COMPACT CARBON-BASED MEMBRANE REACTORS FOR ANAEROBIC BIODEGRADATION OF AZO-DYES FROM WASTEWATER

Alberto Giménez Pérez

Compact carbon-based membrane reactors for anaerobic biodegradation of azo-dyes from wastewater

DOCTORAL THESIS

Alberto Giménez Pérez

Supervised by:

Dr. Josep Font Capafons
Department of Chemical Engineering

UNIVERSITAT
ROVIRA i VIRGILI

A Thesis submitted in partial fulfillment of the requirements of the degree of doctor from the Universitat Rovira i Virgili in the Chemical, Environmental and Process Engineering Program

Tarragona 2016

UNIVERSITAT ROVIRA I VIRGILI
COMPACT CARBON-BASED MEMBRANE REACTORS FOR ANAEROBIC BIODEGRADATION OF AZO-DYES FROM WASTEWATER
Alberto Giménez Pérez

UNIVERSITAT
ROVIRA i VIRGILI

Department of Chemical Engineering
University of Rovira i Virgili,
Avinguda Països Catalans, 26
43007, Tarragona, Spain.
Tel: +34-977-558506
Fax: +34-977-558544

CERTIFIQUE:

Que el present treball, titulat “Compact carbon-based membrane reactors for anaerobic biodegradation of azo-dyes”, que presenta Alberto Giménez Pérez per a l’obtenció del títol de Doctor, ha estat realitzat sota la meva direcció al Departament Enginyeria Química d’aquesta universitat i acompleix els requeriments per poder optar a Menció Internacional.

Tarragona, 1 de setembre de 2016

Dr. Josep Font Capafons

UNIVERSITAT ROVIRA I VIRGILI
COMPACT CARBON-BASED MEMBRANE REACTORS FOR ANAEROBIC BIODEGRADATION OF AZO-DYES FROM WASTEWATER
Alberto Giménez Pérez

UNIVERSITAT
ROVIRA i VIRGILI

Department of Chemical Engineering
University of Rovira i Virgili,
Avinguda Països Catalans, 26
43007, Tarragona, Spain.
Tel: +34-977-558506
Fax: +34-977-558544

I hereby acknowledge that the present work entitled with “Compact carbon-based membrane reactors for anaerobic biodegradation of azo-dyes”, presented by Alberto Giménez Pérez to obtain the degree of doctor by the University Rovira i Virgili, has been carried out under my supervision at the Departament of Chemical Engineering and fulfils the requirements to be recognised with the International Mention.

Tarragona, September 1, 2016

The thesis supervisor

Dr. Josep Font Capafons

UNIVERSITAT ROVIRA I VIRGILI
COMPACT CARBON-BASED MEMBRANE REACTORS FOR ANAEROBIC BIODEGRADATION OF AZO-DYES FROM WASTEWATER
Alberto Giménez Pérez

To my beloved family,

UNIVERSITAT ROVIRA I VIRGILI
COMPACT CARBON-BASED MEMBRANE REACTORS FOR ANAEROBIC BIODEGRADATION OF AZO-DYES FROM WASTEWATER
Alberto Giménez Pérez

Acknowledgements

First of all, I would like to express my sincere gratitude and appreciation to my supervisor Dr. Josep Font, for giving me the opportunity to work with him. His support, patience, encouragement, and immense knowledge were key motivations throughout my Ph.D. This thesis would not be possible without his continuous guidance and advice.

I would also like to thank all the members of the PISET (formerly CREPI) research group who support me and give me inestimable advice throughout the Ph.D. project development. It was a pleasure to work with you all. In particular, my special gratitude go to Yonhara Garcia and Judith Chirinos for your invaluable help, making easier our common goal. I would also thank Dr. Agustí Fortuny for all the technical support at the laboratory.

I would like to acknowledge the Spanish Government (MINECO) for the financial support to carry out my Ph.D. thesis. My sincere thanks also go to Prof. Pagona Konstantinos, Santosh Bikkarolla and Ali Murad from Carbon-based materials group, University of Belfast. I thank you for making possible my research stay and for devoting so much attention to me. I thank also you for introduce me in the graphene's world.

I would like to gratefully acknowledge Dr. Salome Soares, Dr. Tono Martinez and Dr. Azael Fabregat, for their acceptance to participate in the evaluation committee of this thesis. Furthermore, Dr. Jaume Giralt, Dr. Agustí Fortuny and Dr. Kelly Briceño are acknowledged for being substitutes in the above mentioned committee and Dr. Manuel Macias and Dr. Patricia H. for being external advisors of this thesis.

Me gustaría agradecer el apoyo de mis abuelos, de mis padres y hermanos. A pesar de estar separados por unos cuantos kilómetros, vuestros ánimos y apoyos han hecho mucho más fácil este camino. Mi agradecimiento más especial a Rosa, por su comprensión y optimismo contagioso en los momentos difíciles.

UNIVERSITAT ROVIRA I VIRGILI
COMPACT CARBON-BASED MEMBRANE REACTORS FOR ANAEROBIC BIODEGRADATION OF AZO-DYES FROM WASTEWATER
Alberto Giménez Pérez

Sumario

La contaminación de las aguas es una amenaza para la sostenibilidad del planeta y su importancia es cada vez mayor debido al crecimiento demográfico que se ha experimentado a lo largo de las últimas décadas. Este crecimiento trae consigo una amplia expansión del sector industrial. En este ámbito, los colorantes se emplean para diferentes fines como son la producción de papel, ropa, cosméticos, alimentos… La eliminación de colorantes en aguas residuales es un tema que atrae el interés científico por varios motivos. En primer lugar, los procesos de tratamiento aerobios ampliamente implantados en las estaciones depuradoras de aguas residuales son ineficaces ante estos compuestos. Además, el carácter biotóxico de algunos de estos colorantes podría dañar la biomasa que por carácter general domina estos procesos. Y no hace falta decir que su vertido directo a los ríos o mar acarrearía un daño irreparable a las especies que en ellos habitan. Por estas razones, procesos diferentes y específicos deben ser estudiados e implantados para conseguir la eliminación de estos compuestos.

Los colorantes de tipo azo representan el grupo más numeroso de estos compuestos sintéticos. En su estructura química presentan uno o varios enlaces azo que dificultan su degradación. Ésta puede ser abordada de forma física, físico-química, química o biológica. La técnica física más utilizada se basa en la filtración, normalmente nanofiltración debido al pequeño tamaño de estos compuestos; también la adsorción se incluye en este apartado. Los métodos físico-químicos normalmente consisten en coagular-flocular las partículas colorantes y posteriormente decantarlas. Por el contrario, la práctica totalidad de los tratamientos químicos se basan en la aplicación de diferentes oxidantes en una variada gama de condiciones de operación. En los casos anteriores, ya sea por generar un efluente secundario contaminado o por los costes asociados al tratamiento, el resultado no satisface los requerimientos. En este sentido, los tratamientos biológicos son mucho más prometedores.

En el ámbito de la biodegradación se ha comprobado que estos compuestos se pueden mineralizar bajo condiciones anaerobias, no obstante, es necesario introducir una segunda fuente de carbón que sea oxidada y actúe como fuente de electrones para reducir el colorante. Hay substancias presentes en este tipo de medios, algunas de ellas provienen de la degradación del propio colorante, como las quinonas que actúan como portador de electrones facilitando el proceso. Aun así se ha comprobado que éste es el

paso limitante del proceso y es por ello que materiales externos electro-conductores han sido introducidos en estos sistemas con objeto de ser estudiados.

Estudios previos realizados por este mismo grupo de investigación comprobaron el efecto positivo que se produce al introducir carbón activado en la degradación anaerobia del colorante Acid Orange 7, también llamado Orange II. Se propuso un sistema de lecho empacado con material carbonoso que potenciaba en gran medida la degradación de este compuesto. No obstante, este novedoso sistema presentó algunos inconvenientes como son la sobreproducción de biomasa y ensuciamiento del lecho, lo que provoca el bloqueo hidráulico del mismo. Ante este problema, no fue posible aplicar sistemas de limpieza adecuados. Además el sistema no incluye ningún tipo de elemento separador capaz de retener la biomasa u otras partículas sólidas, por tanto eventualmente son arrastradas con el efluente y la introducción posterior de sistemas de separación se hace totalmente necesaria para conseguir un agua tratada de alta calidad.

Por ello, este trabajo plantea el uso de un innovador sistema en el cual se combina el material portador de electrones y el elemento separador en una misma unidad. Esto se consigue mediante la preparación de membranas de carbón soportadas sobre elementos cerámicos. Estos materiales presentan poros en el rango de la nanofiltración por lo que permiten la retención de la totalidad de los compuestos que llevan a cabo la degradación. Además, la capa de carbono facilita el tránsito de electrones del mismo modo que lo hacía el lecho empacado de carbon activado. La síntesis de la membrana requiere condiciones específicas que son discutidas a lo largo de la tesis, de esta forma se consigue preparar una superficie uniforme y completamente recubierta de carbono. Este novedoso sistema permite velocidades de degradación del colorante azo Acid Orange 7, 80-100% (32 $g \cdot m^{-3} \cdot dia^{-1}$) similares al restos de técnicas reportadas en los últimos años. Además, en casos esporádicos de elevado ensuciamiento sobre la membrana, este puede ser eficientemente eliminado a través de técnicas de limpieza ampliamente utilizadas en este campo.

Una vez comprobado el rendimiento favorable de la técnica propuesta, la segunda parta de la tesis se enfocó al desarrollo de la membrana. Se estudiaron las variables que influyen en su rendimiento para la degradación de colorantes. Por ello, se modificaron variables como la cantidad de carbono que incorporan las membranas, o la porosidad del soporte cerámico, entre otros factores. De esta forma, se ha observado que membranas que contienen una cantidad de carbono mayor, tienden a ofrecer un mayor

rendimiento en esta aplicación, lo cual confirma el papel clave del conductor de electrones. Por otro lado también se observó que membranas rugosas favorecen la degradación del compuesto. Esto es debido a que este tipo de superficies favorecen un mayor crecimiento de biomasa a la vez que una mayor capacidad de adsorción.

La tercera parte de la tesis abordó el estudio de sistemas con cámaras segregadas como alternativa al tratamiento de estos colorantes. Estos sistemas permiten el tratamiento independiente de dos corrientes con cargas de contaminantes totalmente diferentes. Compuestas de dos celdas de reacción, en una de ellas se oxida y en la otra se reduce, existiendo un flujo de electrones y de protones que como novedad en este caso se transmiten a través de las membranas ya implementadas y estudiadas en los apartados anteriores de la tesis.

Finalmente se abordó la síntesis de nuevos materiales carbonosos que a priori ofrezcan mejores condiciones para transportar los electrones que el carbón activado. Con este objetivo, se ha preparado grafeno parcialmente oxidado; posteriormente empleado en la preparación de membranas del mismo tipo que las discutidas en la primera parte de la tesis y que podrían ser empleadas en la misma aplicación o en cualquier otro proceso basado en las mismas etapas.

UNIVERSITAT ROVIRA I VIRGILI
COMPACT CARBON-BASED MEMBRANE REACTORS FOR ANAEROBIC BIODEGRADATION OF AZO-DYES FROM WASTEWATER
Alberto Giménez Pérez

Sumari

La contaminació de les aigües és una amenaça per a la sostenibilitat del planeta i la seva importància és cada vegada major a causa del creixement demogràfic que s'ha experimentat al llarg de les ultimes dècades. Aquest creixement porta una àmplia expansió del sector industrial. En aquest àmbit, els colorants han estat utilitzats per a diferents aplicacions com la producció de paper, roba, cosmètics, aliments... L'eliminació de colorants en aigües residuals és un tema d'interès científic per diversos motius. En primer lloc, els processos de tractaments aerobis àmpliament implementats a les estacions depuradores d'aigües residuals són ineficaços per a l'eliminació d'aquests compostos. D'altra banda, el caràcter biotòxic d'alguns d'aquests colorants podria danyar la biomassa que per caràcter general domina aquests processos. No fa falta dir que el seu abocament directe al riu o mar suposaria un dany irreparable a les espècies que en ells hi viuen. Per aquestes raons, processos diferents i específics han de ser estudiats i implementats per aconseguir l'eliminació d'aquests compostos.

Els colorants tipus azo representen el grup més nombrós d'aquests compostos sintètics. A la seva estructura química presenten un o múltiples enllaços tipus azo que dificulten la seva degradació. Les vies d'eliminació són físiques, físico-químiques, químiques o biològiques. La tècnica física més utilitzada es basa en la filtració, normalment nanofiltració a causa de la petita mida dels porus d'aquests compostos; també l'adsorció pot incloure's en aquest apartat. Els mètodes físico-químics consisteixen en coagular-flocular les partícules colorants per posteriorment decantar-les. La pràctica totalitat dels tractaments químics es basen en l'aplicació de diferents oxidants en un ampli ventall de condicions d'operació. En els casos anteriors, ja sigui per generar un efluent secundari contaminat o pels costos associats als tractaments, el resultat no satisfà els requeriments. En aquest sentit, els tractaments biològics són molt més prometedors.

A l'àmbit de la biodegradació s'ha comprovat que es poden mineralitzar sota condicions anaeròbies, tot i que és necessari introduir una segona font de carboni que serà oxidada i actuarà com a font d'electrons per reduir el colorant. Existeixen substàncies presents a aquest tipus de medis, algunes d'elles provinents del mateix colorant, com per exemple les quinones que actuen com portadors d'electrons facilitant el procés. Encara així s'ha comprovat que aquest es el pas limitant del procés i per això diferents materials externs electro-conductors han estat introduïts i estudiats als darrers anys.

Els estudis prèviament realitzats pel nostre grup d'investigació van comprovar l'efecte positiu que es produeix en introduir carbó activat en la degradació anaeròbia del colorant Acid Orange 7, també anomenat Orange II. Es va proposar un sistema de llit empacat amb material carbonós que potenciava significativament la degradació d'aquest compost. No obstant això, aquest innovador sistema va presentar alguns inconvenients com són la sobreproducció de biomassa i embrutiment del llit, que provoca el bloqueig hidràulic d'aquest. Davant aquest problema, no va ser possible aplicar sistemes de neteja adequats. Addicionalment, el sistema no incloïa cap element separador amb capacitat de retenir la biomassa u altres partícules sòlides, per això eventualment podien ser arrossegades amb l'efluent. En conseqüència, la introducció d'elements secundaris de separació es feia totalment necessària per aconseguir aigua tractada d'alta qualitat.

Aquest treball presenta l'ús d'un innovador sistema que combina el portador d'electrons i l'element separador en un mateix element. Això s'aconsegueix mitjançant la preparació de membranes de carboni suportades per materials ceràmics. Aquests materials presenten porus que poden situar-se al rang de la nanofiltració pel que ajuden a la retenció de la totalitat de la biomassa que duu a terme la degradació. A més a més, la capa de carboni facilita el trànsit d'electrons de la mateixa forma que ho feia el llit empacat. La síntesi de la membrana requereix condicions específiques que són discutides al llarg de la tesi, d'aquest forma s'aconsegueix la preparació d'una superfície uniforme i completament recoberta de carboni. Aquest innovador sistema permet velocitats de degradació del colorant azo Acid Orange 7 similars als estudiats anteriorment pel nostre grup d'investigació, 80-100% (32 $g \cdot m^{-3} \cdot dia^{-1}$). A més, en cas d'embrutiment de la membrana, aquest pot ser eficientment eliminat a través de tècniques de neteja àmpliament empleades en aquest camp.

Una vegada comprovat el rendiment favorable de la tècnica proposada, la segona part de la tesi s'enfocà en el desenvolupament de la membrana. Es van estudiar les variables que influeixen sobre el rendiment en la degradació de colorants. Per a això, es van modificar variables com la quantitat de carboni que incorporen les membranes o la porositat de la membrana suport, entre d'altres factors. D'aquesta forma, s'ha observat que les membranes que contenen una major quantitat de carboni tendeixen a oferir un major rendiment en aquesta aplicació, cosa que confirma el paper clau del conductor d'electrons. D'altra banda, també es va observar que les membranes rugoses afavoreixen la degradació del compost. Això és degut a que aquest tipus de superfícies

este tipo de superfícies faciliten un major creixement de biomassa, a la vegada que una major capacitat d'adsorció.

La tercera part de la tesi aborda l'estudi de sistemes amb cambres segregades com alternativa al tractament d'aquests colorants. Aquests sistemes permeten el tractament independent de dos corrents amb càrregues de contaminants totalment diferents. Compostes de dues cel·les de reacció, en una s'oxida i a l'altra es redueix, existint un flux d'electrons i de protons que com a novetat en aquest cas es transmeten a través de les membranes ja implementades i estudiades als apartats anteriors de la tesi.

Finalment es va estudiar la síntesi de nous materials carbonosos que a priori poden oferir millors condicions per transportar electrons que el carboni activat. Amb aquest objectiu, es va preparar grafè parcialment oxidat; posteriorment empleat per a la preparació de membranes del mateix tipus que les discutides a la primera part de la tesi i que podrien ser empleades a la mateixa aplicació o a qualsevol altre procés fonamentat en les mateixes etapes.

UNIVERSITAT ROVIRA I VIRGILI
COMPACT CARBON-BASED MEMBRANE REACTORS FOR ANAEROBIC BIODEGRADATION OF AZO-DYES FROM WASTEWATER
Alberto Giménez Pérez

Summary

The water pollution is a threat to the sustainability of the planet and its importance it is increasing due to the population growth that has been experienced over the past decades. This population growth brings an extensive expansion of the industrial sector, where the synthetic dyes are used for purposes such as production of paper, clothing, cosmetics, food... The removal of dyes in wastewater is an issue that attracts the scientific interest for many reasons. First, aerobic treatment processes widely implemented in wastewater treatment plants are ineffective for this purpose. In addition, the biotoxic character of some of these dyes could affect the biomass generally occurring in these processes. Of course, the direct discharge into rivers or the sea would cause irreparable harm to the aquatic ecosystem. Therefore, different and specific processes must be studied and implemented to achieve the degradation of these substances.

Azo dyes represent the largest group of these synthetic compounds. In their chemical structure, they contain one or more azo bonds that difficult their degradation. There are four different methods of degradation, physical, physico-chemical, chemical and biological. The physical technique most used is based on filtration, the nanofiltration is usually applied for this purpose due to the small size of the synthetic dyes; also adsorption can be included in this group. Physico-chemical methods usually consist of azo dyes coagulation-flocculation and subsequent settling. On the other hand, almost all the chemical treatments are based on the oxidation, using a wide variety of oxidants applied in a broad range of operation conditions. In the above cases, due to either the generation of a secondary contaminated effluent or the associated costs, the result does not fulfil the requirements. In this sense, the biological treatments are much more promising.

Regarding biological methods, it has been found that azo dyes can be mineralized under anaerobic conditions; however, it is necessary to introduce a secondary source of carbon that is oxidized and acts as an electron donor to reduce the dye. There are substances present in such media, some of them derived from the degradation of the dye itself, such as quinones that take the role of electron carrier facilitating the process. However, it has been found that the electron transfer is the limiting-step, thus external electro-conductive materials have been introduced into these systems in order to be studied.

Our previous studies proved the positive effect produced by introducing activated carbon in the anaerobic degradation of the dye Acid Orange 7, also called Orange II. A packed-bed system with carbonaceous material greatly enhanced the mineralization of this compound. However, this new system presented some drawbacks such as biomass over production and fouling, causing the accumulation of material into the system. Efficient cleaning procedures could not be applied. In addition, it should be noted that the bed system does not include any separation element to retain the biomass or other solid particles being dragged with the effluent, which forces the introduction of secondary clarifiers to obtain high-quality treated water.

Therefore, this thesis deals with the use of an innovative system in which the electron carrier and separation element are combined in a single unit. This is achieved by preparing ultrathin carbon films supported on ceramic elements. These membranes present pores in the range of nanofiltration so allow the retention of all the biomass that carry out the biodegradation. Furthermore, the carbon layer facilitates the transport of electrons. The membrane synthesis requires specific conditions widely discussed throughout the thesis to get a uniform surface and completely covered with carbon. This new technique allows similar rates of degradation of azo dye Acid Orange 7, 80-100% (32 $g \cdot m^{-3} \cdot day^{-1}$) in comparison with other alternative systems such as packed-bed reactors. Furthermore, in case of severe fouling it can be efficiently removed by conventional cleaning techniques widely used in this field.

After proving the efficiency of the proposed technique, the second part of the thesis was focused on the optimization of the membrane synthesis. Different preparation factors that may affect the azo dye removal were studied. Therefore, variables such as the amount of carbon of the membranes or the support pore size among other factors were evaluated. It was found that the membranes containing higher amounts of carbon reach better performances for this application. This confirms the key role of the activated carbon as electron exchanger. Furthermore, it was also observed that rough membranes favor the biodegradation. This is because these surfaces facilitate the biomass growth in addition to provide a higher adsorption capacity.

The third part of the thesis was addressed to the study of a redox system with separated chambers as an alternative to the treatment of these dyes. These systems allow the independent treatment of two completely different pollutant streams. Composed of two cells connected through a carbon membrane, the oxidation takes place in one of them

and the reduction is carried out in the other one; while a flow of electrons and protons is maintained through the ceramic supported carbon membrane, which was studied in the preceding chapters of this thesis.

Finally, the synthesis of new carbonaceous materials offering, a priori, better capacity for electron transport than amorphous activated carbon was investigated. For this purpose, partially oxidized graphene powder was prepared and subsequently used in the preparation of ceramic supported membranes. The graphene membranes could be used for the same application or in any process controlled by the same steps.

UNIVERSITAT ROVIRA I VIRGILI
COMPACT CARBON-BASED MEMBRANE REACTORS FOR ANAEROBIC BIODEGRADATION OF AZO-DYES FROM WASTEWATER
Alberto Giménez Pérez

List of Content

CHAPTER 1 ..... ***1***

Introduction ***1***

1.1 Water: General considerations 3

1.2 Azo dyes removal 3
1.2.1 Azo dyes 5
1.2.2 The role of a redox mediator 7
1.2.3 Ceramic supported carbon membranes 8
1.2.4 Synthesis of novel redox mediators 10

1.3 Hypothesis and objectives. 12

References 13

CHAPTER 2 ..... ***19***

Enhanced anaerobic biodegradation of azo dyes using ceramic-supported carbon membranes ***19***

2.1 Introduction 20

2.2 Materials and methods. 21
2.2.1 Chemicals 21
2.2.2 Preparation of CSCM 22
2.2.3 Lab-scale CSCM bioreactor 23
2.2.4 Analytical methods 24

2.3 Results and discussion 25
2.3.1 Membrane characterization 25
2.3.2 Anaerobic biodegradation of AO7 30

2.4 Conclusions 35

References 36

Supplementary material 41

CHAPTER 3 ..... ***49***

Optimized synthesis of ceramic-supported carbon membranes for azo dye degradation in anaerobic biofilms ***49***

3.1 Introduction 51

3.2 Experimental 53
3.2.1 Chemicals 53
3.2.2 Membrane synthesis and characterization. 53
3.2.3 CSCM bioreactor system. 54
3.2.4 Analytical methods 55

3.3 Results and discussion 56
3.3.1 Carbon membrane characterization. 56

3.4 Conclusions 65

References 66

Supplementary material 71

CHAPTER 4 73

Double chamber bioreactor systems with ceramic supported carbon membranes for the removal of azo dyes 73

4.1 Introduction 75

4.2 Materials and methods 77
4.2.1 Chemicals 77
4.2.2 Ceramic and carbon membranes 78
4.2.3 Redox system operation 79
4.2.4 Analytical techniques 81

4.3 Results 82
4.3.1 Membranes characterization 82
4.3.2 AO7 biodegradation. 83

4.4 Conclusions 94

References 95

CHAPTER 5 101

Synthesis of N-doped and non-doped partially oxidised graphene membranes supported over ceramic materials 101

5.1 Introduction 103

5.2 Experimental 105
5.2.1 Membrane precursor preparation. 105
5.2.2 Membrane supports 106
5.2.3 Synthesis of graphene (GO or NrGO) membranes 107
5.2.4 Membrane characterisation. 107
5.2.5 Membrane filtration tests. 108

5.3 Results and discussion 109
5.3.1 Graphene (GO or NrGO) synthesised powder characterisation 109
5.3.2 Membrane characterisation 114
5.3.3 Interactions on the membrane surface 119
5.3.4 Membrane permeation tests 119
5.3.5 Influence of membrane thickness 121
5.3.6 Support pore size influence on membrane preparation. 123

5.4 Conclusions 125

References 126

Supplementary material 132

CHAPTER 6 135

General conclusions and future work 135

6.1 General conclusions 136

6.2 Future work..... 138

List of Figures

Figure 1.1 Colored lab gloves..... 3

Figure 1.2 Red polluted water flows into the Jian River in Luoyang (China)..... 4

Figure 2.1 AO7 dye removal plant..... 24

Figure 2.2 ESEM membrane characterization. Cross-sectional view of the ceramic support (a) and CSCM (b), and front view of the ceramic support (c) and CSCM (d). 27

Figure 2.3 AFM image. CSCM height profile..... 29

Figure 2.4 CSCM ($J_{W,\ CSCM}$) and ceramic support (J_W, C_S) permeability at 25 ºC ... 29

Figure 2.5 AO7 anaerobic biodegradation in CSCM reactors and non-modified ceramic supports from the start-up until the achievement of steady state..... 31

Figure 2.6 Reproducibility of the bioreactor experiments. [Feed AO7 concentration: 50 $mg \cdot l^{-1}$; flux: 0.05 $l \cdot m^{-2} \cdot h^{-1}$; temperature: 37 ºC]. 34

Figure 2.7 Influence of the flux on the steady AO7 conversion. [LMH: $L \cdot m^{-2} \cdot h^{-1}$; feed AO7 concentration: 50 $mg \cdot l^{-1}$; temperature: 37 ºC]..... 35

Figure A2.1 Synthesis procedure for the preparation of CSCM..... 41

Figure A2.2 Carbon infiltrations in the ceramic support..... 41

Figure A2.3 ESEM analysis of CSCM defects: carbonization hole (a), polymer deposition-related cracks (b) 42

Figure A2.4 Polymer (carbon precursor) deposited over the ceramic support..... 42

Figure A2.5 EDx analysis of the CSCM (a) and ceramic support (b), respectively. . 44

Figure A2.6 Ceramic support: AFM height profile 44

Figure A2.7 Decolorization over the biological degradation process..... 44

Figure A2.8 Ceramic support (white disk) and CSCM (black disk)..... 45

Figure A2.9 Membrane's holder and bioreactor..... 45

Figure A2.10 Influence of the contact time (flux) on the AO7 removal..... 47

Figure 3.1 CSCM bioreactor system..... 55

Figure 3.2 Support pore size influence on the membrane thickness: (a) CSCM 15-10, (b) CSCM 50-10, (c) CSCM 150-10..... 57

Figure 3.3 3D surface height profiles; CSCM 150-2 (a) and CSCM 15-10 (b) 59

Figure 3.4 Evolution of the AO7 conversion for the different CSCM..... 63

Figure A3.1 CSCM and ceramic support (CS) permeability; precursor solution composition: 2 and 10% wt. 71

Figure 4.1 Proposed biodegradation mechanism for TAR (a), AOG (b), and AO7 (c) 76

Figure 4.2 Double-cell bioreactor 80

Figure 4.3 Carbon membrane (a, c) and Ceramic support (b, d) surfaces and thickness, respectively 83

Figure 4.4 Double-cell bioreactor performance under different experimental conditions 85

Figure 4.5 CSCM Bioreactors after 0 (a) and 15 (b) days of operation. 87

Figure 4.6 Influence of the dye concentration ([NaAc:AO7] 10:1, temperature 37ºC). 88

Figure 4.7 First-order kinetic model for the AO7 88

Figure 4.8 Effect of the mass ratio between the external carbon source and the azo dye. [AO7 initial concentration: 50 $mg \cdot L^{-1}$, [NaAc: AO7] = 2:1, temperature 37ºC]. 90

Figure 4.9 Comparison of the biodegradation of different azo dyes 91

Figure 4.10 Kinetic of the biodegradation of different azo dyes 91

Figure 4.11 Optical microscope (a) and TEM (b-d) images of a biofilm samplepp .. 94

Figure 5.1 Dead-end filtration experimental setup: (1) nitrogen gas cylinder; (2) gas pressure regulator; (3) relief valve; (4) feed tank; (5) membrane holder; (6) weighing scale. 108

Figure 5.2 ESEM (a) and TEM (b) images of GO powder synthesised by a modification of Hummer's method 110

Figure 5.3 ESEM (a) and TEM (b) images of NrGO powder synthesised by Solvo-thermal method**.** 111

Figure 5.4 Raman spectrum of GO and NrGO powder. 112

Figure 5.5 XRD characterisation of GO and NrGO powder 113

Figure 5.6 High resolution C 1s XPS spectra of GO (a) and NrGO (b); high resolution N 1s XPS spectra of NrGO (c); elemental composition of GO and NrGO (d) 114

Figure 5.7 ESEM images: GO (a, c, e) and NrGO (b, d, f) disks, membrane surface, and cross-sectional view, respectively 116

Figure 5.8 AFM images: GO (a, b) and NrGO (c, d) membrane topography 2D, and 3D 118

Figure 5.9 GO membrane over ZrO2 surfaces. Interaction mechanism 119

Figure 5.10 Pure water flux. [GO or NrGO deposited: 0.1 mg; ceramic support: 0.04 µm; hydraulic pressure difference: 0.2 bar] 120

Figure 5.11 Dependence of the pure water flux on the GO deposited [ceramic support: 0.4 µm**]**..... 122

Figure 5.12 Influence of the support pore size on the permeate flux. [GO coated: 0.1 and 0.2 mg; hydraulic pressure difference: 0.2 bar; T = 20 ºC] 123

Figure A5.1 Synthesised GO after (a) and before (b) the centrifuge process..... 132

Figure A5.2 Synthesised NrGO powder (reflux method). 132

Figure A5.3 Synthesised NrGO membrane (Solvothermal method). 133

Figure A5.4 Synthesised NrGO powder (Solvothermal method). 133

Figure A5.5 GO (a) and NrGO (b) membranes, respectively..... 134

List of Tables

Table 2.1. Ceramic support properties..... 23

Table 2.2 ESEM-EDX analysis; composition (wt. %) of the carbon membrane and ceramic support..... 28

Table 2.3 Membrane flux resistances. 30

Table A2.1. Experimental data..... 47

Table 3.1. Synthesized carbon membranes..... 54

Table 3.2. Influence of the preparation conditions on the membrane thickness, roughness, and carbon composition. 58

Table 3.3 Hydraulic resistances (m^{-1}) [ΔP: 40000 Pa] 60

Table 3.4 Electrical resistance (Ω·m)..... 62

Table 4.1 Ceramic support properties..... 78

Table 5.1 Elemental composition of GO or NrGO composite membranes (wt. %). 115

Table 5.2 Intrinsic GO layer and support resistances. [Hydraulic pressure difference = 0.2 bar; T = 20 ºC; GO coated: 0.1 mg] 124

UNIVERSITAT ROVIRA I VIRGILI
COMPACT CARBON-BASED MEMBRANE REACTORS FOR ANAEROBIC BIODEGRADATION OF AZO-DYES FROM WASTEWATER
Alberto Giménez Pérez

CHAPTER 1

Introduction

The first chapter of this thesis presents general considerations about wastewater management and, specially, azo dyes. This part presents a brief description of the conventional water treatments and some alternatives for the removal of commercial azo dyes. The chapter emphasizes on the biological methods and the role of the activated carbon to enhance the biodegradation. Finally, it introduces the contents discussed in this thesis.

UNIVERSITAT ROVIRA I VIRGILI
COMPACT CARBON-BASED MEMBRANE REACTORS FOR ANAEROBIC BIODEGRADATION OF AZO-DYES FROM WASTEWATER
Alberto Giménez Pérez

1.1 Water: General considerations.

Clean water is absolutely necessary for any life organism. Therefore, humans are bound to maintain the quality of this natural resource to achieve a sustainable development for everyone on earth. Due to the population growth on earth and the industrialization, the demand of water is continuously increasing. According the United Nations Environment Programme (UNEP), annual global freshwater withdrawal has grown from 3790 km^3 (of which consumption accounted for 2070 km^3 or 61%) in 1995, to 4430 km^3 (of which consumption accounted for 2304 km^3 or 52%) in 2000 (Shiklomanov, 1999). On the other hand, the published studies by the European Commission about the global climate change predict high vulnerability in the Southern regions of Spain, Italy or Greece where already suffer from scarcity of water resources.

For all these reasons, a proper management of the water resources is totally vital. Polluted water sources must be decontaminated and reused for new purposes. New methods should be developed to deal with toxic or non-biodegradable compounds. On the other side, human population's consciousness, which is in notable growth, should head for a decrease on the water consumption the next decades.

1.2 Azo dyes removal

Azo dyes are massively produced and subsequently applied for different commercial purposes: cosmetics, paper, textiles (Figure 1.1) or food; its use has increased enormously throughout the last decades [1]. Their chemical structures contain a single or multiple strong azo bonds that furnish specific color to the molecules and provide robustness.

Figure 1.1 Colored lab gloves*

* Ocon Chemicals Ltd. (http://oconchemicals.ie/)

These compounds are classified as highly toxic by the main health protection organisms. Consequently, their waste management is constantly being regulated. Some azo dyes have been completely banned in some countries. If not, the discharge limits have been considerably reduced. These compounds frequently occur in the effluents from textile industries; 1 kg of cloth produced generates about 40-65 liters of wastewater [2]. It is estimated that billions of tones of azo contaminated water are annually produced around the world [3]. The colored water is not only sometimes highly toxic for aquatic organisms, it is also unacceptable for society (Figure 1.2). On the other hand, these synthetic compounds are designed to be extremely resistant to degradation, especially those that are used for the fabrication of clothes. Thus, many conventional treatments are inefficient for their removal.

Figure 1.2 Red polluted water flows into the Jian River in Luoyang (China)*

*Alpha Press (http://www.dailymail.co.uk/)

1.2.1 Azo dyes.

This kind of dyes is usually recalcitrant to typical waste treatment processes; thus the study of new techniques more efficient on the azo dye removal is highly demanded. The treatments can be classified as physical, physico-chemical, chemical, and biological. Physical or physico-chemical methods concentrate the pollutant in a new stream that needs secondary treatments; for example, physical methods based on coagulation or flocculation [4]. Moreover, the coagulation stage requires the use of chemicals. Other physical methods, i.e. filtration, require high investment for complex equipment in addition to present serious problems of operation, i.e. membrane fouling [5]. Adsorption methods can be highly efficient for azo dye removal [6,7]. However, the cost of the adsorbents and their regeneration restrain its use. Other chemical methods such as advanced oxidation processes (AOP) have been reported with removal efficiencies higher than 90%, for example processes involving the Electro-Fenton process. The Fenton's reagent (H_2O_2, Fe^{2+}) generates hydroxyl radicals ($^{\cdot}OH$) by simultaneous reduction of dioxygen and ferrous ions over a specific electrode [8]. The hydroxyl radicals react with the azo dyes mineralizing the problematic molecules into CO_2 and H_2O. However, the associated costs of these treatments are too high [9].

Biological processes are an alternative more cost-effective and environmentally-friendly than other approaches because they avoid the use of chemicals [10]. The effectiveness of microbial decolorization depends on the adaptability and the activity of the selected microorganisms. Consequently, a large number of species has been tested for the decolorization and mineralization of various commercial dyes in recent years [11–15]. The most widely used azo dyes, such as Acid Orange 7 or Reactive Black 5, are typically chosen as model compounds [16,17]. These compounds are defined by the number of azo bonds or the type of functional groups.

The biological treatment starts with anaerobic reactors where the azo bond is broken and several intermediate metabolites are released. These compounds, aromatic amines, usually present a toxicity that can be even higher than that of the dye original one [17]. The degradation metabolites, i.e. sulfanilic acid, are usually mineralized under aerobic conditions [13]. Hence, sequential anoxic-aerobic bioreactors enhance the mineralization of these synthetic molecules as has been proven in previous reported studies [10]. It has been demonstrated that mixed cultures favor the development and adaptation of microbial strains that are able of degrading these compounds under the

cited variable conditions. Microbial discoloration can occur via two principal mechanisms: biosorption and degradation, or a combination of both [18]. Biomass from algae, yeast, filamentous fungi and bacteria has been used to remove dyes by biosorption [17]. The biosorption capacity of a microorganism is associated to the heteropolysaccharide and lipid components of the cell wall, establishing solid attractive forces between the azo dye and the cell wall [18–21]. On the other hand, the azo dye degradation presents limitations, since these compounds contain electron-deficient xenobiotic components such as azo bonds (–N=N–), which significantly complicate the microbial mineralization [4, 33–36]. The cleavage of the azo bond takes place with the help of an external electron source and a redox mediator that enhances the electron transfer [13, 41–43]. The degradation mechanism is preferable as it is not restricted by the biomass adsorption capacity and the pollutant is not just retained but actually destroyed.

The biodegradation is altered by different parameters as the azo dye structure, carbon and nitrogen sources, salinity, pH, temperature, dye concentration and the presence or absence of oxygen [18]. Azo dyes structure defines the facility for being degraded; compounds that contain electron-deficient components are easily mineralized; moreover, dye molecules with complex structures, i.e. several functional groups such as sulfonic acid groups. The azo dyes chemical structure influences the rate of degradation [19]. Carbon and nitrogen are essential for the decolorization process. Carbon substrates have different roles. They provide the energy needed for the survival and growth of the microorganisms. On the other hand, carbon substrates are also necessary as electron source [20]. The addition of organic nitrogen sources, such as peptone, can regenerate NADH, which acts as an electron donor for the reduction of azo dyes; hence also enhancing the process. Finally, parameters like pH, salinity, dye concentration and oxygen also affect the process [2]. It has been found that sodium concentration higher than 3000 mg/L inhibits seriously the activity of most bacterial groups [18]. The increase of the dye concentration reduces progressively the decolorization rate [5]. The process is also dependent on the pH of the solution; this parameter defines the dye solubility and, hence, sometimes the color of the solution [21]. The optimal pH for color removal is often between 6.0 and 10.0 [5]. Yet, the temperature has a notably importance on the enzymatic production and microbial growth; thus, it defines the degradation performance. Operating temperatures in the range 30-40 ºC have been

found optimal for this process [22]. In relation to the election of the electron donor, different substrates as sodium acetate, glucose, sodium formate, sodium succinate, sodium citrate and sodium pyruvate have been proven as process enhancers [18].

1.2.2 The role of a redox mediator.

The impact of the redox mediator is probably the most significant. The transfer of electrons between the electron sources to the dye is considered the rate-limiting step [5]. It has been proven that the electron density around the azo bonds is related to the removal rate. For this reason, several studies reported the external addition of redox mediators for enhancing the degradation. Different redox mediators have demonstrated a positive impact on this process such as flavin-based compounds, quinones, or humic acids [5]. The election of activated carbon as redox mediator also relies on other secondary advantages since this compound also acts as physical support for microorganisms and adsorbent, which sometimes promotes the dye retention so that its degradation. The combination of these factors makes carbonaceous materials as ideal substrate for the studied application.

Granulated and powder AC (GAC and PAC, respectively) have been usually tested throughout last decades. Granulated AC can be retained more easily into the bioreactors, therefore its use is preferential. This material has been introduced in different types of bioreactors. Several examples of sequential batch reactors (SBR) have been described; the introduction of GAC into SBR showed a positive impact on the biological degradation of Orange II [23]. Upflow anaerobic sludge blanket (UASB) reactors have been combined with PAC for degrading a model compound (Yellow Gold RNL); the azo dye was highly degraded (73-94%) with a hydraulic retention time of 24 h. Membrane bioreactors with an AC packed zone have also been successfully tested with some model compounds [24], i.e. Acid Orange II. Mezohegyi et al. [25] investigated the anaerobic reduction of Acid Orange 7 in upflow anaerobic packed bed (UPBR) bioreactors achieving over 99% conversion. The packed bed was mainly conformed by GAC, which facilitates the formation of an immobilized active biofilm. Two significant problems were observed in this system. The first one is related with the over production of biomass, which triggered the blocking of the bioreactor. Non simple cleaning methods can be applied in that situation. The second problem regards the retention of the desired substances inside the reactors. In the absence of a micro-pore filter, some

components such as PAC or microorganisms can be dragged out from the system. This implies the need of secondary clarifiers and higher operational costs.

Taking into account the proven positive effect of the activated carbon for the biodegradation of azo dyes, this thesis deals with a novel approach where the carbon is incorporated through supported films. This configuration presents several advantages in comparison to previous techniques- The carbon material is immobilized over ceramic materials guarantying its retention inside the bioreactor, the membrane can be cleaned much more easily than other systems such as packed-bed reactors, the degradation is focused over the active biofilm growth onto the carbon membrane, and the membrane acts as biomass retention system. Hence, this process intensification means a reduction on the volume needed and simplifies the operation in comparison to other recent alternatives found in the literature.

1.2.3 Ceramic supported carbon membranes.

The first part of this thesis is focused on the development of carbon membranes and its subsequent application into bioreactors. The synthesis and application of this type of membranes was previously reported for gas separation processes [26]. Ceramic supported carbon membranes (CSCM) were prepared by carbonization of commercial polymer onto ultrafiltration ceramic membranes. A commercial polyimide, Matrimid 5218®, was chosen as carbon precursor. This polymer has been extensively used in the preparation of carbon films or composites for many purposes. Matrimid 5218® presents exceptional properties such as high molecular weight or absence of water in the final product. Preliminary studies were made to find suitable synthesis parameters, for instance the amount of precursor, precursor deposition way or carbonization techniques. The final objective was to prepare a membrane perfectly covered without cracks or holes that could increase notably the original permeation of the ceramic support. Moreover, the combination of the support pore size and precursor amount determines the permeation of the synthesized membranes. Taking into account the final application in membrane bioreactors, the hydraulic contact time must be long enough for reaching acceptable dye removal rates at normal transmembrane pressures (TMP). Therefore, these parameters were modified in order to synthesize membranes that provide the desired properties. Cracking problems related to the deposition and carbonization stage

were overcome by modifying the support coating parameters or the carbonization heating programmer.

After synthesizing a membrane that accomplish with the specifications, it was coupled in a bioreactor and tested for the elimination of a model compound, Acid Orange II. Mixed microbial sludge from a municipal WWTP was used as biomass inoculum. The experiments were maintained for weeks in order to prove the robustness of this technique. Additionally, the effect of the biomass contact time or experimental reproducibility was also analyzed.

The second part of this work was dedicated to further study of the membrane synthesis process so as to enhance the dye degradation. The membrane structure is dependent on synthesis parameters such as ceramic support pore size or polymer amount employed. These parameters determines the adsorption and redox mediator capacity, membrane roughness, or permeability; thus its suitability for this application. After the synthesis, an extensive structural characterization study was completed. Complementary studies on permeability were also included. Next, their performances on degrading azo dyes were compared to find out which are the more convenient synthesis parameters taking into account the proposed application.

The third part of this thesis was dedicated to simultaneous oxidation-reduction in separated chambers for the removal of recalcitrant compounds, again azo dyes. This allows treating two different contaminated effluents, one in anaerobic conditions, i.e. the azo dye-containing effluent, and the other in aerobic conditions, where the effluent must contain readily biodegradable organic compounds. The electrons are totally exchanged between the oxidation and reduction chamber through the carbon membrane placed between both chambers. There is not external electron circulation, so no energy is obtained, thus the electron current is exclusively dedicated to the biodegradation. This way, the biodegradation process is intensified and high rates of mineralization can be obtained. The other important difference falls to the membrane role. To achieve that goal, electro-conductive porous membranes were prepared through polymer carbonization onto ceramic supports.

A lab-scale double chamber bioreactor was designed to process several model azo dyes such as Acid Orange 7. Ceramic supported carbon membranes, CSCMs, were synthesized and subsequently employed to separate both chambers but simultaneously

favoring the electrons and protons flux. The study deals with the performance of the CSCMs and the influence of different operating parameters. Some of the studied variables were the concentration ratio between the oxidized and reduced components, the carbon precursor amount or the support pore size.

1.2.4 Synthesis of novel redox mediators.

The last part of the thesis was assigned to the graphene films synthesis. Graphene is a monolayer of carbon atoms packed into a two-dimensional (2D) honeycomb lattice [27]. This is a basic element of other configurations such as carbon nanotubes (1D) or stacked into 3D graphite. Their unique thermal, mechanical and electrical properties open a wide range of possibilities of application. Due to its high optical transparency (>97% for monolayer) and mobility (>200,000 $cm^{-2}/V \cdot s$), graphene has been regarded as the most potential material for flexible transparent electrodes of super-capacity, touch screen and solar cells [28,29]. This outstanding electrical conductivity becomes graphene in the ideal candidate to replace amorphous carbons in case that the electron transfer is the rate-limiting step. Moreover, depending on the oxidation state, highly oxidized graphene oxide (GO) present a 3D porous structure with excellent adsorption capacity [30], which is sometimes demanded if this process plays an important role. Two examples of environmental application where adsorption and electron transfer are critical points are anaerobic biodegradation of recalcitrant pollutants, for instance azo dyes, or any photocatalytic degradation.

Graphene can be synthesized by several methods; the election of the most proper method depends on the application requirements. These methods employ graphite sources or non-graphitic sources. Both pathways involve physical and chemical processes, or a combination of both. In 2004, Novoselov et al. reported electronic measurements of a single-layer graphene [28]. These sheets were obtained by micromechanical cleavage of graphite. This procedure is also known as the scotch tape method. This method is simple and special equipment is not required. A tape is put onto the desired area of graphite and the adhesive is carefully peeled-off. They realized that repeating several times this procedure, the numbers of graphite layers decreases. This way, they reduced the thickness of these films from few-layers to single-layers. The time consuming step of micromechanical cleavage is the identification of a single layer

of graphene [31]. Unfortunately, this method is not easily scalable to satisfy the demand associated to all the possible applications of this material.

A totally different approach based on chemically cleavage and exfoliation is employed for synthesizing partially oxidized graphene, the Hummers method [32]. In 1958, this author reported an alternative route for the synthesis of graphene oxide by using $KMnO_4$ and $NaNO_3$ in concentrated H_2SO_4. Large highly oxidized graphene oxide (GO) films can be produced following this technique. Once GO is prepared, it can be reduced to increase its electrical conductivity. Each reduction process defines the reduced GO (rGO) properties and its performance in a potential application. The different reductive processes are based on thermal, chemical or multi-stage reduction [33]. Thermal reduction consists on reducing GO films by thermal annealing at high temperatures, i.e. 600-1000ºC [34], and inert atmosphere. The exfoliation takes place because of the abruptly expansion of gases such as CO_2 created because of the decomposition of GO functional groups. Therefore, this process not only decompose the oxygen functional groups presents in GO, but also exfoliates the material. This is a proper method to produce bulk graphene, however, uniquely small and wrinkle films. The effect of these gases evolved throughout the process is the cause of the imperfections along the sheets; in order to prevent this explosive process, the heating must be slow, which makes the process time consuming and more expensive.

On the other hand, chemical reduction of GO can be achieved by adding Hydrazine. This reagent is usually incorporated into GO solutions, obtaining non-soluble few-layers sheets of graphene. Other examples of reductants are sodium borohydride or ascorbic acid.

The most important technique for manufacturing graphene from non-graphitic sources is chemical vapor deposition (CVD). This method consists on the decomposition of hydrocarbons at high temperatures and deposition of graphitic layers onto metal surfaces [35]. This technique allows the preparation of high-quality graphene that can be used for transparent organic electronics [31]. However, note that the transfer of the graphene sheet from the metal support, where it has been growth, for being used in a final application it is a delicate step because of the structure can be easily damaged.

This part of the thesis goes into depth of the graphene synthesis. Graphene oxide powders with different oxidizing grades were prepared. A modified Hummers method

was followed to synthesize GO powder. Next, GO was reduced via chemical reducing agents. In this study, nitrogen doped reduced graphene oxide (NrGO) is synthesized through hydrothermal reaction of graphene oxide with ammonia and hydrazine. This carbon material exhibits an electrical conductivity many orders of magnitude higher than GO or other carbon structures. The second part of this chapter was the novel development of partially oxidized graphene membrane supported over Titania-Zirconia supports. To the best of our knowledge, the only report in the literature of this kind of materials, studies the preparation of highly oxidized graphene films over porous alumina tubular supports [36]. In the present study, the graphene oxygen content was reduced in order to enhance its electrical conductivity. Moreover, the use of zirconia supports with different pore sizes was evaluated. Regarding the film preparation, there are different techniques widely used for casting, e.g. dip or spray coating, however, vacuum-filtration allows an absolute control over the amount deposited onto the substrate. For this reason, the chosen technique for creating these composites was vacuum-filtration. The effect of multiple variables on the membrane preparation was extensively investigated, for instance the ceramic support pore size, the membrane thickness, the oxidizing degree, and the combination of all this factors. Complementary, the experimental reproducibility or the robustness of these membranes was also discussed. These membranes can be useful in any process where redox mediators and separation is required. Some examples are the biodegradation of recalcitrant pollutants; in this case activated carbon is being used as electron carrier. GO or rGO exhibits better electro-conductive properties than amorphous carbons, thus their replacement can mean even higher degradation rates. A different application is photocatalytic processes in wastewater treatments. This composite membrane provides an electro-conductive surface and guarantees the retention of non-desirable matter.

1.3 Hypothesis and objectives.

One hypothesis of this thesis is based on the capacity of supported biologically activated carbon films for the removal of azo dyes. If the carbon is deposited in form of a layer covering a ceramic filtration element, this material still must act as redox mediator and overcomes some operational problems related to fouling and biomass retention, thus

enhancing the performance of previous reported technologies. Its preparation and application for the reduction of the azo dyes is discussed (**Chapter 2**). After proving this fact, the membrane structure is modified so as to optimize its performance on these biological processes (**Chapter 3**). Different aspects such as membrane roughness, pore size, or thickness are evaluated.

A different hypothesis is tested in (**Chapter 4**), where it is proven that the anaerobic reduction of the azo dye and the aerobic oxidation of the carbon source can be simultaneous conducted in different chambers, which are connected through a synthesized carbon membrane allowing the flux of electrons and protons. In this way, the external carbon source could be any organic wastewater readily biodegradable and the addition of other compounds is no longer needed in the effluent containing the azo dye.

The last part of this thesis starts from the hypothesis that other carbon materials with superior properties than activated carbon in terms of electro-conductivity, e.g. graphene and derived materials, must perform better in the anaerobic reduction of azo dyes. Thus, **Chapter 5** deals with the synthesis of partially oxidized graphene and its subsequent usage for preparing graphene-based membranes. These new advanced materials present potential to be applied in similar processes as those discussed in this thesis.

References.

[1] A. Spagni, S. Casu, S. Grilli, Decolourisation of textile wastewater in a submerged anaerobic membrane bioreactor, Bioresour. Technol. 117 (2012) 180–185. doi:10.1016/j.biortech.2012.04.074.

[2] G. Mezohegyi, F.P. van der Zee, J. Font, A. Fortuny, A. Fabregat, Towards advanced aqueous dye removal processes: A short review on the versatile role of activated carbon, J. Environ. Manage. 102 (2012) 148–164. http://dx.doi.org/10.1016/j.jenvman.2012.02.021.

[3] Z. Wang, M. Xue, K. Huang, Z. Liu, Textile Dyeing Wastewater Treatment, (2010) 91–116.

[4] Y.-Y. Lau, Y.-S. Wong, T.-T. Teng, N. Morad, M. Rafatullah, S.-A. Ong, Coagulation-flocculation of azo dye Acid Orange 7 with green refined laterite soil, Chem. Eng. J. 246 (2014) 383–390. doi:10.1016/j.cej.2014.02.100.

[5] R.G. Saratale, G.D. Saratale, J.S. Chang, S.P. Govindwar, Bacterial decolorization and degradation of azo dyes: A review, J. Taiwan Inst. Chem. Eng. 42 (2011) 138–157. doi:10.1016/j.jtice.2010.06.006.

[6] A. Guzmán-Vargas, E. Lima, G.A. Uriostegui-Ortega, M.A. Oliver-Tolentino, E.E. Rodríguez, Adsorption and subsequent partial photodegradation of methyl violet 2B on Cu/Al layered double hydroxides, Appl. Surf. Sci. 363 (2016) 372–380. doi:10.1016/j.apsusc.2015.12.050.

[7] R.S. Ribeiro, N.A. Fathy, A.A. Attia, A.M.T. Silva, J.L. Faria, H.T. Gomes, Activated carbon xerogels for the removal of the anionic azo dyes Orange II and Chromotrope 2R by adsorption and catalytic wet peroxide oxidation, Chem. Eng. J. 195–196 (2012) 112–121. doi:10.1016/j.cej.2012.04.065.

[8] L. Fu, S.-J. You, G. Zhang, F.-L. Yang, X. Fang, Degradation of azo dyes using in-situ Fenton reaction incorporated into H2O2-producing microbial fuel cell, Chem. Eng. J. 160 (2010) 164–169. doi:10.1016/j.cej.2010.03.032.

[9] M. Tammaro, A. Salluzzo, R. Perfetto, A. Lancia, A comparative evaluation of biological activated carbon and activated sludge processes for the treatment of tannery wastewater, J. Environ. Chem. Eng. 2 (2014) 1445–1455. doi:10.1016/j.jece.2014.07.004.

[10] G. Mezohegyi, E, U.I. Castro, C. Bengoa, F. Stuber, J. Font, et al., Effective Anaerobic Decolorization of Azo Dye Acid Orange 7 in Continuous Upflow Packed-Bed Reactor Using Biological Activated Carbon System, Ind. Eng. Chem. Res. 46 (2007) 6788–6792. doi:10.1021/ie061692o.

[11] A. Pandey, P. Singh, L. Iyengar, Bacterial decolorization and degradation of azo dyes, Int. Biodeterior. Biodegradation. 59 (2007) 73–84. doi:http://dx.doi.org/10.1016/j.ibiod.2006.08.006.

[12] M.V. Tuttolomondo, G.S. Alvarez, M.F. Desimone, L.E. Diaz, Removal of azo dyes from water by sol–gel immobilized Pseudomonas sp., J. Environ. Chem. Eng. 2 (2014) 131–136. doi:10.1016/j.jece.2013.12.003.

[13] Y. García-Martínez, C. Bengoa, F. Stüber, A. Fortuny, J. Font, A. Fabregat, Biodegradation of acid orange 7 in an anaerobic–aerobic sequential treatment system, Chem. Eng. Process. Process Intensif. 94 (2015) 99–104. doi:http://dx.doi.org/10.1016/j.cep.2014.12.011.

[14] M.F. Coughlin, B.K. Kinkle, P.L. Bishop, High performance degradation of azo dye Acid Orange 7 and sulfanilic acid in a laboratory scale reactor after seeding with cultured bacterial strains., Water Res. 37 (2003) 2757–63. doi:10.1016/S0043-1354(03)00069-1.

[15] H.-Z. Zhao, Y. Sun, L.-N. Xu, J.-R. Ni, Removal of Acid Orange 7 in simulated wastewater using a three-dimensional electrode reactor: removal mechanisms and dye degradation pathway., Chemosphere. 78 (2010) 46–51. doi:10.1016/j.chemosphere.2009.10.034.

[16] S.J. You, R. a. Damodar, S.C. Hou, Degradation of Reactive Black 5 dye using anaerobic/aerobic membrane bioreactor (MBR) and photochemical membrane reactor, J. Hazard. Mater. 177 (2010) 1112–1118. doi:10.1016/j.jhazmat.2010.01.036.

[17] D. Méndez-Paz, F. Omil, J.M. Lema, Anaerobic treatment of azo dye Acid Orange 7 under fed-batch and continuous conditions, Water Res. 39 (2005) 771–778. http://dx.doi.org/10.1016/j.watres.2004.11.022.

[18] M. Solís, A. Solís, H.I. Pérez, N. Manjarrez, M. Flores, Microbial decolouration of azo dyes: A review, Process Biochem. 47 (2012) 1723–1748. doi:10.1016/j.procbio.2012.08.014.

[19] R. Brás, A. Gomes, M.I.A. Ferra, H.M. Pinheiro, I.C. Gonçalves, Monoazo and diazo dye decolourisation studies in a methanogenic UASB reactor, J. Biotechnol. 115 (2005) 57–66. doi:10.1016/j.jbiotec.2004.08.001.

[20] G. Mezohegyi, F. Gonçalves, J.J.M. Órfão, A. Fabregat, A. Fortuny, J. Font, et al., Tailored activated carbons as catalysts in biodecolourisation of textile azo dyes, Appl. Catal. B Environ. 94 (2010) 179–185. doi:10.1016/j.apcatb.2009.11.007.

[21] V. Yousefi, H.-R. Kariminia, Statistical analysis for enzymatic decolorization of acid orange 7 by Coprinus cinereus peroxidase, Int. Biodeterior. Biodegradation.

64 (2010) 245–252. doi:10.1016/j.ibiod.2010.02.003.

[22] F.P. van der Zee, S. Villaverde, Combined anaerobic–aerobic treatment of azo dyes—A short review of bioreactor studies, Water Res. 39 (2005) 1425–1440. doi:10.1016/j.watres.2005.03.007.

[23] S.-A. Ong, E. Toorisaka, M. Hirata, T. Hano, Treatment of azo dye Orange II in aerobic and anaerobic-SBR systems, Process Biochem. 40 (2005) 2907–2914. doi:10.1016/j.procbio.2005.01.009.

[24] F.I. Hai, K. Yamamoto, F. Nakajima, K. Fukushi, Bioaugmented membrane bioreactor (MBR) with a GAC-packed zone for high rate textile wastewater treatment, Water Res. 45 (2011) 2199–2206. doi:10.1016/j.watres.2011.01.013.

[25] G. Mezohegyi, C. Bengoa, F. Stuber, J. Font, A. Fabregat, A. Fortuny, Novel bioreactor design for decolourisation of azo dye effluents, Chem. Eng. J. 143 (2008) 293–298. doi:10.1016/j.cej.2008.05.006.

[26] K. Briceño, A. Iulianelli, D. Montané, R. Garcia-Valls, A. Basile, Carbon molecular sieve membranes supported on non-modified ceramic tubes for hydrogen separation in membrane reactors, ICCE-2011. 37 (2012) 13536–13544. doi:10.1016/j.ijhydene.2012.06.069.

[27] A.K. Geim, K.S.S. Novoselov, The rise of graphene, Nat Mater. 6 (2007) 183–191. doi:10.1038/nmat1849.

[28] K.S. Novoselov, A.K. Geim, S. V Morozov, D. Jiang, Y. Zhang, S. V Dubonos, et al., Electric Field Effect in Atomically Thin Carbon Films, Sci. . 306 (2004) 666–669. doi:10.1126/science.1102896.

[29] Q. Zheng, Z. Li, J. Yang, J. Kim, Graphene oxide-based transparent conductive films, Prog. Mater. Sci. 64 (2014) 200–247. doi:10.1016/j.pmatsci.2014.03.004.

[30] L. Sun, H. Yu, B. Fugetsu, Graphene oxide adsorption enhanced by in situ reduction with sodium hydrosulfite to remove acridine orange from aqueous solution., J. Hazard. Mater. 203–204 (2012) 101–10. doi:10.1016/j.jhazmat.2011.11.097.

[31] K.E. Whitener, P.E. Sheehan, Graphene synthesis, Diam. Relat. Mater. 46 (2014) 25–34. doi:10.1016/j.diamond.2014.04.006.

[32] J. William S. Hummers, R.E. Offeman, Preparation of Graphitic Oxide, J. Am. Chem. Soc. 80 (1958) 1339. doi:10.1021/ja01539a017.

[33] S. Pei, H.-M. Cheng, The reduction of graphene oxide, Carbon N. Y. 50 (2012) 3210–3228. doi:10.1016/j.carbon.2011.11.010.

[34] A. Ganguly, S. Sharma, P. Papakonstantinou, J. Hamilton, Probing the Thermal Deoxygenation of Graphene Oxide using High Resolution In Situ X-Ray based Spectroscopies, J. Phys. Chem. C. 115 (2011) 17009–17019. doi:10.1021/jp203741y.

[35] J. Campos-Delgado, A.R. Botello-Méndez, G. Algara-Siller, B. Hackens, T. Pardoen, U. Kaiser, et al., CVD synthesis of mono- and few-layer graphene using alcohols at low hydrogen concentration and atmospheric pressure, Chem. Phys. Lett. 584 (2013) 142–146. doi:10.1016/j.cplett.2013.08.031.

[36] X. Hu, Y. Yu, J. Zhou, Y. Wang, J. Liang, X. Zhang, et al., The improved oil/water separation performance of graphene oxide modified Al2O3 microfiltration membrane, J. Memb. Sci. 476 (2015) 200–204. doi:10.1016/j.memsci.2014.11.043.

UNIVERSITAT ROVIRA I VIRGILI
COMPACT CARBON-BASED MEMBRANE REACTORS FOR ANAEROBIC BIODEGRADATION OF AZO-DYES FROM WASTEWATER
Alberto Giménez Pérez

CHAPTER 2

Enhanced anaerobic biodegradation of azo dyes using ceramic-supported carbon membranes

Defect-free carbon membranes supported over ceramic disks were prepared by carbonization of Matrimid® 5218, a commercial polymer. The structure and composition of the carbon layer were characterized by microscopy techniques. Subsequently, they were applied to anaerobically process wastewater containing low concentration of Acid Orange 7, as model compound. The degradation was conducted in a biofilm supported over the carbon membrane, where the wastewater was continuously filtrated through. After a period of acclimation and incubation, the azo dye conversion exceeded 80% from the feed dye concentration (50 $mg \cdot L^{-1}$) and a flux of 0.05 $L \cdot m^{-2} \cdot h^{-1}$. Sulfanilic acid, a derived dye reduction metabolite, was also significantly degraded (> 95%) while the chemical oxygen demand was halved. The presence of a carbon layer enhanced the removal rate over four times in comparison to the performance of commercial ceramic membranes. The carbon layer played an essential role as electron mediator favoring the dye reductive treatment and as retention system for biomass and its derivatives, resulting in an intensified one-step treatment for azo dyes removal from wastewater.

Research paper submitted to

Industrial & Engineering Chemistry Research

Enhanced anaerobic biodegradation of azo dyes using ceramic-supported carbon membranes

Alberto Giménez-Perez, Kelly Briceño, Christophe Bengoa, Azael Fabregat, Agustí Fortuny, Frank Stüber

Manuscript ID: *ie-2016-03178z*

2.1 Introduction.

Over 0.7 million tons of synthetic organic dyes are annually produced worldwide. The azo based class constitutes the largest group of synthetic dyes, being approximately an 70% of production (Saratale et al., 2011). These compounds are employed in many industrial sectors such as textile, food, cosmetics and paper, which generate huge amounts of colored wastewater (Brás et al., 2001).

Most azo dyes are recalcitrant to degradation in a typical wastewater treatment plant (WWTP) due to their xenobiotic nature, thus occurring in its effluents (Zhang et al., 2015). The discharge of these hazardous wastes into rivers, oceans, and lakes strongly affects their aquatic ecosystems as, for instance, these compounds reduce significantly the sunlight transmission, what has a severe impact on photosynthetic organisms (dos Santos et al., 2007; Feng et al., 2012; Fernando et al., 2014).

These pollutants can be degraded by physical, chemical or biological methods (Saratale et al., 2011). Advanced oxidation process (AOPs) are commonly applied to degrade dyes; the oxidative dissolution of organic pollutants in wastewater is achieved using hydroxyl radicals (·OH) generated using ozone, ultraviolet (UV) light, a semiconductor photocatalyst, hydrogen peroxide, ultrasound, or a Fenton reagent (Glaze et al., 1987). AOPs present disadvantages such as high running costs for ozone generation and difficulties with operational parameters in the addition of hydrogen peroxide (Suzuki et al., 2015).

Physical methods such as filtration techniques have also been successfully applied in textile industry; however, their main drawbacks are high investment cost and fouling (Zhang et al., 2013). Physicochemical methods based on coagulation-flocculation or adsorption provide low color removal efficiency (Lau et al., 2014). Moreover, these group exhibit a common disadvantage, a concentrated secondary waste stream is created and further treatments are needed (Solanki et al., 2013).

On the contrary, biological treatments –mostly in anaerobic conditions- provide an environmental-friendly alternative avoiding the use of chemicals and derived production of huge amounts of sludge (Brás et al., 2005; dos Santos et al., 2007). The decoloration takes usually place after a period of anaerobic acclimation of a mixed microbial consortium to the bioxenotic compounds (Khehra et al., 2005; Yu et al., 2015). Over this

period, new adapted microbial strains are developed allowing the mineralization of azo dyes into less harmful forms (Stolz, 2001).

Different bioreactor configurations have been tested for azo dye removal over the last decades such as packed-bed (Mielgo et al., 2001), continuous flow stirred-tank (CSTR) (Ong et al., 2005), upflow anaerobic sludge blanket (UASB) (Brás et al., 2005) or membrane bioreactors (MBR) (Spagni et al., 2012).

However, the anaerobic reduction of azo dyes is considered as a relatively slow process (Pandey et al., 2007; Supaka et al., 2004). Bacterial azo reduction is generally classified as a non-specific reduction process that is enhanced by redox mediators, shuttling electrons from bacteria to the azo dyes (Keck et al., 1997). For this reason, the influence of redox mediators has been extensively tested for azo dye reduction and its synergistic effect evidenced, in particular, when biologically activated carbon (BAC) was used (Mezohegyi et al., 2008, 2010).

This study proposes a novel approach through ceramic-supported carbon membranes (CSCM) as biologically active surfaces. To the best of our knowledge, there are not previous studies using carbon membranes to enhance the biodegradation of azo dyes. These CSCMs incorporate a carbon layer deposited onto ZrO_2-TiO_2 support elements. The carbon film plays a triple role. In first place, it behaves as redox mediator for the oxidation of an secondary electron source, e.g. sodium acetate, and the reduction of the azo dye (Mezohegyi et al., 2007). Also, it is a pollutant immobilizer by adsorption into the surface (Mezohegyi et al., 2012). Finally, it acts as physical support for the biofilm (Fig. 2) [22]. Moreover, the membrane performs as a retention system avoiding the use of secondary clarifiers, then allowing complete removal of microorganisms, a significant disinfection capability (Brik et al., 2006; Hai et al., 2011; Konsowa et al., 2011), or the use of highly aged, concentrated sludge (Kapdan and Ozturk, 2005).

2.2 Materials and methods.

2.2.1 Chemicals.

Regarding the carbon membrane synthesis, a commercial polyimide-type polymer, Matrimid® 5218 (3, 3′, 4, 4′-benzophenonetetracarboxylic dianhidride and diamino-

phenylindane, Huntsman Advanced Materials) was used as carbon precursor and 1-methyl-2-pyrrolidone (NMP, 99.5%, Sigma Aldrich) as precursor solvent.

Azo dye Orange II (also named Acid Orange 7, C.I. AO7) sodium salt (dye content 99%, Sigma Aldrich, ref. O8126), an acid dye massively used in textile processes, was selected as model azo colorant. Sulfanilic acid (SA), a dye reduction metabolite, was also obtained from Sigma Aldrich (min. 99%, ref. S5263). Sodium acetate (99%, Aldrich ref. 11019-1) was used as secondary carbon source, which is a readily biodegradable co-substrate allowing the biofilm to grow and providing electrons for the azo reduction. The basal media used to support the microorganism growth contained the following compounds ($mg \cdot l^{-1}$): $MnSO_4 \cdot H_2O$ (0.15), $CuSO_4 \cdot 5H_2O$ (0.28), $ZnSO_4 \cdot 7H_2O$ (0.46), $CoCl_2 \cdot 6H_2O$ (0.26), $(NH_4)_6Mo_7O_{24}$ (0.28), $MgSO_4 \cdot 7H_2O$ (15.20), $CaCl_2$ (13.48), $FeCl_3 \cdot 6H_2O$ (29.06), NH_4Cl (190.90), KH_2PO_4 (8.50), $Na_2HPO_4 \cdot 2H_2O$ (33.40), K_2HPO_4 (21.75). All required chemicals were supplied by Sigma Aldrich.

2.2.2 Preparation of CSCM.

The carbon membranes were synthesized using a protocol adapted from previous works (Briceño et al., 2012a; Cardenas-Robles et al., 2013; Fuertes and Centeno, 1998; Ismail and David, 2001). Commercial ceramic disks, typically dedicated to ultrafiltration, were employed as supports for the membrane preparation. The supports and corresponding holders were purchased from TAMI Industries (Nyons, France) and their properties are listed in Table 2.1. The selected carbon precursor was a commercial polyimide (PI), Matrimid® 5218, which has been widely used for carbon coatings (Rungta et al., 2012) because there is no polyamic acid precursor in the products; moreover, it is fully imidized during its manufacture eliminating the presence of water as by-product, which facilitates the preparation of defect-free coatings (Fuertes et al., 1999). Polymer solutions were prepared by dissolving 10% wt. of PI in NMP with a mechanical stirrer for 3 h. The mixture was prepared under vacuum to remove completely all the air bubbles from the solution.

Table 2.1. Ceramic support properties

Ø (mm)	Area (cm^2)	Thickness (mm)	MWCO (kDa)[a]	Composition
47	13.1	2.5	50 *[b]	$ZrO_2 - TiO_2$

[a] MWCO: Molecular Weight Cut-Off.
[b] Membrane pore size : 40 nm. Estimated from the molecular weight cut-off (MWCO) by Crystal water manufacturer.

A small amount (5 ml) of PI solution was uniformly spread onto the support surface through the spin coating technique (SPIN150i-NPP desktop version, SPS). A two-step spinning program was applied; an initial ramp for 10 s at 500 rpm followed by a final spun at 3000 rpm for 30 s. After the polymer impregnation, the membranes were cured in air atmosphere at 110 °C for 24 h, washed with methanol, and finally heat-treated at 100 °C for 2 h to completely remove the solvent since any trace causes defects on the membrane surface. Finally, the carbonization of the polymer film was carried out in a horizontal tubular furnace (Kosmon S.A.) under constant nitrogen gas flow (0.9 $l \cdot min^{-1}$) at 700 ºC and atmospheric pressure. Below 200 ºC, the heating ramp rate was set at 4 $ºC \cdot min^{-1}$ and over 200 ºC it was decreased to 1 $ºC \cdot min^{-1}$ to prevent cracking. Next, a complete membrane characterization focused on the surface, thickness and composition was carried out to assess its suitability for the proposed application.

2.2.3 Lab-scale CSCM bioreactor.

Fig. 1 schematically depicts the anaerobic system. The CSCM reactor consisted of a filtration cell (Tami industries) holding the 47 mm diameter CSCM with a retentate chamber of 5 mL. The synthetic wastewater was comprised of sodium acetate (150 $mg \cdot l^{-1}$), AO7 mono-azo dye (50 $mg \cdot l^{-1}$), and the basal media with microelements described previously, all dissolved in deionized water. The 200 mL feed storage tank was maintained at 1±1 ºC into a fridge to prevent the growth of microorganisms, thus avoiding the sodium acetate consumption outside the bioreactor. Low redox potentials are necessary to assure anaerobic conditions and obtain high color removal rates (Lourenço et al., 2001). The redox potential throughout the system was always kept below -400 mV (referred to a combined Pt//Ag/AgCl redox electrode) by bubbling nitrogen gas. Once the anaerobic conditions were established, a small sample (0.1 ml) of anaerobic sludge was inoculated onto the membrane surface. This inoculum was

obtained by partial digestion of aerobic activated sludge (5 L) under anaerobic conditions for a week; the aerobic activated sludge was collected from a municipal WWTP located in Reus (Spain). Subsequently, the wastewater was continuously fed to the anaerobic CMSM bioreactor (Fig. 1), which was operated in dead-end filtration mode at 37±1 ºC to promote the occurrence of microbial strains capable of completely mineralizing the azo dye (Khehra et al., 2005). The bioreactor flux was held up constant at 0.05 $L \cdot m^{-2} \cdot h^{-1}$ and the permeate volume was automatically monitored by means of an analytical balance (A&D GF1200). Nitrogen gas served to pressurize the system and control the flux through the membrane by manually setting the transmembrane pressure (TMP). Over the experiments, membrane fouling led to a slight progressive transmembrane pressure increase (0.1 bar) to keep constant flux. The pH was not controlled by adding external substances; its value was monitored varying from 6.5 to 7.1 in the reactor outlet. It was measured by a Crison lab pH-meter with a Slimtrode pH electrode (Hamilton, ref. 238150).

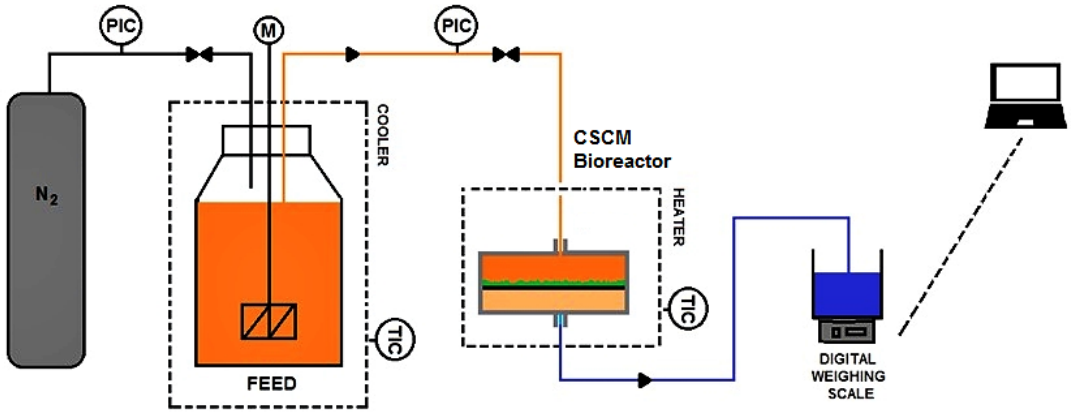

Figure 2.1 AO7 dye removal plant.

At the end of the operation, the membrane was cleaned applying backward flushing with deionized water for 2 minutes at 4 bar. Finally, the carbon layer was re-examined by microscopy techniques to discard any structural damage owing to the use.

2.2.4 Analytical methods.

AO7, SA and sodium acetate were measured by HPLC (Agilent 1220 Infinity), on a C18 Hypersil ODS column (2.1 x 50 mm, particle size of 5 µm) with a flow rate of 1 $ml \cdot min^{-1}$ under a gradient of methanol (M) / water (W) mobile phase using the following program: 0-5 min, 0/100 M/W; 5-10 min, 25/75 M/W; 10-12 min, 50/50

M/W; 12–15 min, 0/100 M/W. The UV detection wavelengths were 487, 252, and 210 nm for AO7, SA and sodium acetate, respectively. Note that effluent samples of 1 ml were pre-filtered through a 0.22 µm PVDF filter (Whatman®) at room temperature before performing the analysis. The detection of 1-amino-2 naphtol was performed by HPLC-MS (Agilent 6410A) following the same HPLC analytical programme previously described.

The composite membranes were examined by means of an environmental scanning electron microscopy, ESEM, (FEI Quanta 600), coupled with an Oxford Inca Energy Dispersive X-ray (EDX) system for chemical composition analysis. Membrane surfaces were also characterized by atomic force microscopy (AFM Pico Plus 2500 from Molecular Imaging, Bid-Service, LLC, Freehold, NJ, USA). The images were recorded in tapping mode with a resonance frequency of 1 Hz in air at room temperature and then processed by WSxM 5.0 software (Horcas et al., 2007). Silicon nitride cantilevers (NP-S, Brucker) with a nominal spring constant of 0.12 $N \cdot m^{-1}$ and a resonant frequency of 23 kHz were used.

Chemical oxygen demand (COD) was determined by dichromate method according to the standard method 5220D (APHA, 17th Edition, 1989).

2.3 Results and discussion.

2.3.1 Membrane characterization.

2.3.1.1 Microscopy characterization.

The membrane and support structures were investigated by ESEM technique. Figure 2a shows the ceramic support cross-sectional view where the upper layer (ZrO_2) is clearly visible. On the top of this layer takes place the carbon precursor deposition. After its carbonization, the carbon coated film formation is evident and its thickness was found around 12 µm (Fig. 2b). However, some deeper infiltrations of carbon material could appear, which are probably attributed to the formation of gases and subsequently precipitation throughout the carbonization process. In any case, the ceramic supports were efficiently coated by homogeneous carbon layers as the comparison of Figures 2c-d evidences. No defects were identified in terms of appreciable areas without coatings. Also, a decrease of the support pore size is expected given the different texture and

grain size observed. A rough study of the pore size distribution based on AFM imaging was performed by SPIP^{TM} software. More than 80% of the total pores were found in the range 1-20 nm, so the synthesis process reduced the support pore size (40 nm) more than 50%. Hence, the carbon membrane can be nearly classified into the nanoporous membrane family.

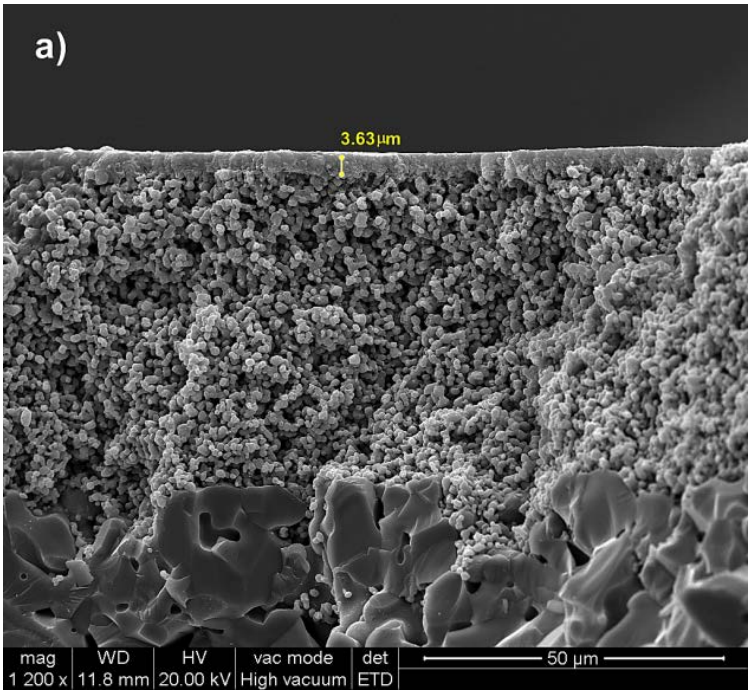

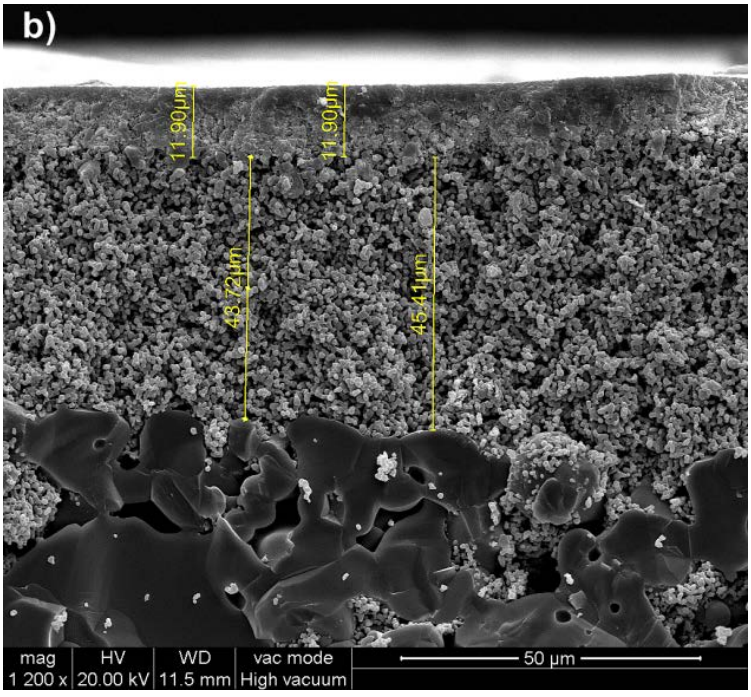

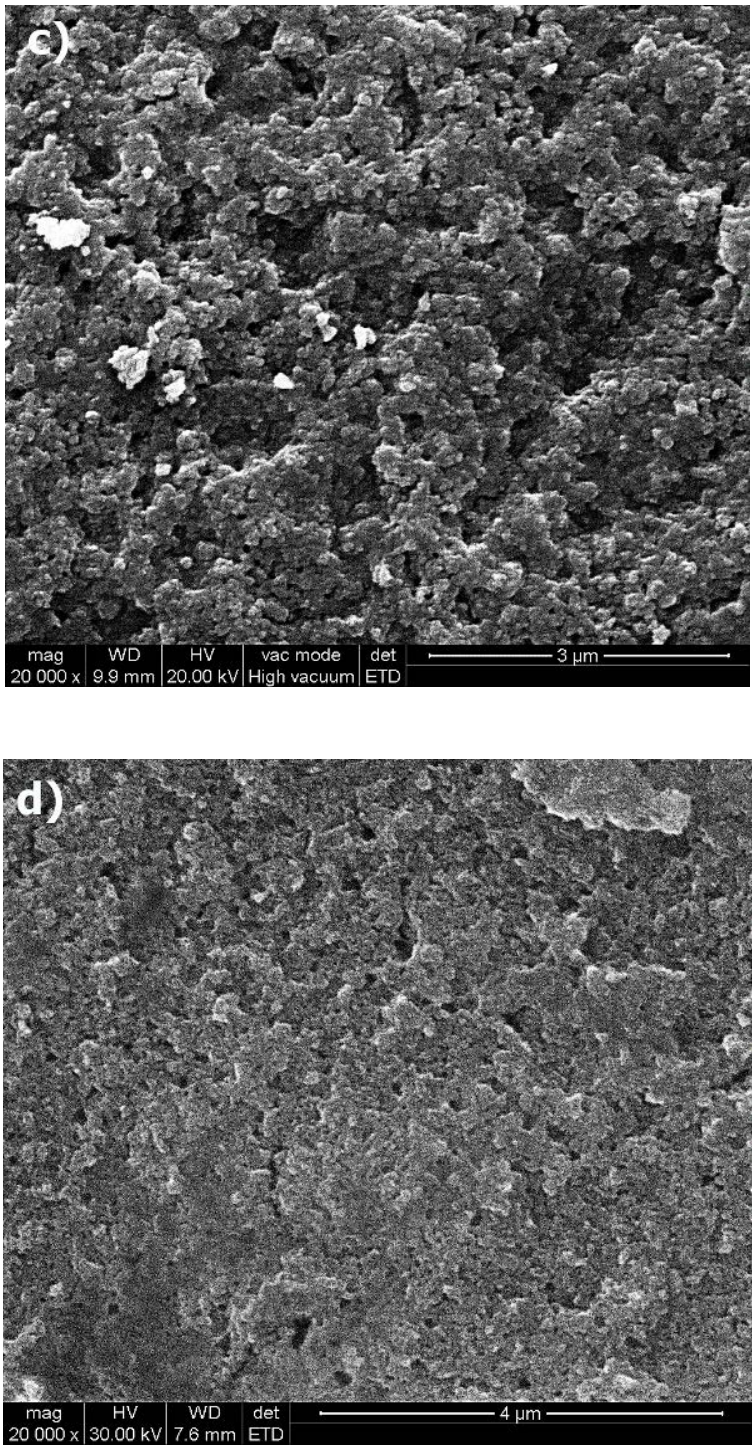

Figure 2.2 ESEM membrane characterization. Cross-sectional view of the ceramic support (a) and CSCM (b), and front view of the ceramic support (c) and CSCM (d).

ESEM–EDX inspection of the structure was conducted to measure the elemental chemical composition at two different depths (Table 2.2). The analysis suggests a typical composite membrane, where the denser superficial film, rich in carbon, demonstrates the formation of a mixed layer, which is due to the precursor penetration

into the zirconia (ZrO_2) upper layers of the ceramic support. Instead, at the deepest position, the original thicker microporous substrate, essentially made of titanium and oxygen, prevails.

Table 2.2 ESEM-EDX analysis; composition (wt. %) of the carbon membrane and ceramic support.

	C	**O**	**Ti**	**Zr**
Carbon membrane	25.4	28.5	0.5	45.6
Ceramic support	0.0	44.0	52.2	3.8

ESEM analysis technique was also conducted to detect membrane structural defects on the synthesized carbon layers (Fig. A.1 in the supplementary material). Two different types of defects were occasionally observed: single holes with variable size (Fig. A.1a) or longitudinal cracks (Fig. A.1b). Membrane defects must be completely avoided since small superficial defects increase significantly the liquid permeation and make the membrane useless in a given application. The proper selection of the spin coating rotation rate has found to be decisive. The use of speeds below 500 rpm gave imperfect, thicker and non-homogeneous membranes. On the contrary, spinning speeds over 3000 rpm promoted an excellent dispersion of the polymer solution. On the other hand, the carbonization stage was also critical to prevent the formation of imperfections; the pyrolysis atmosphere must be maintained strictly under vacuum or inert conditions in order to prevent undesired burn off and chemical damage of the membrane precursor (Ismail and David, 2001). At the finally selected synthesis conditions, the CSCM obtained were free of coverage defects.

AFM technique was also randomly applied to different membrane areas (10x10 μm) including a root mean square (RMS) roughness analysis. Fig. 3 displays an example. Considering average values, the roughness decreased from 110.2 to 57.8 nm after coating the carbon film. Thus, despite this decrease, the CSCM can be considered as rough, which may affect positively to the studied application due to the greater available surface area, so the bacteria are more robustly attached to the surface (Shimp and Pfaender, 1982).

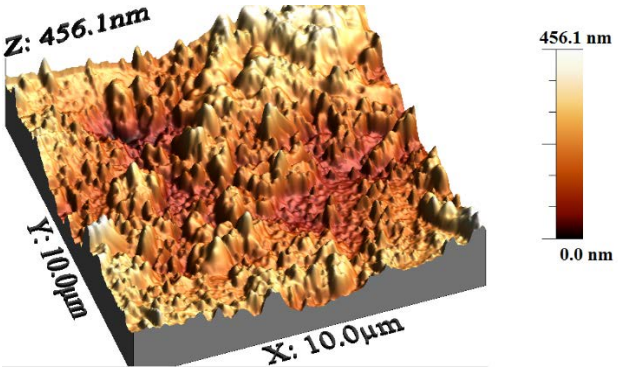

Figure 2.3 AFM image. CSCM height profile.

2.3.1.2 Permeability tests.

Before modification, the permeability of the commercial supports was determined at several hydraulic pressure differences (ΔP). The operating pressures were chosen in concordance with the studied application where the flux defines the biomass contact time and, thus, the removal reached. Once the carbon membrane synthesis was completed, these tests were repeated in order to evaluate the influence of the additional carbon layer on the permeability. As can be observed in Figure 4, the water flux decreases around 30-40% in comparison to the ceramic support permeability.

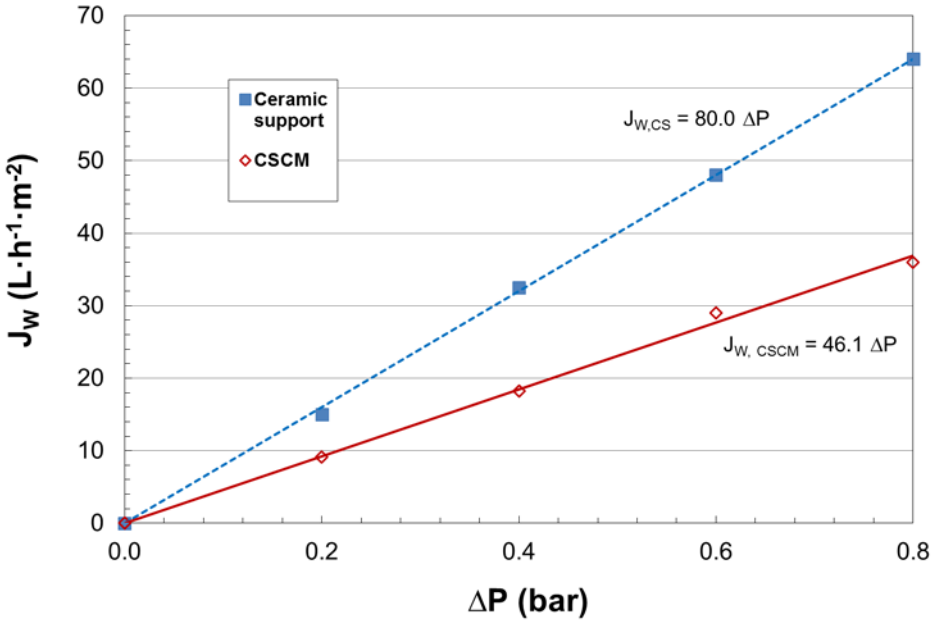

Figure 2.4 CSCM ($J_{W, CSCM}$) and ceramic support ($J_{W, CS}$) permeability at 25 ºC.

The overall hydraulic membrane resistance R_m (m^{-1}) was calculated using the following equation:

$$R_m = \sum R_i = \sum R_s + R_c = \frac{\Delta P}{\eta \cdot J_w} \quad \textbf{(1)}$$

where, R_s is the ceramic support resistance (m^{-1}), R_c is the carbon layer resistance (m^{-1}), ΔP is the hydraulic pressure difference (Pa), J_w is the pure water flux ($m^3 \cdot m^{-2} \cdot s^{-1}$), and η is the water viscosity ($kg \cdot m^{-1} \cdot s^{-1}$). As the resistance of the support, R_s, can be obtained from its original pure water flux, the additional resistance provided by the carbon layer, R_c, can be inferred (Table 2.3).

Table 2.3 Membrane flux resistances.

$\mathbf{R_m \cdot 10^{-12}}$ **(m^{-1})**	$\mathbf{R_s \cdot 10^{-12}}$ **(m^{-1})**	$\mathbf{R_c \cdot 10^{-12}}$ **(m^{-1})**
7.71±0.21	4.54±0.14	3.25±0.23

As shown in Table 2.3, the thin carbon layer contributes to the total CSCM resistance with an additional term in the same order of magnitude than that originally given by the ceramic support, which indicates the presence of a highly dense carbonaceous layer.

2.3.2 Anaerobic biodegradation of AO7.

2.3.2.1 Performance of CSCM bioreactor.

The studies were initially focused on the azo-dye physical adsorption over the carbon membrane in order to discern its potential contribution to the dye removal. AO7 solutions were filtrated under identical flux (0.05 $L \cdot m^{-2} \cdot h^{-1}$) as well as the rest of operation conditions previously described for the biological tests, but in the absence of microorganisms. After 12 hours of operation, permeate and feed solution showed the same concentration, which means that the carbon layer has become equilibrated at the feed dye concentration, so adsorption does not exist anymore. This also discards any other via of dye disappearance. The amount of AO7 removed was estimated to be 0.003 mg/cm^2.

Therefore, in the biodegradation experiments, it is expected that the adsorption could contribute to the dye removal just during the first 12 h as maximum. Hereon, the dye elimination must be exclusively ascribed to the biodegradation because of the biofilm presence. Taking into account that each biodegradation test was extended for weeks, it is conclusively proved that physical adsorption is no relevant for the correct interpretation of the results.

The biodegradation test starts with the inoculation of a mixed microbial consortium. The biomass requires a minimum of 5-10 days of acclimation and incubation as can be inferred from Fig. 5. This value is in agreement with previous studies in different systems (Ong et al., 2005). Once that period concludes, the adapted microorganisms offer high removal rates.

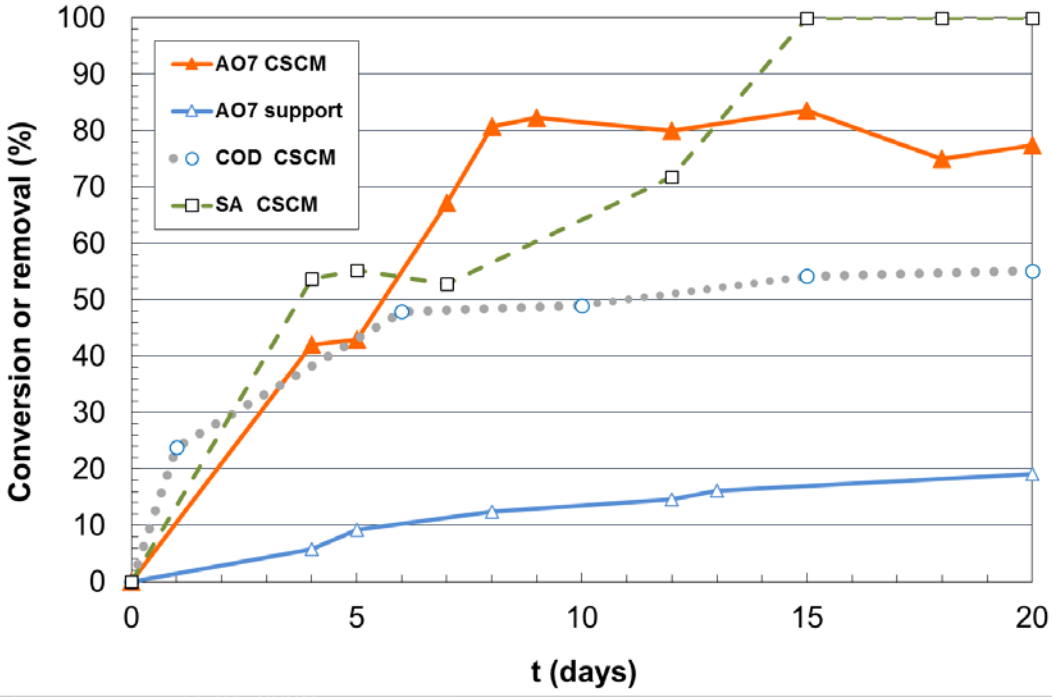

Figure 2.5 AO7 anaerobic biodegradation in CSCM reactors and non-modified ceramic supports from the start-up until the achievement of steady state. [Feed AO7 concentration: 50 $mg \cdot l^{-1}$; flux: 0.05 $l \cdot m^{-2} \cdot h^{-1}$; temperature: 37 ºC].

AO7 steady-state levels were attained after 12 days approximately. At a flux rate of 0.05 $l \cdot m^{-2} \cdot h^{-1}$, conversion values above 80% are achieved. It must be pointed out that the biodegradation by means of non-modified ceramic support, i.e. without the carbon layer, drives to steady values below 20% of AO7 conversion. This fact clearly

demonstrates that the deposited carbon layer plays a critical role on the overall biodegradation process.

A scaled equipment of the studied system would be based on a typical plate and frame configuration, which usually shows an area to volume ratio around 500 $m^2 \cdot m^{-3}$ (Nunes and Peinemann, 2006). Therefore, the proposed system would supposedly be able to treat about 38 $g \cdot m^{-3} \cdot day^{-1}$ of AO7. This estimated dye loading rate is in concordance with most novel techniques dealing with this kind of compounds previously described in the literature, such as PBRs or sequential anaerobic-aerobic systems, i.e. 25-75 $g \cdot m^{-3} \cdot day^{-1}$ load rates and 80-100% removal efficiencies (Saratale et al., 2011).

It must be noted that in our system, the removal of SA was also relevant reaching almost complete elimination, while other alternatives (van der Zee and Villaverde, 2005) need a secondary stage (typically aerobic) for the subsequent mineralization of this dye biodegradation product. It is expected that a highly-aged microbial consortium, instead of a fresh pure culture, achieves a higher degree of biodegradation and mineralization due to the synergistic metabolic activities of the microbial community (Saratale et al., 2011). Moreover, the biofilm is supported over a membrane with narrower pores, in comparison to conventional ones, so the degradation products could be better retained and metabolized. These could be among other reasons the cause of the high removal rates obtained, thus giving an efficient, compact single step treatment.

In turn, 1-amino-2-naphthol (1A2N), the other AO7 cleavage metabolite, was not detected by HPLC-MS analysis. However, aminophenols are known to undergo rapid autoxidation reactions upon exposure to oxygen (Brás et al., 2005), so despite the samples were immediately analyzed it could have disappeared because they were not meanwhile maintained under anoxic conditions.

HPLC analyses showed that that the external carbon source, i.e. acetate, which is readily degradable was completely digested since it was not detected in the exiting effluent. In addition, biomass or its derivates were not observed in the permeate, proving that the almost nanoporous membrane guarantees their retention. Therefore, the COD in the treated effluent can be exclusively assigned to the azo dye and its small size degradation metabolites. As evidenced in Fig. 5, at steady-state conditions, the single anaerobic step halves the inlet COD of the azo dye, which was calculated to be 73 $mg \cdot L^{-1}$.

Overall, this novel approach offered higher azo dye mineralization than those reported in previous studies focused on packed-bed reactors (PBRs) (Mezohegyi et al., 2008). Furthermore, non-serious biofouling problems were detected even though the system was running for three weeks. This fact can be explained by the difference on size between the biomass and the membrane pores. This membrane presents pores much smaller than microorganisms, so they cannot enter the pores to constrict them, thus the biofouling is limited to the external side of the membrane. After the biological tests, the membrane was cleaned by back-flushing, and the original permeate flux was recovered. Further characterization of the used CSCM discarded structural changes due to the operation.

This ease of operation is an important advantage regarding to other systems that combine carbon and anaerobic microorganism to mineralize azo dyes, such as PBRs. A potential overproduction of biomass can be controlled by quick and efficient cleaning methods. Moreover, an additional advantage is that membrane reactors guarantee the retention of all the biomass into the bioreactor.

2.3.2.2 Experimental reproducibility.

Two different membranes were synthesized following exactly the same experimental procedure, above described, and subsequently evaluated for the biodegradation of AO7 (Fig. 6). Both bioreactors (referred to as B-CSCM1 and B-CSCM2) were operated under the same conditions; starting with the same protocol but different inoculum batch. Note that these experiments were not performed simultaneously and the non-selected sludge batch used was collected in different moments from the same tank of a conventional WWTP. The experiments roughly reproduced the start-up evolution but, what it is more important, both attained almost identical AO7 conversion, i.e. 80%, at steady operation, which proves the robustness of the preparation protocol and corresponding performance of the biodegradation process. The different activity showed throughout the microbial acclimation period can be attributed to the use of mixed microbial cultures (Saratale et al., 2011) as well as small variations in the operation.

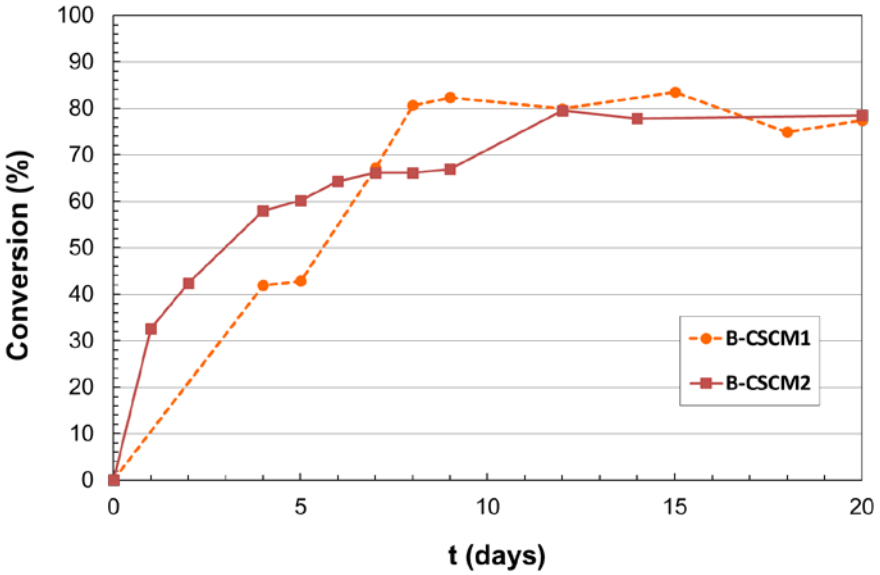

Figure 2.6 Reproducibility of the bioreactor experiments.
[Feed AO7 concentration: 50 mg·l^{-1}; flux: 0.05 l·m^{-2}·h^{-1}; temperature: 37 ºC].

2.3.2.3 Effect of the contact time.

The influence of the contact time on the removal of AO7 was also checked. As the biodegradation takes place over the biofilm, this is a surface process where the reaction time is directly related to the flux as it determines the time that the dye is exposed to the action of the microorganisms. Therefore, the operation flux was used to contrast the contact time influence. Three independent experiments were conducted at different fluxes (0.05, 0.11 and 0.15 L·m^{-2}·h^{-1}) but constant feed dye concentration until the steady-state was reached. As expected (García-Martínez et al., 2015), Fig. 7 evidences that the AO7 conversion decreases at shorter contact times; thus the reported value around 80% conversion, i.e. 82%, is achieved at 0.05 L·m^{-2}·h^{-1}, but decreased up to 53% at 0.11 L·m^{-2}·h^{-1}, and still reaches a 41% at 0.15 L·m^{-2}·h^{-1}. The reactor performance was modeled using a simple plug-flow configuration accepting that the reaction only occurs while the effluent crosses the biofilm. However, the residence time was substituted by the inverse of the flux, assuming that the biofilm thickness is identical irrespective of the applied flux. Under such conditions, it was found that the biodegradation proceeds following very closely a first reaction order with respect to the inverse of the flux (Appendix A in the supplementary material). Many researchers postulate that this kind of biodegradation follows Michaelis-Menten kinetics given its biological base (Ding et al., 2010; Mezohegyi et al., 2008, 2007; van der Zee et al.,

2000; Wuhrmann et al., 1980). It is well-known that Michaelis-Menten approaches to a first order reaction in excess of biomass, therefore the results suggest that there is still an excess of biofilm available for additional dye biodegradation.

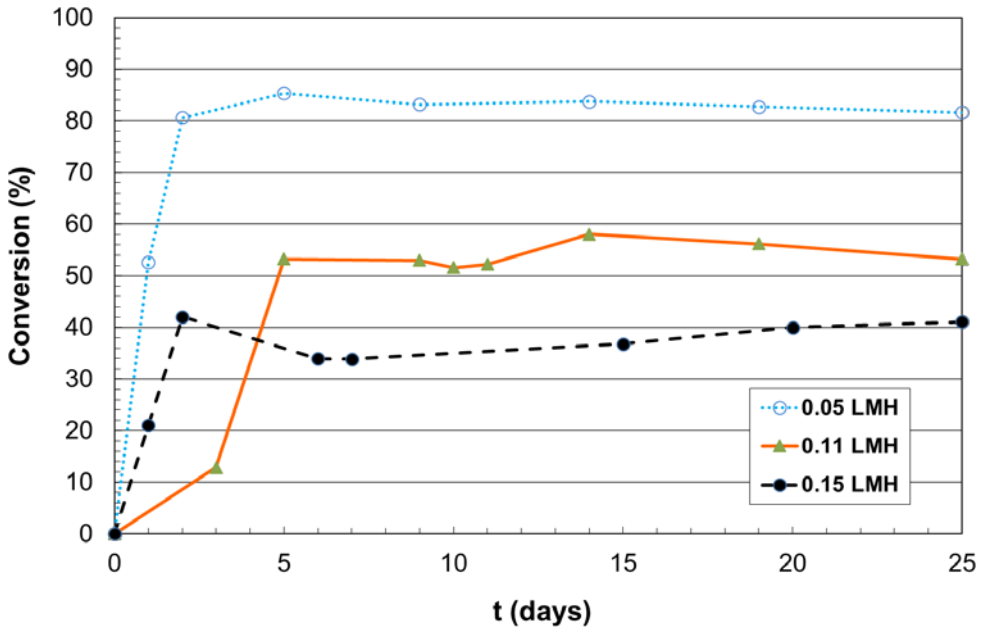

Figure 2.7 Influence of the flux on the steady AO7 conversion.
[LMH: $L \cdot m^{-2} \cdot h^{-1}$; feed AO7 concentration: 50 $mg \cdot l^{-1}$; temperature: 37 ºC].

2.4 Conclusions.

Robust and defect-free ceramic-supported carbon membranes (C-ZrO_2-TiO_2) were successfully prepared. The coating of the ceramic support was found to be the most crucial step in the membrane preparation. The spin coating technique provided defect-free films at high spinning rates (3000 rpm). Both the membrane synthesis and its posterior application were proven to be reproducible.

CSCM bioreactors exhibited an excellent degradation activity intensifying the azo dye removal process. AO7 conversions increased more than four times in presence of the carbon layer. CSCM bioreactors showed mostly complete SA degradation under strictly anaerobic conditions. This outstanding performance could be explained because of the proposed alternative dealt with an efficient biologically carbon layer assembled in form of a nearly nanoporous structure as well as the use of highly-aged mixed microbial consortium, making easier the mineralization of this specific biorefractory compound. Additional advantages are the absence of microorganisms in the exiting effluent

(permeate) and the low system clogging, as the system did not actually show significant fouling-related problems for weeks.

It has been demonstrated that this novel approach improves existing azo dye degradation methods assuring higher mineralization in a very compact system. Futures studies should be focused on modifying the carbon layer surface to increase its electron transfer ability, which is critical in this kind of redox-based biodegradation processes.

References

Brás, R., Gomes, A., Ferra, M.I.A., Pinheiro, H.M., Gonçalves, I.C., 2005. Monoazo and diazo dye decolourisation studies in a methanogenic UASB reactor. J. Biotechnol. 115, 57–66. doi:10.1016/j.jbiotec.2004.08.001

Brás, R., Isabel A. Ferra, M., Pinheiro, H.M., Gonçalves, I.C., 2001. Batch tests for assessing decolourisation of azo dyes by methanogenic and mixed cultures. J. Biotechnol. 89, 155–162. doi:10.1016/S0168-1656(01)00312-1

Briceño, K., Iulianelli, A., Montané, D., Garcia-Valls, R., Basile, A., 2012a. Carbon molecular sieve membranes supported on non-modified ceramic tubes for hydrogen separation in membrane reactors. ICCE-2011 37, 13536–13544. doi:10.1016/j.ijhydene.2012.06.069

Briceño, K., Montané, D., Garcia-Valls, R., Iulianelli, A., Basile, A., 2012b. Fabrication variables affecting the structure and properties of supported carbon molecular sieve membranes for hydrogen separation. J. Memb. Sci. 415–416, 288–297. doi:10.1016/j.memsci.2012.05.015

Cardenas-Robles, A., Martinez, E., Rendon-Alcantar, I., Frontana, C., Gonzalez-Gutierrez, L., 2013. Development of an activated carbon-packed microbial bioelectrochemical system for azo dye degradation. Bioresour. Technol. 127, 37–43. doi:10.1016/j.biortech.2012.09.066

Ding, H., Li, Y., Lu, A., Jin, S., Quan, C., Wang, C., Wang, X., Zeng, C., Yan, Y., 2010. Photocatalytically improved azo dye reduction in a microbial fuel cell with rutile-cathode. Bioresour. Technol. 101, 3500–5. doi:10.1016/j.biortech.2009.11.107

dos Santos, A.B., Cervantes, F.J., van Lier, J.B., 2007. Review paper on current technologies for decolourisation of textile wastewaters: Perspectives for anaerobic biotechnology. Bioresour. Technol. 98, 2369–2385. doi:http://dx.doi.org/10.1016/j.biortech.2006.11.013

Feng, J., Cerniglia, C.E., Chen, H., 2012. Toxicological significance of azo dye metabolism by human intestinal microbiota. Front. Biosci. (Elite Ed). 4, 568–86.

Fernando, E., Keshavarz, T., Kyazze, G., 2014. Complete degradation of the azo dye Acid Orange-7 and bioelectricity generation in an integrated microbial fuel cell, aerobic two-stage bioreactor system in continuous flow mode at ambient temperature. Bioresour. Technol. 156, 155–162. doi:10.1016/j.biortech.2014.01.036

Fuertes, A.B., Centeno, T.A., 1998. Carbon molecular sieve membranes from polyetherimide. Microporous Mesoporous Mater. 26, 23–26. doi:10.1016/S1387-1811(98)00204-2

Fuertes, A.B., Nevskaia, D.M., Centeno, T.A., 1999. Carbon composite membranes from Matrimid® and Kapton® polyimides for gas separation. Microporous Mesoporous Mater. 33, 115–125.

García-Martínez, Y., Bengoa, C., Stüber, F., Fortuny, A., Font, J., Fabregat, A., 2015. Biodegradation of acid orange 7 in an anaerobic–aerobic sequential treatment system. Chem. Eng. Process. Process Intensif. 94, 99–104. doi:http://dx.doi.org/10.1016/j.cep.2014.12.011

Glaze, W.H., Kang, J.-W., Chapin, D.H., 1987. The Chemistry of Water Treatment Processes Involving Ozone, Hydrogen Peroxide and Ultraviolet Radiation. Ozone Sci. Eng. 9, 335–352. doi:10.1080/01919518708552148

Horcas, I., Fernández, R., Gómez-Rodríguez, J.M., Colchero, J., Gómez-Herrero, J., Baro, A., 2007. WSXM: A software for scanning probe microscopy and a tool for nanotechnology. Rev. Sci. Instrum. 78, 013705. doi:10.1063/1.2432410

Ismail, A.F., David, L.I.B., 2001. A review on the latest development of carbon membranes for gas separation. J. Memb. Sci. 193, 1–18. doi:10.1016/S0376-7388(01)00510-5

Keck, A., Klein, J., Kudlich, M., Stolz, A., Knackmuss, H.J., Mattes, R., 1997.

Reduction of azo dyes by redox mediators originating in the naphthalenesulfonic acid degradation pathway of Sphingomonas sp. strain BN6. Appl. Environ. Microbiol. 63, 3684–3690.

Khehra, M., Saini, H., Sharma, D., Chadha, B., Chimni, S., 2005. Decolorization of various azo dyes by bacterial consortium. Dye. Pigment. 67, 55–61. doi:10.1016/j.dyepig.2004.10.008

Lau, Y.-Y., Wong, Y.-S., Teng, T.-T., Morad, N., Rafatullah, M., Ong, S.-A., 2014. Coagulation-flocculation of azo dye Acid Orange 7 with green refined laterite soil. Chem. Eng. J. 246, 383–390. doi:10.1016/j.cej.2014.02.100

Lourenço, N.D., Novais, J.M., Pinheiro, H.M., 2001. Effect of some operational parameters on textile dye biodegradation in a sequential batch reactor. J. Biotechnol. 89, 163–174. doi:http://dx.doi.org/10.1016/S0168-1656(01)00313-3

Mezohegyi, G., Bengoa, C., Stuber, F., Font, J., Fabregat, A., Fortuny, A., 2008. Novel bioreactor design for decolourisation of azo dye effluents. Chem. Eng. J. 143, 293–298.

Mezohegyi, G., Gonçalves, F., Órfão, J.J.M., Fabregat, A., Fortuny, A., Font, J., Bengoa, C., Stuber, F., 2010. Tailored activated carbons as catalysts in biodecolourisation of textile azo dyes. Appl. Catal. B Environ. 94, 179–185. doi:10.1016/j.apcatb.2009.11.007

Mezohegyi, G., Kolodkin, A., Castro, U.I., Bengoa, C., Stuber, F., Font, J., Fabregat, A., Fortuny, A., 2007. Effective Anaerobic Decolorization of Azo Dye Acid Orange 7 in Continuous Upflow Packed-Bed Reactor Using Biological Activated Carbon System. Ind. Eng. Chem. Res. 46, 6788–6792. doi:10.1021/ie061692o

Mezohegyi, G., van der Zee, F.P., Font, J., Fortuny, A., Fabregat, A., 2012. Towards advanced aqueous dye removal processes: A short review on the versatile role of activated carbon. J. Environ. Manage. 102, 148–164.

Mielgo, I., Moreira, M., Feijoo, G., Lema, J., 2001. A packed-bed fungal bioreactor for the continuous decolourisation of azo-dyes (Orange II). J. Biotechnol. 89, 99–106. doi:10.1016/S0168-1656(01)00319-4

Nunes, S.P., Peinemann, K.V., 2006. Membrane Technology, second ed. ed, Membrane Technology: in the Chemical Industry. Wiley-VCH, Weinheim.

doi:10.1002/3527608788

Ong, S.-A., Toorisaka, E., Hirata, M., Hano, T., 2005. Treatment of azo dye Orange II in aerobic and anaerobic-SBR systems. Process Biochem. 40, 2907–2914. doi:10.1016/j.procbio.2005.01.009

Pandey, A., Singh, P., Iyengar, L., 2007. Bacterial decolorization and degradation of azo dyes. Int. Biodeterior. Biodegradation 59, 73–84. doi:http://dx.doi.org/10.1016/j.ibiod.2006.08.006

Rungta, M., Xu, L., Koros, W.J., 2012. Carbon molecular sieve dense film membranes derived from Matrimid® for ethylene/ethane separation. Carbon N. Y. 50, 1488–1502.

Saratale, R.G., Saratale, G.D., Chang, J.S., Govindwar, S.P., 2011. Bacterial decolorization and degradation of azo dyes: A review. J. Taiwan Inst. Chem. Eng. 42, 138–157. doi:http://dx.doi.org/10.1016/j.jtice.2010.06.006

Shimp, R.J., Pfaender, F.K., 1982. Effects of Surface Area and Flow Rate on Marine Bacterial Growth in Activated Carbon Columns. Appl. Environ. Microbiol. 44, 471–477. doi:0099-2240/85/

Solanki, K., Subramanian, S., Basu, S., 2013. Microbial fuel cells for azo dye treatment with electricity generation: a review. Bioresour. Technol. 131, 564–71. doi:10.1016/j.biortech.2012.12.063

Spagni, A., Casu, S., Grilli, S., 2012. Decolourisation of textile wastewater in a submerged anaerobic membrane bioreactor. Bioresour. Technol. 117, 180–185. doi:http://dx.doi.org/10.1016/j.biortech.2012.04.074

Stolz, A., 2001. Basic and applied aspects in the microbial degradation of azo dyes. Appl. Microbiol. Biotechnol. 56, 69–80. doi:10.1007/s002530100686

Supaka, N., Juntongjin, K., Damronglerd, S., Delia, M., Strehaiano, P., 2004. Microbial decolorization of reactive azo dyes in a sequential anaerobic–aerobic system. Chem. Eng. J. 99, 169–176. doi:10.1016/j.cej.2003.09.010

Suzuki, H., Araki, S., Yamamoto, H., 2015. Evaluation of advanced oxidation processes (AOP) using O3, UV, and TiO2 for the degradation of phenol in water. J. Water Process Eng. 7, 54–60. doi:10.1016/j.jwpe.2015.04.011

van der Zee, F.P., Lettinga, G., Field, J.A., 2000. The role of (auto)catalysis in the mechanism of an anaerobic azo reduction. Water Sci. Technol. 42, 301–308.

van der Zee, F.P., Villaverde, S., 2005. Combined anaerobic–aerobic treatment of azo dyes—A short review of bioreactor studies. Water Res. 39, 1425–1440. doi:http://dx.doi.org/10.1016/j.watres.2005.03.007

Wuhrmann, K., Mechsner, K., Kappeler, T., 1980. Investigation on rate --- Determining factors in the microbial reduction of azo dyes. Eur. J. Appl. Microbiol. Biotechnol. 9, 325–338. doi:10.1007/BF00508109

Yu, L., Zhang, X.-Y., Wang, S., Tang, Q.-W., Xie, T., Lei, N.-Y., Chen, Y.-L., Qiao, W.-C., Li, W.-W., Lam, M.H.-W., 2015. Microbial community structure associated with treatment of azo dye in a start-up anaerobic sequenced batch reactor. J. Taiwan Inst. Chem. Eng. 54, 118–124. doi:10.1016/j.jtice.2015.03.012

Zhang, B., Wang, Z., Zhou, X., Shi, C., Guo, H., Feng, C., 2015. Electrochemical decolorization of methyl orange powered by bioelectricity from single-chamber microbial fuel cells. Bioresour. Technol. 181, 360–2. doi:10.1016/j.biortech.2015.01.076

Zhang, J., Wang, L., Zhang, G., Wang, Z., Xu, L., Fan, Z., 2013. Influence of azo dye-TiO2 interactions on the filtration performance in a hybrid photocatalysis/ultrafiltration process. J. Colloid Interface Sci. 389, 273–83. doi:10.1016/j.jcis.2012.08.062

Supplementary material

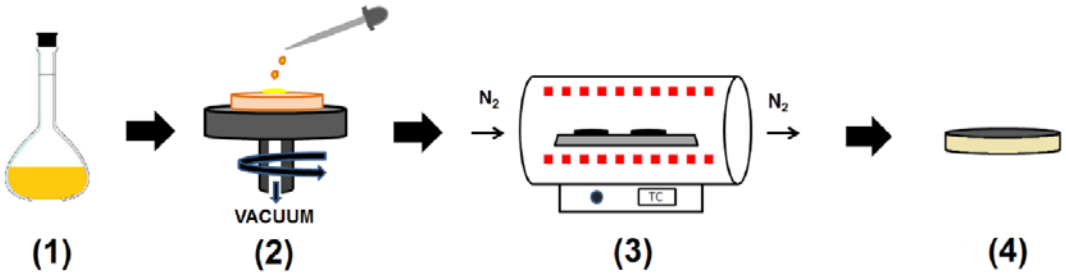

Figure A2.1 Synthesis procedure for the preparation of CSCM.

Microscopy characterization.

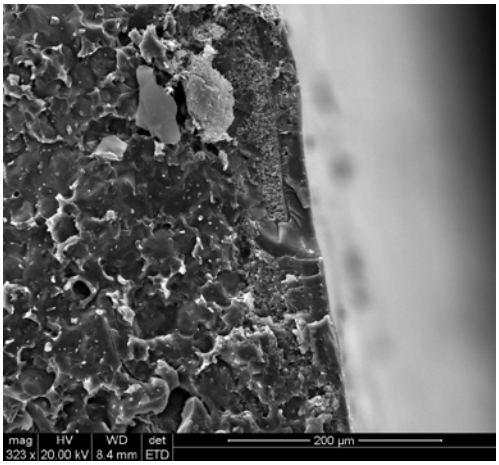

Figure A2.2 Carbon infiltrations in the ceramic support

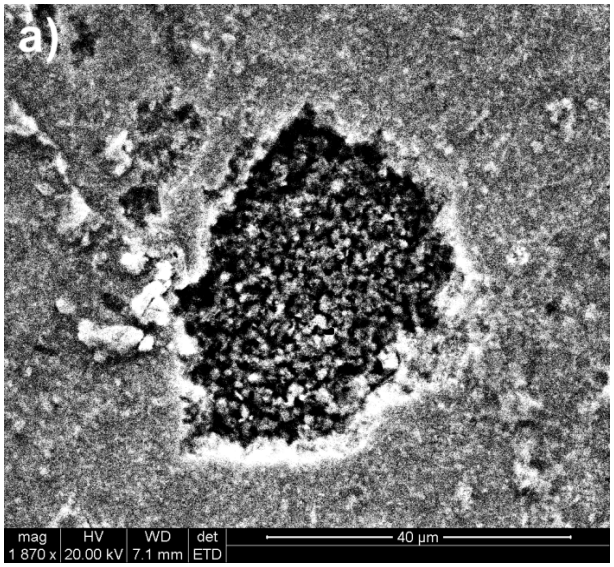

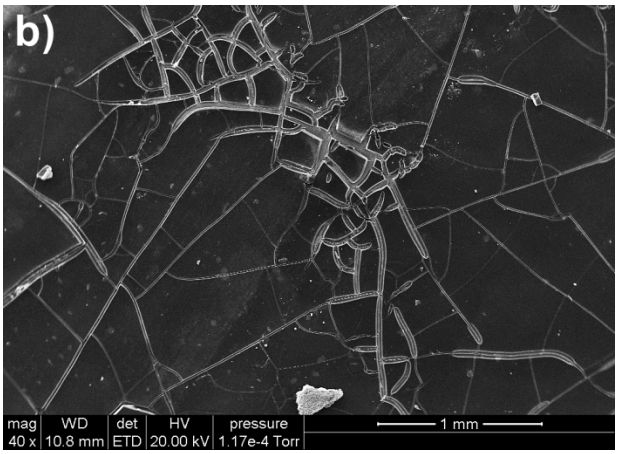

Figure A2.3 ESEM analysis of CSCM defects: carbonization hole (a), polymer deposition-related cracks (b).

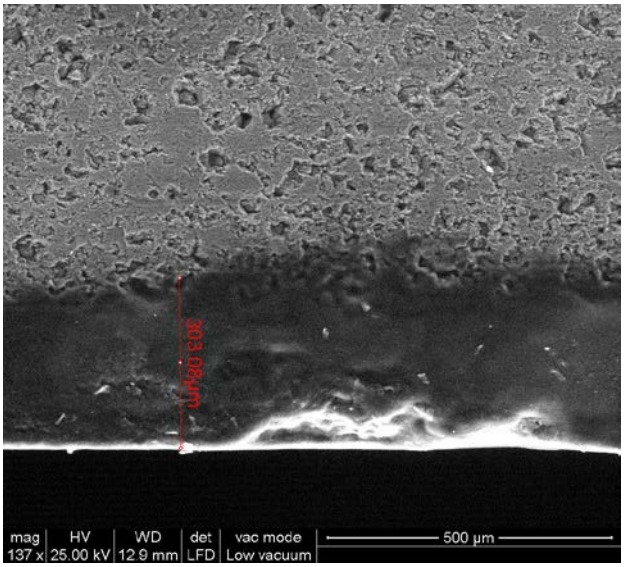

Figure A2.4 Polymer (carbon precursor) deposited over the ceramic support.

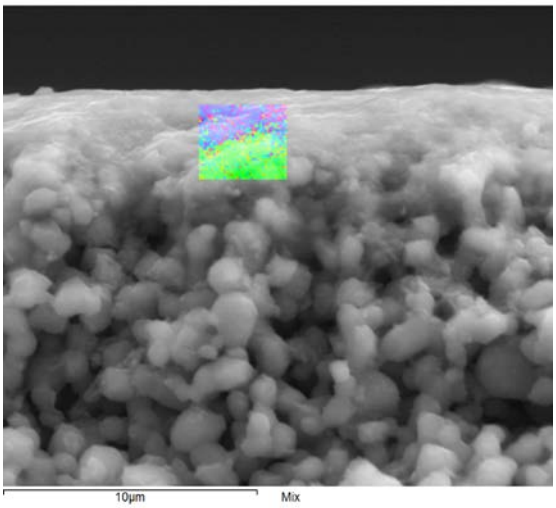
10µm
Mix

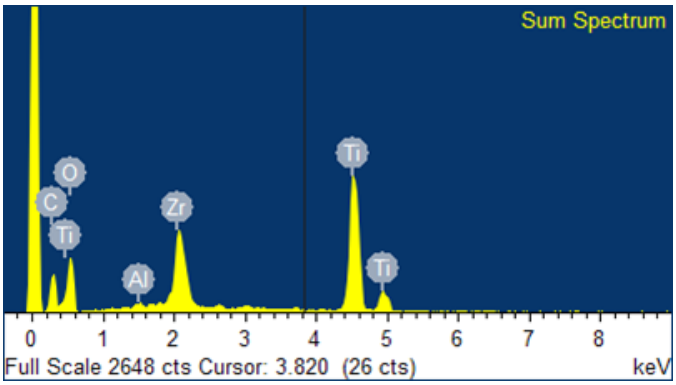
Sum Spectrum
O
C
Ti
Zr
Al
Ti
Ti
0
1
2
3
4
5
6
7
8
Full Scale 2648 cts Cursor: 3.820 (26 cts)
keV

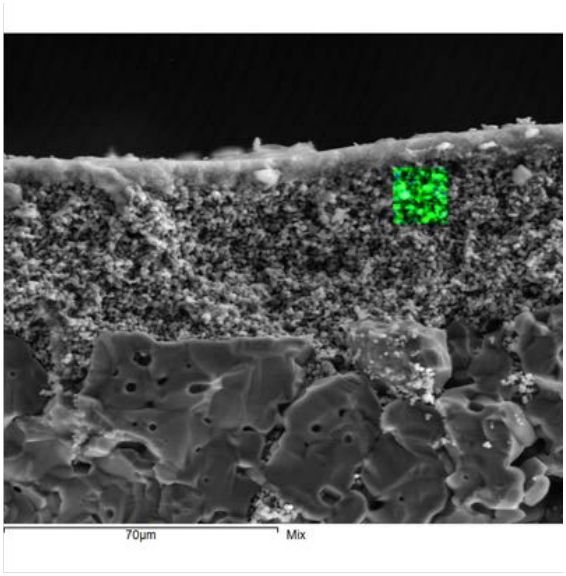
70µm
Mix

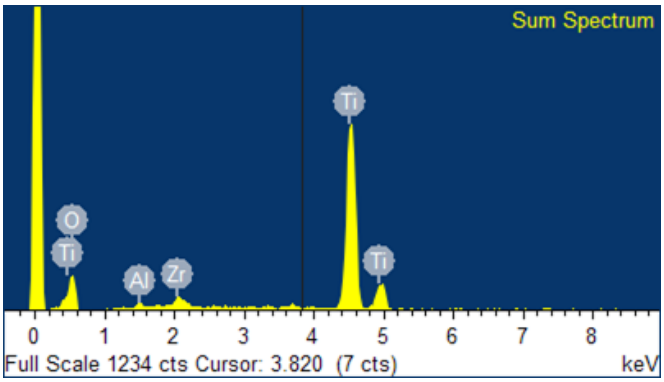

Figure A2.5 EDx analysis of the carbon membrane and ceramic support. [Comment: Red; Carbon, Green Titania; Blue Zirconia]

Figure A2.6 Ceramic support: AFM height profile.

Figure A2.7 Decolorization over the biological degradation process. After 0 (a), 7 (b) and 10 (c) days of operation.

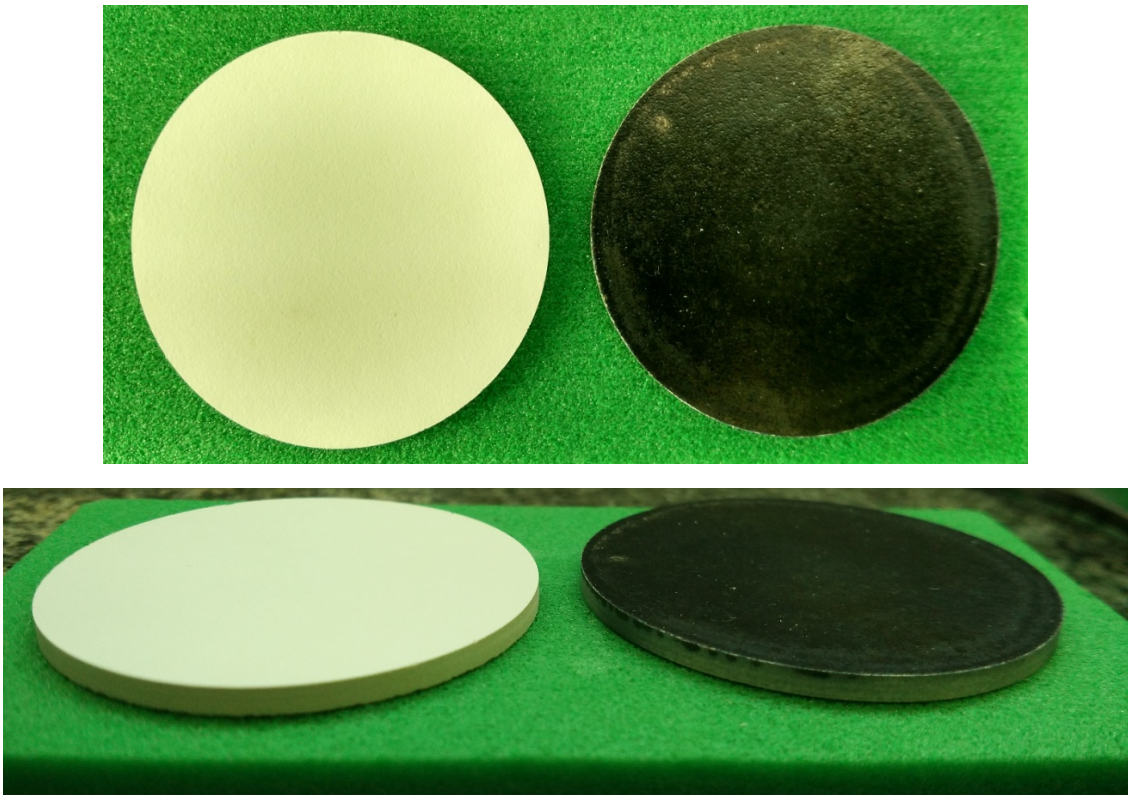

Figure A2.8 Ceramic support (white disk) and CSCM (black disk).

Figure A2.9 Membrane's holder and bioreactor.

A2.2 Influence of the contact time.

A2.2.1 First-order kinetics

A simplified modeling of the process shows that the biodegradation proceeds closely following a first order of reaction with respect to the inverse of the flux, as equivalent variable to the residence time.

The integrated form of a *first-order kinetics* equation is

$$\ln\frac{[AO7]}{[AO7]_0} = -\,k\cdot t \qquad \textbf{(A.1)}$$

Considering the inverse of the flux as residence time equivalent and replacing concentrations with conversion,

$$1-X = \exp(-k'/J) \qquad \textbf{(A.2)}$$

A2.2.2 Michaelis-Menten kinetics

However, it is expected that the process follows Michaelis-Menten kinetics since is a biobased degradation. The first step in any enzyme process is a reversible reaction between the enzyme (E) and the substrate (S), leading to the formation of an intermediate enzyme-substrate (ES), which then undergoes practically irreversible decomposition, yielding a reaction product (P) and the original enzyme.

$$E + S \overset{K_1}{\leftrightarrow} ES \overset{k_2}{\rightarrow} E + P \qquad \textbf{(A.3)}$$

Then, the corresponding Michaelis-Menten kinetic equation gives the reaction rate,

$$r_{AO7} = -\frac{K_1\cdot[AO7]}{k_2+[AO7]} \qquad \textbf{(A.4)}$$

Finally, the integrated equation considering the inverse of the flux as residence time equivalent and replacing concentrations with conversion,

$$\frac{1}{J} = \frac{[AO7]_0}{K'_1}\cdot X - \frac{k'_2}{K'_1}\cdot\ln(1-X) \qquad \textbf{(A.5)}$$

Table A2.1. Experimental data

J ($L \cdot m^{-2} \cdot h^{-1}$)	X
0.06	0.82
0.10	0.53
0.15	0.41

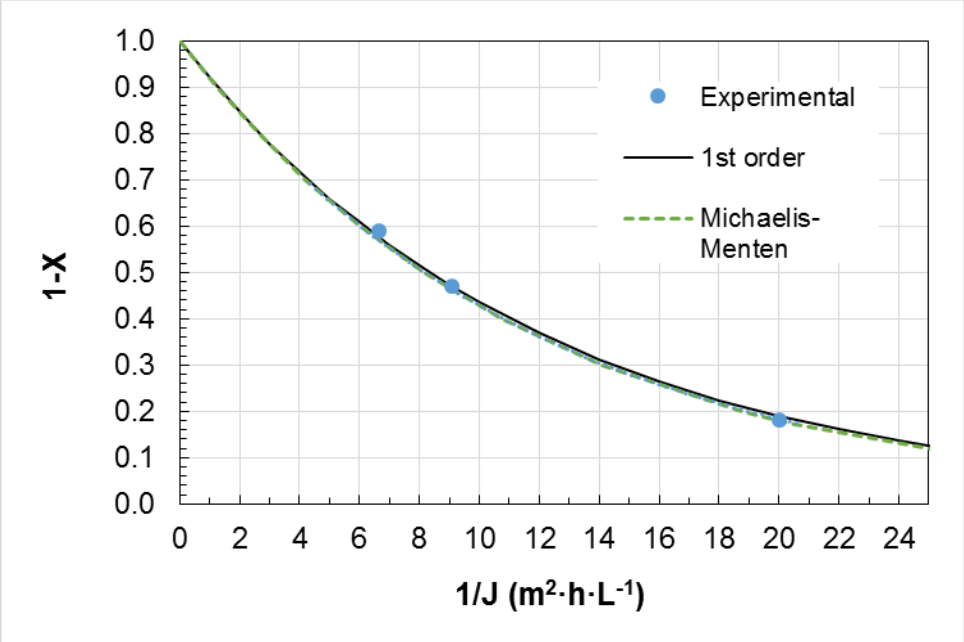

Figure A2.10 Influence of the contact time (flux) on the AO7 removal.

UNIVERSITAT ROVIRA I VIRGILI
COMPACT CARBON-BASED MEMBRANE REACTORS FOR ANAEROBIC BIODEGRADATION OF AZO-DYES FROM WASTEWATER
Alberto Giménez Pérez

CHAPTER 3

Optimized synthesis of ceramic-supported carbon membranes for azo dye degradation in anaerobic biofilms

Carbon-based materials have been broadly used in wastewater treatments dealing with redox, adsorption or photocatalytic processes. The conductive properties of these materials allow performing as redox mediator and enhance the biodegradation of biorefractory compounds. The present study lies in the synthesis of carbon materials in form of thin membranes to promote the degradation of wastewater containing a low concentration of the azo dye Acid Orange 7. The study deals with the influence of the membrane synthesis conditions on the performance to remove azo dyes. The membranes were prepared by carbonization of a commercial polyimide (Matrimid® 5218) over ZrO_2-TiO_2 supports. The amount of carbon precursor (2-10% wt.) and the support pore size (15, 50, and 150 kDa cutoff) were examined. These factors determined the membrane thickness (5-11 μm) and surface characteristics such as root mean square roughness (31-67 nm). All the membranes were tested for the anaerobic biodegradation of the dye over immobilized biofilms under an equivalent dye loading rate of 38 $g \cdot m^{-3} \cdot day^{-1}$. The presence of the carbon membrane increased two to five times the biodegradation rates. The amount of carbon material and the membrane roughness were found to be related to the azo dye removal differences.

Research paper submitted to

Journal of Membrane Science

Optimized synthesis of ceramic-supported carbon membranes for azo dye degradation in anaerobic biofilms

Alberto Giménez-Pérez, Kelly Briceño, Christophe Bengoa, Azael Fabregat, Agustí Fortuny, Frank Stüber, Josep Font

Manuscript ID: MEMSCI_2016_382

UNIVERSITAT ROVIRA I VIRGILI
COMPACT CARBON-BASED MEMBRANE REACTORS FOR ANAEROBIC BIODEGRADATION OF AZO-DYES FROM WASTEWATER
Alberto Giménez Pérez

3.1 Introduction.

Around one million tons of dyes are annually produced worldwide, half of them azo compound class [1], and straightaway used in different applications. Among others, textiles, cosmetics, food, pharmaceuticals, leathers or paper printing therefore occurring in their wastewater effluents [2]. Most azo dyes are considered as biotoxic and/or mutagenic to life, and consequently must be mineralized before discharging to the environment [3,4]. Unfortunately, these compounds are classified as biorefractory pollutants, hence they cannot be efficiently degraded through conventional methods implemented in municipal wastewater treatment plants [5].

The toxicology of these compounds is a major concern for the European authorities. The use of azo dyes in the European countries have been regulated over the last years through the REACH Regulation (EC) 1907/2006 including previous EU directives (2004/21/EC, 2003/3/EC and 2002/61/EC), which limits their occurrence in industrial wastewater. Azo dyes are composed of one or more R_1-N=N-R_2 units. These compounds are often considered toxic after reduction and cleavage of the azo bond, which can lead to the release of aromatic compounds [4]. In this study, Acid Orange 7 (AO7) was selected as model compound because of its well-known structure and wide use. Its reduction releases sulphanilic acid (SA) with equivalent toxicity to the unreduced dye, and 1-amino-2 naphtol (1A2N), whose associated toxicity is around 100 times higher than that of the formers [4].

Synthetic dyes can be degraded by physical, chemical or biological approaches [6]. Physical and chemical methods, mostly based on coagulation-flocculation or adsorption of dyes, provide low color removal and generate huge amounts of residual sludge, thus preventing their use [7]. Likewise, filtration techniques have been successfully used in textile industry. However, they still retain some inconveniences mainly due to their high investment cost and fouling [8]. Additionally, all these methods exhibit a common disadvantage, a concentrated secondary waste stream is created and further treatments are needed [9].

Meanwhile, bioremediation consists in the application of biological techniques to neutralize or remove pollutants. The biological approach provides notable benefits, for instance, near complete mineralization with no further treatments needed, cost-effective processes, and less environmental impact [10]. In case of dealing with azo dyes, the microorganisms must undergo an acclimatization period to these bioxenotic

compounds, hence creating new resistant strains with the ability of transforming toxic pollutants into non-hazardous derived compounds [11]. Several studies have demonstrated that the microbial decolorization is associated to the action of enzymes [12], such as Laccase [13] or lignin peroxidase [14]. Different organisms such as fungi, algae, plants or bacteria are potentially able to degrade azo dyes [15,16]. Bacterial degradation implies the use of mixed [17] or pure cultures [18]. An individual strain typically allows faster degradation, but generally cannot degrade completely these pollutants. On the contrary, mixed cultures reach deeper level of mineralization [12] because of the synergistic action from the different metabolic activities of the microbial community, thus degrading both the azo dye and its intermediate derived products [19,20]. Anaerobic bacteria are commonly used for this purpose [21].

Several reactor configurations have been tested over the last decades for such biological systems, among them, packed-bed [22], upflow anaerobic sludge blanket (UASB) [2] or membrane bioreactors (MBR) [23]. Most of the succeeding configurations have used granular sludge or active biofilms over different supports, which increases the biomass concentration and facilitates the degradation [24,25]. Moreover, since the transport of electrons is usually described as the rate-limiting step for the azo dye reduction, carbon materials have been employed as redox mediators to increase the color removal due to their ability of transporting electrons in redox systems [26,27]. The electrons are exchanged between the oxidation of a secondary readily degradable carbon source, such as sodium acetate, and the reduction of the azo dye.

Carbon-based membranes can be prepared depositing thin polymer films onto ceramic supports, followed by its carbonization at high temperatures [28–32]. Ceramic supported carbon membranes (CSCM) have been usually employed in gas separation processes [32–35], however their potential in aqueous processes is still to be explored. In the approach here introduced, CSCM are employed to treat colored wastewater by promoting the formation of an immobilized biofilm, yet the carbon layer plays a multiple role as physical support and retention system for biomass, redox mediator, and adsorbent enhancing the removal.

This study examines the influence of the biologically activated carbon surface on the azo dye removal and is focused on the carbon membrane synthesis conditions and subsequent impact on the azo dye biodegradation rate. The use of different ceramic supports and carbon precursor concentrations defines the membrane structure, which in

turn influences the azo dye removal. To the best of our knowledge, no such studies have been carried out on carbon membranes and removal of azo dyes.

3.2 Experimental.

3.2.1 Chemicals.

A commercial polyimide, Matrimid® 5218 (3, 3′, 4, 4′-benzophenonetetracarboxylic dianhidride and diamino-phenylindane) from Huntsman Advanced Materials, was used as carbon membrane precursor and 1-methyl-2-pyrrolidone (NMP) (content 99.5%, Sigma Aldrich) as precursor solvent.

AO7 (content 99%, Sigma Aldrich ref. O8126) was selected as model azo colorant. Sodium acetate (Sigma Aldrich, ref. 11019-1, 99%) was used as co-substrate being both the secondary carbon source for anaerobic sludge and the electron donor for the azo reduction. The basal media for microorganism growth contained the following compounds ($mg \cdot l^{-1}$): $MnSO_4 \cdot H_2O$ (0.15), $CuSO_4 \cdot 5H_2O$ (0.28), $ZnSO_4 \cdot 7H_2O$ (0.46), $CoCl_2 \cdot 6H_2O$ (0.26), $(NH_4)_6Mo_7O_{24}$ (0.28), $MgSO_4 \cdot 7H_2O$ (15.20), $CaCl_2$ (13.48), $FeCl_3 \cdot 6H_2O$ (29.06), NH_4Cl (190.91), KH_2PO_4 (8.52), $Na_2HPO_4 \cdot 2H_2O$ (33.43), K_2HPO_4 (21.75). All the basal media compounds were purchased from Sigma Aldrich.

3.2.2 Membrane synthesis and characterization.

CSCMs were synthesized through deposition and subsequent carbonization of thin polymer films onto ceramic supports. Carbon precursor (Matrimid® 5218) solutions were prepared with 1-methyl-2-pyrrolidone (NMP) as solvent; two different precursor concentrations were investigated: 2 and 10% wt. Ceramic supports for carbon layer deposition were commercial ultrafiltration ceramic disks, with a nominal molecular weight cut-off (MWCO) either of 15, 50 and 150 kDa, manufactured by TAMI Industry (Nyons, France). The polymer solutions (3 ml) were spread onto the support surfaces by the spin-coating technique. An initial spun at 500 rpm for 10 s was applied, followed by a final stage at 3000 rpm for 30 s. Once the ceramic was coated and the solvent slowly evaporated, the carbonization took place at 700 ºC and atmospheric pressure. Below 200 ºC, the heating ramp rate was set at 4 $ºC \cdot min^{-1}$ and over 200 ºC it was decreased to

1 ºC·min^{-1} to prevent the occurrence of surface breaks, adapting a heating protocol elsewhere published [29]. All CSCMs were prepared following exactly the same procedure, where only the ceramic substrate pore size and carbon precursor concentration were varied (Table 1).

Table 3.1. Synthesized carbon membranes.

Code	Support MWCO (kDa)	Matrimid® 5218 (% wt.)
CSCM-15-2	15	2
CSCM-15-10	15	10
CSCM-50-2	50	2
CSCM-50-10	50	10
CSCM-150-2	150	2
CSCM-150-10	150	10

The membrane permeability was measured by means of a lab-scale filtration cell; this is a critical property taking into account that, within the typical operating pressure range (0-2 bar), the permeability must be in concordance with the biomass contact time needed to reach significant AO7 removal rates.

The electrical resistance of the carbon film was measured through a multi-height microposition four point probing system (Lukas Lab SP4) combined with a Keithley K2420 SourceMeter.

3.2.3 CSCM bioreactor system.

Figure 1 shows a scheme of the lab scale CSCM bioreactors system. Synthetic feed wastewater (200 ml) containing AO7 (50 mg·l^{-1}), sodium acetate (150 mg·l^{-1}) and the basal media previously described was maintained into a fridge at low temperature (1±1 ºC) to prevent the readily degradable carbon source (sodium acetate) biodegradation. The bioreactor temperature was set at 37±1 ºC to furnish optimum growth conditions for anaerobic microbial strains. The whole experimental system was held up under nitrogen atmosphere to generate anaerobic conditions. The redox potential (ORP) was continuously monitored and controlled to maintain its value under

-400 mV. The CSCM was mounted into a TAMI® (Nyons, France) filtration cell, where the synthesized carbon membrane was placed in the retentate side. This side consists of a vertical cylinder, 47 mm in diameter and 2.2 mm in height.

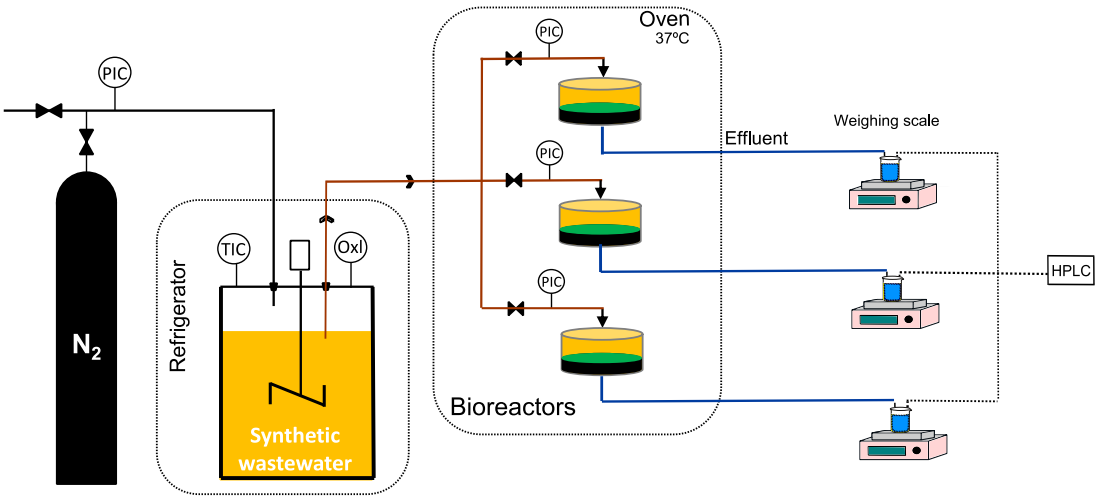

Figure 3.1 CSCM bioreactor system.

The experiment started once a seed of anaerobic sludge was inoculated into the bioreactor (1 ml). The mixed culture of anaerobic sludge was obtained by partial digestion of aerobic sludge collected from a municipal WWTP (Reus, Spain) under anaerobic conditions for a week. The bioreactors were subsequently operated at constant feed rate (0.06 $L \cdot m^{-2} \cdot h^{-1}$) in dead-end filtration mode. Nitrogen gas was used as pressure driven force as well as to maintain an anaerobic atmosphere throughout the system. In some tests membrane fouling forced a slight progressive increase in the transmembrane pressure (TMP) to operate the process under constant-flux conditions. All the experiments were run until steady-state conditions were achieved. The pH was monitored in the permeate (Crison ph-meter BASIC 20) and its value ranged between 6.5 and 7.4, however, no external substances were added to control it. After each run, the membranes were examined by microscopy techniques for verifying the integrity of their structure after operation.

3.2.4 Analytical methods.

AO7 and sodium acetate were measured by HPLC (Agilent 1220 Infinity), using a C18 Hypersil ODS column (2.1 x 50 mm, particle size of 5 µm) with a flow rate of 1

$ml \cdot min^{-1}$ under a gradient of methanol/water mobile phase using the following program: 0-5 min, 0/100; 5-10 min, 25/75; 10-12 min, 50/50; 12–15 min, 0/100. The UV detection wavelengths were 487 and 210 nm for AO7 and sodium acetate, respectively. The effluent samples of 1 ml were pre-filtered through a 0.22 µm PVDF filter (Whatman®) at room temperature before performing the analysis.

The synthesized membranes were examined by means of Environmental Scanning Electron Microscopy, ESEM (FEI Quanta 600), coupled with an Oxford Inca Energy Dispersive X-ray (EDX) system for chemical composition analysis. Membrane surfaces were also characterized by atomic force microscopy, AFM (Pico Plus 2500 from Molecular Imaging, Bid-Service, LLC, Freehold, NJ, USA). The images were recorded in tapping mode with a resonance frequency of 1 Hz in air at room temperature and then processed by WSxM 5.0 software [36]. Silicon nitride cantilevers (NP-S, Brucker) with a nominal spring constant of 0.12 $N \cdot m^{-1}$ and a resonant frequency of 23 kHz were used.

Chemical oxygen demand (COD) was determined by dichromate method according to the standard method 5220D (APHA, 17th Ed., 1989).

3.3 Results and discussion.

3.3.1 Carbon membrane characterization.

3.3.1.1 Microscopy techniques.

The synthesized membranes were characterized by ESEM. All carbon membrane surfaces were found to be homogeneous under the chosen preparation protocol previously described and the further conditions listed in Table 3.1. As shown in Figure 2a-c and Table 3.2, the deposited layer thickness varied notably depending on the synthesis parameters.

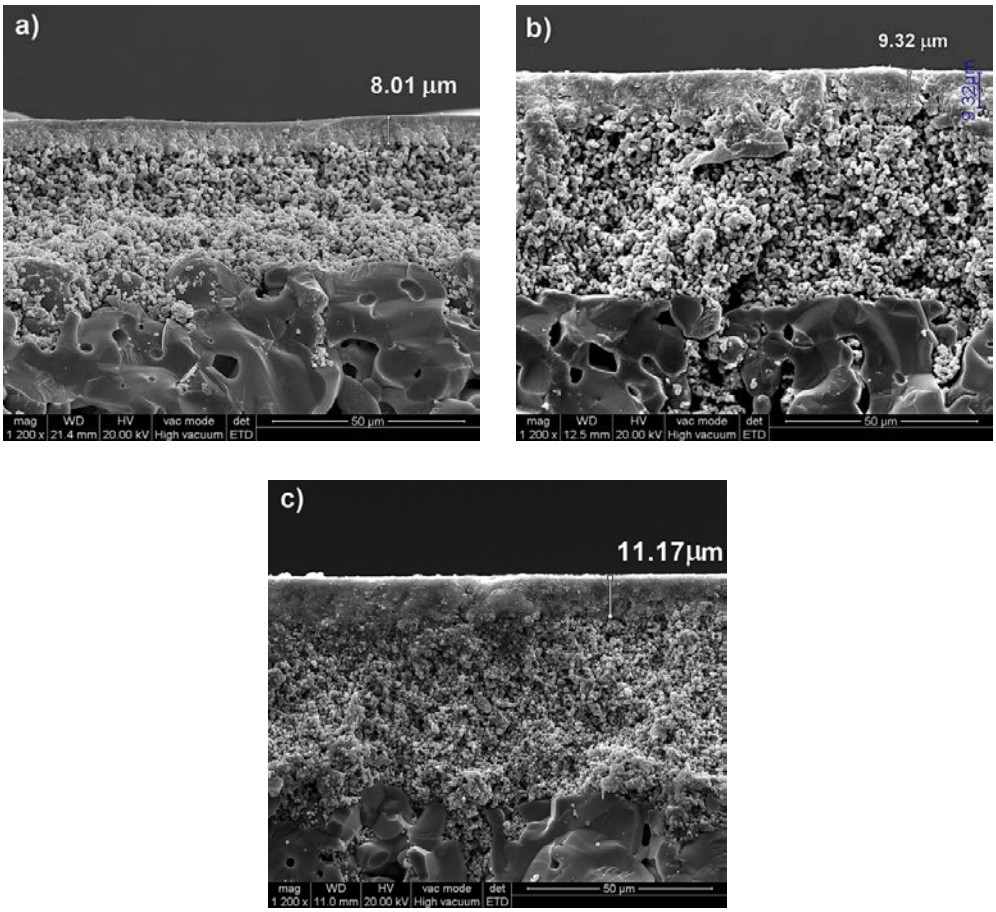

Figure 3.2. Support pore size influence on the membrane thickness: (a) CSCM 15-10, (b) CSCM 50-10, (c) CSCM 150-10.

The use of supports with larger pore sizes allowed the carbon precursor penetration into the CS granular interstices. On the contrary, as the CS pore size decreased, the infiltration of the precursor was restrained, thus the precursor accumulated onto the superficial ceramic substrate, which finally results in thinner but denser membranes.

Table 3.2. Influence of the preparation conditions on the membrane thickness, roughness, and carbon composition.

Membrane code	**Thickness** (µm)	**Roughness** (RMS*)	**Carbon** (% wt.)
CSCM 15-2	5.67	67.35	25.42
CSCM 50-2	6.35	75.43	3.34
CSCM 150-2	7.91	86.67	1.54
CSCM 15-10	8.01	31.26	35.98
CSCM 50-10	9.32	54.64	18.24
CSCM 150-10	11.17	64.54	2.54

*RMS: root mean square roughness analysis (nm).

As can be discerned from Table 3.2, for a given support, the increase of the precursor composition from 2 to 10% wt. favors the synthesis of thicker membranes; the increments varied between 47 and 40% in case of CSs equivalents to 50 and 150 kDa, respectively.

The composition of the membrane active layer was investigated through X-ray microanalysis (ESEM-EDX) and is also presented in Table 3.2. The X-rays penetration depth is estimated in 5 µm taking into account the chemical elements conforming the membrane and the applied analysis conditions (30 kV). Since the synthesized membranes showed thicknesses around 5.7-11.2 µm, the composition analysis not always represents the whole membrane active layer but rather the more superficial zone. As can be observed in Table 3.2, it is confirmed the use of CSs with greater pore sizes promotes the penetration of the carbon precursor forming a composite (carbon-ceramic) that presents lower carbon concentrations. On the contrary, CSs with smaller pores difficult the precursor infiltration, favoring this way the formation of superimposed carbon films with higher carbon concentrations. The membrane surface was also examined by AFM and 3D height profiles are depicted in Figure 3a, b.

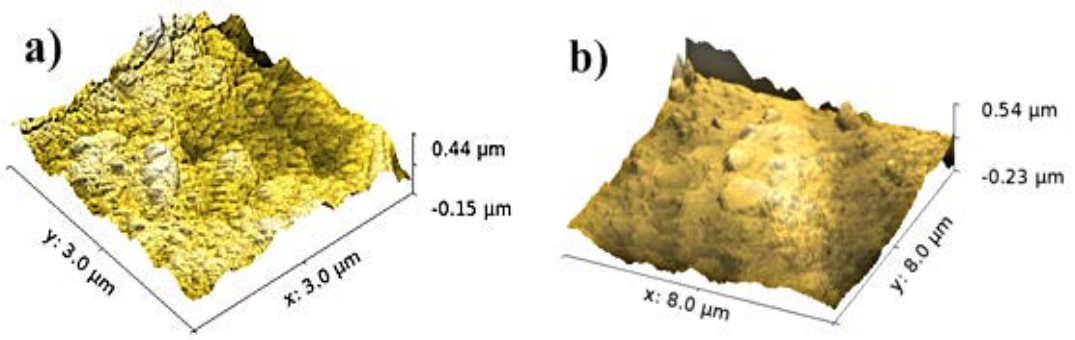

Figure 3.3 3D surface height profiles; CSCM 150-2 (a) and CSCM 15-10 (b)

In principle, rough surfaces are preferred to growth bacteria cultures [37]; thus, a root mean square roughness analysis (RMS) was completed (Table 3.2). It must be noted that the CS disks can be already considered as highly rough; the analyses found values of 120.3, 110.2 and 95.30 nm for 150, 50, and 15 kDa supports, respectively. The deposition of the carbon onto its surface significantly modifies them. As can be observed in Table 3.2, the carbon membrane synthesis reduced in all studied cases the roughness of the ceramic support, e.g. between 47 and 68% in case of CSs equivalents to 150 and 15 kDa, respectively. The effect was more pronounced when larger mass of precursor was deposited. Overall, the carbon membrane composition or thickness can be defined by the preparation conditions following the requirements of a specific application.

3.3.1.2 Membrane hydraulic resistances.

The permeability of the CSCMs and CSs was determined in order to establish the effect of the deposited carbon layer on this property. It must be noted that the membrane flux will determine the productivity of the CSCM bioreactor, in terms of mass of dye removed per unit of time and reactor (membrane) surface area, as it imposes the contact time because of the dead-end mode operation. Table 3.3 shows the measured permeabilities for all the membranes tested; supplementary material including further tests at different transmembrane pressure conditions is also available.

Table 3.3 Hydraulic resistances (m^{-1}) [ΔP: 40000 Pa]

Membrane code	$J_{W,s} \cdot 10^6$ ($m^3 \cdot m^{-2} \cdot s^{-1}$)	$J_{W,m} \cdot 10^6$ ($m^3 \cdot m^{-2} \cdot s^{-1}$)	$R_s \cdot 10^{-12}$ (m^{-1})	$R_m \cdot 10^{-12}$ (m^{-1})	$R_c \cdot 10^{-12}$ (m^{-1})
CSCM-15-2	3.44	0.48	11.6	82.0	70.4
CSCM-50-2	11.90	8.54	3.4	4.7	1.3
CSCM-150-2	25.80	15.51	1.6	2.6	1.0
CSCM-15-10	3.44	0.06	11.6	652.6	641.0
CSCM-50-10	11.90	5.87	3.4	6.8	3.4
CSCM-150-10	25.80	6.95	1.5	5.7	4.2

The membrane synthesis implies the addition of an external carbon precursor to a commercial CS and two different mechanisms take place throughout this process; the CS pores constriction through the carbon precursor penetration, and formation of superimposed carbon layers over the CS. Therefore, as expected, the addition of the carbon layer lowered the permeability (28-98%) given by the original ceramic support. The highest impact on the permeability reduction was found for the membranes supported over the ceramic substrate of smallest pore size; i.e. CSCM-15-2 and CSCM-15-10. In such situation, the accumulation of carbon material onto the support is likely the predominant mechanism. On the contrary, when using lower concentrated solutions of membrane precursor (2% wt.) and CS with MWCO equivalents to 50 and 150 kDa the impact on the permeation was significantly lower (≤ 40%).

It should be noted that carbon membranes prepared over ceramic substrates with MWCO equivalents to 50 and 150 kDa and higher concentrated solutions of membrane precursor (10% wt.), i.e. CSCM-50-10 and CSCM-150-10, offered close permeabilities. This fact suggests that the individual resistance offered by the membrane components, carbon film and ceramic support, were different in each membrane but their combination gives comparable overall membrane resistances; hence, under the cited synthesis conditions, the final permeation seemed to be mostly controlled by the polymer concentration (10% wt.) chosen for the membrane preparation. Further information about the permeability characterization is presented in the supplementary material (section A.1).

The overall membrane resistance R_m (m^{-1}) was calculated using the following equation:

$$R_m = \sum R_i = R_S + R_C = \frac{\Delta P}{\eta \cdot J_W} \quad (1)$$

where R_S is the ceramic support resistance (m^{-1}), R_C is the carbon layer resistance (m^{-1}), ΔP is the hydraulic pressure difference (Pa), J_W is the pure water flux ($m^3 \cdot m^{-2} \cdot s^{-1}$), and η is the viscosity ($kg \cdot m^{-1} \cdot s^{-1}$).

As the resistance of the support, R_S, can be obtained from its original pure water flux, the additional resistance provided by the carbon layer, R_C, can be calculated (Table 3.4). Table 3.4 evidences that except for the membranes supported over CS with MWCO equivalents to 15 kDa, the carbon layer exerted an additional resistance in the same order of magnitude than that already owned by the CS. On the contrary, the carbon film deposited onto the CS with the smallest ceramic pores provided much higher resistance than the others, i.e. CSCM-15-2 and CSCM-15-10. This fact again corroborates that could occur the pores saturation because of the lower volume available or the impossibility of carbon precursor infiltration. Hereon, the membrane precursor settled down onto the support, thus, forming superimposed carbon films that increased to a greater extend the flux resistance. A clear example of this phenomenon, CSCM 15-10, when the resistance associated to the carbon film is more than ten times higher than the one derived of the CS.

Overall, the added carbon layer offers enough resistance to reduce the CS permeation notably (Figure A.1 in the supplementary material). However, the membranes supported over CS with MWCO equivalents to 15 kDa showed a higher reduction on the permeation (≥90%). This is probably due to the fact that in this case the formation of superimposed carbon layers over the CS prevails.

3.3.1.3 Surface conductivity.

Bacterial azo reduction is generally considered as a non-specific reduction process that can be helped by redox mediators, shuttling electrons from the oxidation of a readily degradable secondary carbon source to the reduction semireaction, and thus increasing the biodegradation rates [38]. The CSCM ability to carry electrons is a measure of its suitability for this application. Hence, the electrical resistance of the synthesized carbon layers was measured through a multi-height microposition four point probing system. The obtained values ($\Omega \cdot m$), listed in Table 3.4, are calculated following the Ohm's law:

$$R_e = 4.5324 \cdot \frac{V}{I} \quad (2)$$

where R_e (Ω·m) defines the surface electrical resistance, V the applied electrical current (V), and I correspond to the current through the membrane (A).

Table 3.4 Electrical resistance (Ω·m)

Code	**Current** (μA)	**Intensity** (mV)	**$R_e \cdot 10^7$** (Ω·m)
CSCM-15-2	0.003	45	6.7
CSCM-15-10	0.003	22	3.3
CSCM-50-2	0.001	10	4.5
CSCM-50-10	0.002	12	2.7
CSCM-150-2	0.003	194	29.3
CSCM-150-10	0.003	170	2.5
Standard*	0.003	16	2.4

* Commercial conductive carbon films (PELCO Tabs®)

Electrical measurements indicated similar surface conductivities as commercial carbon films except for those prepared over the CS with the largest pore size. In these cases, the incursion of the carbon precursor into the support pores became larger decreasing the concentration of carbon at the top superficial layers. This implied a drop in the electrical surface conductivity or the membrane ability to transfer electrons. Anyway, all the observed values confirmed the presence of a carbonaceous layer so that the membranes could still be adequate for this application.

3.3.1.4 Performance of the CSCM bioreactors

Initially, the membrane physical adsorption of AO7 was examined in order to check its potential contribution to the overall dye removal. These adsorption experiments were carried out by dead-end filtration of AO7 solutions under the same flux (0.06 $l \cdot m^{-2} \cdot day^{-1}$) and feed dye concentration as the subsequent biodegradation tests. The experiments were performed until permeate and feed solution showed the same concentration. This steady state was reached after 2 and 15 hours of operation for CSCM-150-2 and CSCM-15-10, respectively. This fact evidences that the membranes, rather carbon membranes,

rapidly become saturated, so the contribution of the adsorption ends after 15 hours of operation as maximum. Hereon, the membrane adsorption of any compound can be totally discarded. Thus, the influence of the membrane physical adsorption on the biological experiments has to be taken into account uniquely throughout the first hours within a total period of operation of several weeks.

Later, the synthesized CSCMs but also non-modified CSs were tested for azo dye removal. The membranes were installed in filtration cells performing as bioreactors operated under a constant flux of 0.06 $l \cdot m^{-2} \cdot h^{-1}$ and feed AO7 concentration of 50 $mg \cdot l^{-1}$. The dye concentration was periodically measured in the exiting effluent for almost three weeks. Figure 4 depicts the evolution of AO7 conversion until a recognizable steady-state was reached.

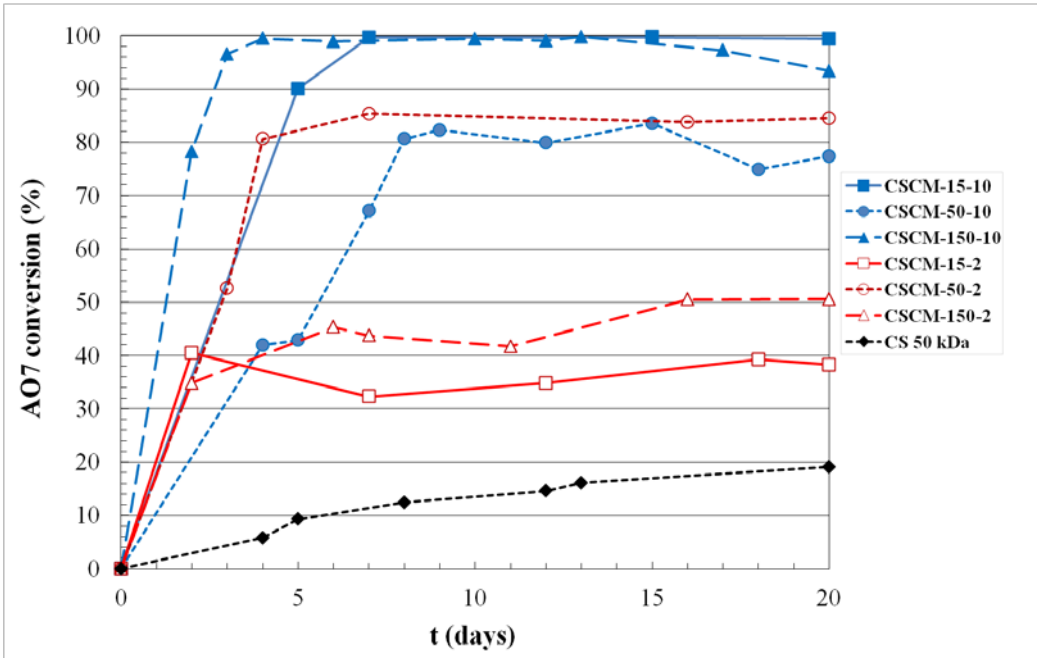

Figure 3.4 Evolution of the AO7 conversion for the different CSCM.

[Temperature: 37 ºC; flux: 0.06 $l \cdot m^{-2} \cdot h^{-1}$]

A blank experiment was carried out by using a CS with an equivalent pore size to 50 kDa in order to evaluate the effect of introducing carbon active films in this biological process. The commercial CS, a disk made of TiO_2 and ZrO_2, was directly used without any kind of modification. In this case, as evidenced in Figure 4, AO7

biological removal is poor, 20% at the highest, after 20 days in operation. On the contrary, all the CSCM bioreactors showed significantly higher AO7 conversion. In all the cases, there was an initial period of acclimation and incubation of the microorganisms, which extended for 3-7 days; where the biomass was progressively adapting to the azo dye and the degradation rate simultaneously increased. After these 3-7 days, a closely stable steady state was maintained offering substantial azo dye biodegradation (40-99%) for near two weeks. All CSCMs enhanced the process in comparison with the performance of non-modified CSs, yielding AO7 conversions 2 to 5 times higher. This fact evidences the positive effect of introducing carbon films in this process.

However, some differences were found on the performance of the several CSCM bioreactors tested. An inspection to Figure 4 clearly suggests some correlation between the amount of carbon and the conversion achieved. Tests that involved CSCM possessing smaller carbon loads such as CSCM 150-2, usually achieved lower AO7 conversions. The lower carbon content reduced its activity as redox mediator as well as the adsorption capacity. Although adsorption does not directly contributes to the removal, it must indeed be a step in the overall mechanism, thus a low carbon load means a decrease on the adsorption capacity making more difficult the retention and subsequent biological reduction of the azo dye. Likewise, CSCM 150-2 presented the highest resistance to electrical flux, which also means a poorer potential for the proposed application. The combination of these factors led to this membrane to provide the lowest biodegradation rate. Contrarily, CSCM-150-10 was able to completely remove the dye. This outstanding performance could also be related to its morphology, in addition to its high carbon content, CSCM-150-10 showed relatively high roughness and permeation compared to the other membranes, which suggests that the carbon contact area was larger besides accessible for biomass. The synergy of these circumstances allowed reaching the highest azo dye biodegradation (almost 100%). A distinct membrane, CSCM 15-10, offered similar performance in comparison with the previously described CSCM 150-10. However, in this case, the application of much higher transmembrane pressure to get the desired flux was required implying higher associated energy cost at comparable operating conditions. In conclusion, the use of CSCM-150-10 should be more recommendable for practical purposes.

Regarding operational problems associated with biofouling, note that the membrane hydraulic pressure difference (ΔP) was slightly increased throughout the operation to maintain the permeate flux constant. However, the increment was around 0.1 bar (CSCM 150-2) and 0.2 bar (CSCM 15-10), which means that despite of the biofilm formation and the accumulation of material, the flux resistance derived from this phenomenon was not a relevant problem from the operational point of view. Once stopped, the membranes were cleaned by back-flushing with distilled water at 4 bar for 5 minutes and the original flux was usually recovered. Overall, membrane fouling was controlled under the operating conditions chosen in this study. Finally, the membranes were re-examined through ESEM discarding in all the cases changes in their structure and morphology due to their use.

3.4 Conclusions.

Defect-free carbon membranes were prepared by impregnation of a polymer onto ceramic surfaces. Polymer solutions were prepared using Matrimid® 5218 as carbon precursor in the composition (% wt.) range from 2 to 10 in NMP solvent. The mixtures were successfully deposited onto ceramic supports with different pore sizes (MWCO of 15, 50 and 150 kDa).

Six different membranes were prepared and, as expected, the synthesis parameters defined carbon membrane properties such as roughness or permeability. Greater pore size ceramic supports promoted the formation of thicker but less carbon concentrated membranes. Contrarily, the use of ceramic substrates with smaller pore sizes difficulted the polymer precursor penetration favoring the creation of a dense superimposed carbon membrane. The membrane permeation decreased notably (25-80%) in comparison with the original ceramic support under the studied conditions. In most cases, the added carbon layer provided an additional resistance to the liquid flux comparable to the ceramic support. The carbon membrane synthesis decreased the original roughness of the ceramic substrates. However, this effect was found less significant if smaller amounts of carbon are incorporated to the support.

In relation to the removal of AO7, the presence of a biologically activated carbon layer enhanced from two to five times the mineralization rate in comparison with non-modified commercial ceramic membranes. Yes, it was found a tendency of higher biodegradation rates by increasing the membrane carbon composition and roughness. Regards the proposed application, the support must be covered by a carbon layer thick enough to guarantee an optimum effect; thus, its greater presence in most cases intensified the process. On the other hand, high membrane roughness favored higher degradation activity because microorganisms prefer this kind of surfaces as physical support; the best performance was found by employing rough membranes with relatively wider pores making the carbon material more accessible for biomass.

Acknowledgements

The Spanish MINECO and FEDER funded this project through the grant (CTM2011-23069 and CTM2015-67970-P). Moreover, the Spanish Ministry of Education, Culture and Sports is greatly acknowledged by providing a pre-doctoral scholarship (BES-2012-059675). The authors' research group is recognized by the *Comissionat per a Universitats i Recerca del DIUE de la Generalitat de Catalunya (2014 SGR 1065)* and supported by the Universitat Rovira i Virgili (2014PFR-URV-B2-35).

References

[1] H. Ollgaard, L. Frost, J. Galster, O.C. Hensen, Survey of azo-colorants in Denmark: Consumption, use, health and environmental aspects, Danish Environmental Protection Agency, Copenhagen (DK), 1998. http://www2.mst.dk/udgiv/publications/1999/87-7909-548-8/pdf/87-7909-546-1.pdf.

[2] R. Brás, A. Gomes, M.I.A. Ferra, H.M. Pinheiro, I.C. Gonçalves, Monoazo and diazo dye decolourisation studies in a methanogenic UASB reactor, J. Biotechnol. 115 (2005) 57–66. doi:10.1016/j.jbiotec.2004.08.001.

[3] J. Feng, C.E. Cerniglia, H. Chen, Toxicological significance of azo dye metabolism by human intestinal microbiota, Front. Biosci. (Elite Ed). 4 (2012) 568–86. doi:10.2741/400 .

[4] A. Gottlieb, C. Shaw, A. Smith, A. Wheatley, S. Forsythe, The toxicity of textile reactive azo dyes after hydrolysis and decolourisation, J. Biotechnol. 101 (2003) 49–56. doi:10.1016/S0168-1656(02)00302-4.

[5] M. Petrović, S. Gonzalez, D. Barceló, Analysis and removal of emerging contaminants in wastewater and drinking water, TrAC - Trends Anal. Chem. 22 (2003) 685–696. doi:10.1016/S0165-9936(03)01105-1.

[6] A.F. Ismail, L.I.B. David, A review on the latest development of carbon membranes for gas separation, J. Memb. Sci. 193 (2001) 1–18. doi:10.1016/S0376-7388(01)00510-5.

[7] Y.-Y. Lau, Y.-S. Wong, T.-T. Teng, N. Morad, M. Rafatullah, S.-A. Ong, Coagulation-flocculation of azo dye Acid Orange 7 with green refined laterite soil, Chem. Eng. J. 246 (2014) 383–390. doi:10.1016/j.cej.2014.02.100.

[8] J. Zhang, L. Wang, G. Zhang, Z. Wang, L. Xu, Z. Fan, Influence of azo dye-TiO2 interactions on the filtration performance in a hybrid photocatalysis/ultrafiltration process, J. Colloid Interface Sci. 389 (2013) 273–83. doi:10.1016/j.jcis.2012.08.062.

[9] M.F. Coughlin, B.K. Kinkle, P.L. Bishop, High performance degradation of azo dye Acid Orange 7 and sulfanilic acid in a laboratory scale reactor after seeding with cultured bacterial strains., Water Res. 37 (2003) 2757–63. doi:10.1016/S0043-1354(03)00069-1.

[10] S.-A. Ong, E. Toorisaka, M. Hirata, T. Hano, Treatment of azo dye Orange II in aerobic and anaerobic-SBR systems, Process Biochem. 40 (2005) 2907–2914. doi:10.1016/j.procbio.2005.01.009.

[11] F.P. van der Zee, S. Villaverde, Combined anaerobic–aerobic treatment of azo dyes—A short review of bioreactor studies, Water Res. 39 (2005) 1425–1440. doi:10.1016/j.watres.2005.03.007.

[12] R.G. Saratale, G.D. Saratale, J.S. Chang, S.P. Govindwar, Bacterial decolorization and degradation of azo dyes: A review, J. Taiwan Inst. Chem.

Eng. 42 (2011) 138–157. doi:10.1016/j.jtice.2010.06.006.

[13] N. Hatvani, I. Mécs, Production of laccase and manganese peroxidase by Lentinus edodes on malt-containing by-product of the brewing process, Process Biochem. 37 (2001) 491–496. doi:10.1016/S0032-9592(01)00236-9.

[14] N. Durán, E. Esposito, Potential applications of oxidative enzymes and phenoloxidase-like compounds in wastewater and soil treatment: a review, Appl. Catal. B Environ. 28 (2000) 83–99. doi:10.1016/S0926-3373(00)00168-5.

[15] F.I. Hai, K. Yamamoto, F. Nakajima, K. Fukushi, L.D. Nghiem, W.E. Price, et al., Degradation of azo dye acid orange 7 in a membrane bioreactor by pellets and attached growth of Coriolus versicolour, Bioresour. Technol. 141 (2013) 29–34. doi:10.1016/j.biortech.2013.02.020.

[16] X. Meng, G. Liu, J. Zhou, Q.S. Fu, Effects of redox mediators on azo dye decolorization by Shewanella algae under saline conditions., Bioresour. Technol. 151 (2014) 63–8. doi:10.1016/j.biortech.2013.09.131.

[17] M.V. Tuttolomondo, G.S. Alvarez, M.F. Desimone, L.E. Diaz, Removal of azo dyes from water by sol–gel immobilized Pseudomonas sp., J. Environ. Chem. Eng. 2 (2014) 131–136. doi:10.1016/j.jece.2013.12.003.

[18] S. Kumar Garg, M. Tripathi, S.K. Singh, J.K. Tiwari, Biodecolorization of textile dye effluent by Pseudomonas putida SKG-1 (MTCC 10510) under the conditions optimized for monoazo dye orange II color removal in simulated minimal salt medium, Int. Biodeterior. Biodegradation. 74 (2012) 24–35. doi:10.1016/j.ibiod.2012.07.007.

[19] M. Solís, A. Solís, H.I. Pérez, N. Manjarrez, M. Flores, Microbial decolouration of azo dyes: A review, Process Biochem. 47 (2012) 1723–1748. doi:10.1016/j.procbio.2012.08.014.

[20] M.F. Coughlin, B.K. Kinkle, P.L. Bishop, Degradation of acid orange 7 in an aerobic biofilm, Chemosphere. 46 (2002) 11–19. doi:10.1016/S0045-6535(01)00096-0.

[21] S.-A. Ong, E. Toorisaka, M. Hirata, T. Hano, Decolorization of Orange II using an anaerobic sequencing batch reactor with and without co-substrates, J. Environ. Sci. 24 (2012) 291–296. doi:10.1016/S1001-0742(11)60766-3.

[22] I. Mielgo, M. Moreira, G. Feijoo, J. Lema, A packed-bed fungal bioreactor for the continuous decolourisation of azo-dyes (Orange II), J. Biotechnol. 89 (2001) 99–106. doi:10.1016/S0168-1656(01)00319-4.

[23] A. Spagni, S. Casu, S. Grilli, Decolourisation of textile wastewater in a submerged anaerobic membrane bioreactor, Bioresour. Technol. 117 (2012) 180–185. doi:10.1016/j.biortech.2012.04.074.

[24] G. Mezohegyi, C. Bengoa, F. Stuber, J. Font, A. Fabregat, A. Fortuny, Novel bioreactor design for decolourisation of azo dye effluents, Chem. Eng. J. 143 (2008) 293–298. doi:10.1016/j.cej.2008.05.006.

[25] G. Mezohegyi, E, U.I. Castro, C. Bengoa, F. Stuber, J. Font, et al., Effective Anaerobic Decolorization of Azo Dye Acid Orange 7 in Continuous Upflow Packed-Bed Reactor Using Biological Activated Carbon System, Ind. Eng. Chem. Res. 46 (2007) 6788–6792. doi:10.1021/ie061692o.

[26] B.E.L. Baêta, H.J. Luna, A.L. Sanson, S.Q. Silva, S.F. Aquino, Degradation of a model azo dye in submerged anaerobic membrane bioreactor (SAMBR) operated with powdered activated carbon (PAC)., J. Environ. Manage. 128 (2013) 462–70. doi:10.1016/j.jenvman.2013.05.038.

[27] G. Mezohegyi, F. Gonçalves, J.J.M. Órfão, A. Fabregat, A. Fortuny, J. Font, et al., Tailored activated carbons as catalysts in biodecolourisation of textile azo dyes, Appl. Catal. B Environ. 94 (2010) 179–185. doi:10.1016/j.apcatb.2009.11.007.

[28] K. Briceño, D. Montané, R. Garcia-Valls, A. Iulianelli, A. Basile, Fabrication variables affecting the structure and properties of supported carbon molecular sieve membranes for hydrogen separation, J. Memb. Sci. 415–416 (2012) 288–297. doi:10.1016/j.memsci.2012.05.015.

[29] K. Briceño, A. Iulianelli, D. Montané, R. Garcia-Valls, A. Basile, Carbon molecular sieve membranes supported on non-modified ceramic tubes for hydrogen separation in membrane reactors, ICCE-2011. 37 (2012) 13536–13544. doi:10.1016/j.ijhydene.2012.06.069.

[30] A.B. Fuertes, T.A. Centeno, Carbon molecular sieve membranes from polyetherimide, Microporous Mesoporous Mater. 26 (1998) 23–26.

doi:10.1016/S1387-1811(98)00204-2.

[31] A.B. Fuertes, T.A. Centeno, Preparation of supported carbon molecular sieve membranes, Carbon N. Y. 37 (1999) 679–684. doi:10.1016/S0008-6223(98)00244-9 .

[32] M. Teixeira, M.C. Campo, D.A. Pacheco Tanaka, M.A. Llosa Tanco, C. Magen, A. Mendes, Composite phenolic resin-based carbon molecular sieve membranes for gas separation, Carbon N. Y. 49 (2011) 4348–4358. doi:10.1016/j.carbon.2011.06.012.

[33] M.C. Campo, F.D. Magalhães, A. Mendes, Separation of nitrogen from air by carbon molecular sieve membranes, J. Memb. Sci. 350 (2010) 139–147. doi:10.1016/j.memsci.2009.12.021.

[34] M.B. Rao, S. Sircar, Nanoporous carbon membranes for separation of gas mixtures by selective surface flow, J. Memb. Sci. 85 (1993) 253–264. doi:10.1016/0376-7388(93)85279-6 .

[35] S. Sircar, M.B. Rao, Nanoporous carbon membranes for gas separation, Membr. Sci. Technol. 6 (2000) 473–496. doi:10.1016/S0927-5193(00)80020-0 .

[36] I. Horcas, R. Fernández, J.M. Gómez-Rodríguez, J. Colchero, J. Gómez-Herrero, A. Baro, WSXM: A software for scanning probe microscopy and a tool for nanotechnology, Rev. Sci. Instrum. 78 (2007) 013705. doi:10.1063/1.2432410.

[37] R.J. Shimp, F.K. Pfaender, Effects of surface area and flow rate on marine bacterial growth in activated carbon columns., Appl. Environ. Microbiol. 44 (1982) 471–7. doi:0099-2240/82/080471-07$02.00/0.

[38] A. Keck, J. Klein, M. Kudlich, A. Stolz, H.J. Knackmuss, R. Mattes, Reduction of azo dyes by redox mediators originating in the naphthalenesulfonic acid degradation pathway of Sphingomonas sp. strain BN6., Appl. Environ. Microbiol. 63 (1997) 3684–3690.

Supplementary material

A3.1) Permeability characterization.

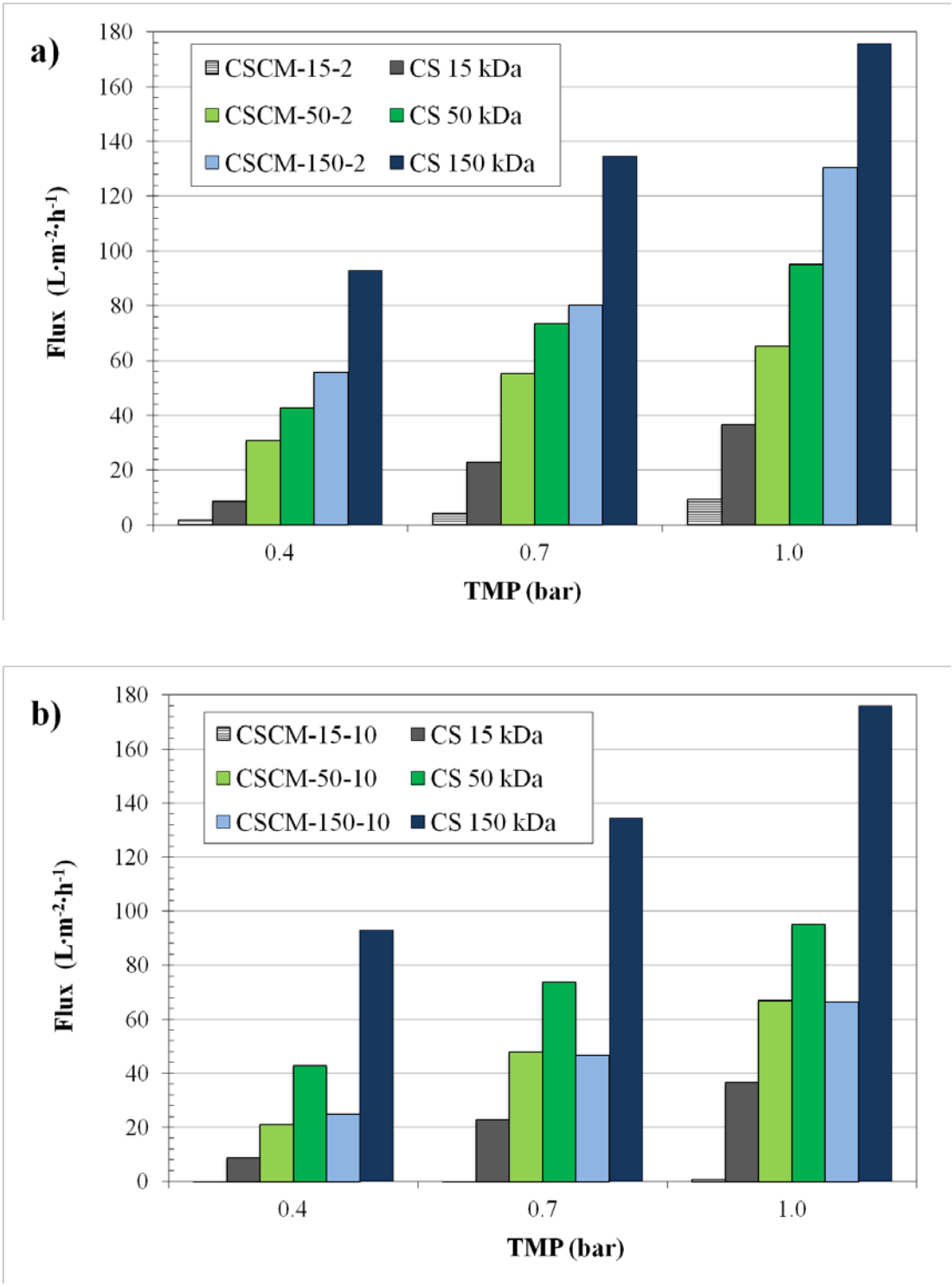

Figure A3.1 CSCM and ceramic support (CS) permeability; precursor solution composition: 2 and 10% wt. (Figure 9a-b, respectively). [LMH: $l \cdot m^{-2} \cdot h$].

UNIVERSITAT ROVIRA I VIRGILI
COMPACT CARBON-BASED MEMBRANE REACTORS FOR ANAEROBIC BIODEGRADATION OF AZO-DYES FROM WASTEWATER
Alberto Giménez Pérez

CHAPTER 4

Double chamber bioreactor systems with ceramic supported carbon membranes for the removal of azo dyes

The next chapter presents a novel integrated double-cell bioreactor for the removal of azo dyes from wastewater. Ceramic supported carbon membranes were prepared by carbonization of polymer onto ceramic porous supports. Next, these materials were employed as electrode acting as an excellent electron shuttle and accelerating the removal of these harmful pollutants from wastewater. The inorganic membrane also acquires the function of separating both chambers allowing both the movement of electrons as the flux of protons generated in the anode chamber. Dye concentrations from 50 $mg \cdot L^{-1}$ to 150 $mg \cdot L^{-1}$ were processed reaching complete removal of Acid Orange-7 and soluble COD under batch conditions. Some harmful intermediates were also significantly degraded such as sulfanilic acid or 1, 2 aminonaphthol hydrochloride into simpler compounds. The effect of the addition of an external carbon source, sodium acetate, as an electron donor was investigated.

Article under preparation

Reductive biodegradation of Acid Orange 7 through a ceramic-supported carbon membrane in a two-chamber bioreactor

Alberto Giménez-Pérez, Christophe Bengoa, Azael Fabregat, Agustí Fortuny, Frank Stüber, Josep Font.

UNIVERSITAT ROVIRA I VIRGILI
COMPACT CARBON-BASED MEMBRANE REACTORS FOR ANAEROBIC BIODEGRADATION OF AZO-DYES FROM WASTEWATER
Alberto Giménez Pérez

4.1 Introduction.

Synthetic azo dyes are being produced for many commercial purposes such as food, cosmetics, paper, textiles, etc [1]. Nowadays, the worldwide production is increasing and literature estimates it around one million tons per year [2]. Most of this production is employed in the textile industry, which means millions of cubic meters of wastewater discharged each year. The toxicity of these compounds is usually high for aquatic and human organisms [3,4]. For this reason, efficient methods must be applied to mineralize these pollutants. Most physical, chemical or physicochemical approaches are expensive due to the equipment investment or operation problems. An additional drawback is sometimes the production of a secondary stream that needs to be treated before discharge into the environment. On the contrary, biological methods are cost-competitive because additional chemicals or electrical power sources are not demanded. Furthermore, an additional advantage is that the pollutants can be completely biomineralized in a single stage of treatment [5]. However, conventional wastewater treatment plants are unable to properly manage these compounds because of their intrinsic chemical stability, so their elimination requires dedicated biological treatments.

Therefore, this study concerns about the biological degradation of commercial azo dyes, such as Acid Orange 7 (AO7), Acid Orange G (AOG) and Tartrazine (TAR), which behave as recalcitrant compounds to conventional aerobic activated sludge processes, thus occurring in the effluent of a typical WWTPs [6,7]. It has been demonstrated that anaerobic conditions are preferred to break the azo bond [8]. Nonetheless, note that a secondary carbon substrate, i.e. glucose or acetate, must be oxidized releasing the electrons needed for the azo dye bond cleavage [9]. The transfer of these electrons has been found the limiting-step for the azo dye reduction. Due to its notable electrical conductivity, carbon materials have been extensively reported as redox mediators in similar decolorization processes [10,11]. Additionally, the carbon provides excellent conditions for the physical support of microorganisms creating robust biofilms over its surface [12]. Another advantage is related to the high adsorption capacity of this inorganic material [13–15] allowing the retention of organic pollutants from wastewater and subsequently their biodegradation [16]. Nevertheless, the reductive biodegradation mechanism can form highly toxic aromatic amines as elsewhere reported [9]. Figure 1 illustrates the structure of AO7, AOG and TAR, and how the breaking of the azo bond

results in amines. Further mineralization of these aromatic amines is usually performed in a secondary aerobic stage [18].

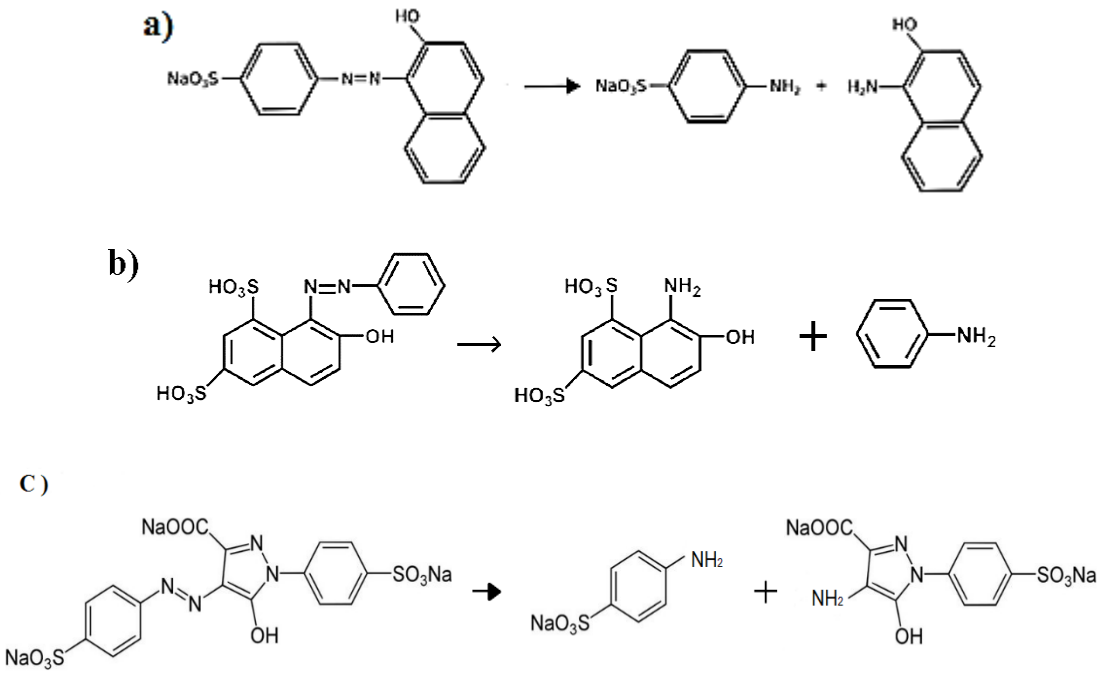

Figure 4.1 Proposed biodegradation mechanism for TAR (a) , AOG (b) [17] , and AO7 (c) [9].

Most studies previously reported in the literature about AO7 biodegradation and carbon materials deal with packed bed reactors [11,12] or the introduction of carbon powder in different configurations of bioreactors [19,20]. This work proposes a novel approach that consists on the application of double-cell bioreactors [21,22]. Recent studies have demonstrated the effectiveness of microbial cells for azo dye degradation and, in some cases, simultaneous electricity production [23]. An additional and significant advantage over other well-known techniques such as MBR is the possibility of treating simultaneously and independently two different wastewater effluents, adjusting the load of each pollutant according their corresponding degradation rate. These redox systems can adopt different configurations through single (SC) or dual (DC) microbial cells. Dual chamber systems present the oxidation and reduction compartments separated by a proton exchange membrane (PEM) [24]. In a typical redox system for azo dye removal, a simple carbon source, i.e. glucose or acetate, is biologically oxidized generating an

electron and proton current at the oxidation cell. With regard to the released electrons, they are carried by the conductive material, i.e. activated carbon [25]. At the reduction chamber, the oxidizing agent (in this case, the azo bond) is reduced due to the acceptation of electrons travelling from the oxidation cell.

The novelty resides in the carbon membrane that separates both chambers allowing the flux of electrons. As previously explained, the biodegradation of azo dyes is limited by the transport of the electrons from the oxidation of a secondary carbon source [10] to the reduction of the azo dye. This novel configuration is designed to enhance the flux electrons enhancing the biological degradation process.

The influence of different parameters on the performance of this new configuration has been examined; among others, the chemical structure of the target dye or the feed dye concentration [16].

4.2 Materials and methods.

4.2.1 Chemicals.

A commercial polymer, i.e. a soluble thermoplastic polyimide (PI), already used for this purpose was purchased from Huntsman Advanced Materials, Matrimid® 5218 (3, 3′, 4, 4′-benzophenonetetracarboxylic dianhidride and diamino-phenylindane). This compound is especially suitable for the preparation of tough and durable coating [26]. For this reason, it was chosen as the carbon precursor for the synthesis of the ultrathin membranes. 1-methyl-2-pyrrolidone (99.5%, Sigma-Aldrich ref. M79204) (NMP), an aprotic solvent with high solubility and low volatility was selected as the precursor solvent in order to prepare the casting solutions required for the membrane synthesis.

The different commercial azo dyes were also supplied by Sigma-Aldrich, AO7 sodium salt (dye content ≥ 99%, ref. O8126), TAR (dye content ≥85%, ref. T0388) and AOG (dye content ≥80%, ref. 861286). Sodium acetate (99%, ref. 11019-1) was used as co-substrate for anaerobic sludge. The microorganism growth media was composed of the next compounds ($mg \cdot L^{-1}$): $MnSO_4 \cdot H_2O$ (0.15), $CuSO_4 \cdot 5H_2O$ (0.28), $ZnSO_4 \cdot 7H_2O$ (0.46), $CoSO_4 \cdot 7H_2O$ (0.31), $(NH_4)_6Mo_7O_{24}$ (0.28), $MgSO_4 \cdot 7H_2O$ (15.20), $Ca(NO_3)_2$

(19.93), $Fe_2(SO_4)_3$ (21.47), KH_2PO_4 (8.50), $Na_2HPO_4 \cdot 2H_2O$ (33.40), K_2HPO_4 (21.75), and K_2HPO_4 (21.75). All basal media compounds were provided by Sigma-Aldrich.

4.2.2 Ceramic and carbon membranes.

Commercial available alumina-titania disks with a pore size equivalent to molecular weight cut off (MWCO) to 1 and 50 kDa, respectively, were provided by TAMI Industries (Nyons, France). Their specific properties are detailed in Table 4.1. The supports with the smaller pore size (1 kDa) were employed without any modification for the studied application. Ceramic substrates of 50 kDa were selected as the supports for the carbon membranes. The carbon precursor solution was composed of Matrimid® 5218 and NMP (solvent). The sequential preparation protocol was composed of several stages. First, the PI pellets were dried for 3 h at 150 ºC to achieve the complete removal of water. Next, polymer solutions were prepared by dissolving 10% wt. of PI in NMP. This mixture was maintained under continuous and vigorous stirring, and vacuum for 3 h to completely remove all the air bubbles from the solution [27]. The presence of air or water in the casted precursor solution may cause serious imperfections in the final structure of the membrane.

Table 4.1. Ceramic support properties.

Ø (mm)	**Area** (cm^2)	**Thickness** (mm)	**Composition**
47	13.1	2.5	$ZrO_2 – TiO_2$

PI solution (2.5 ml) was dropped in the center of the ceramic support and then spread over through the spin coating equipment (SPIN150i-NPP desktop version, SPS). A two-stage *program* was applied; an initial cast for 15 s at 500 rpm continued by a final period at 5000 rpm for 30 s. After the polymer solution casting, the solvent (NMP) was evaporated in air atmosphere at 110 °C for 24 h, washed with methanol, and heat-treated at 80 °C for 2 h to completely remove the solvent; its presence throughout the carbonization process may also cause defects on the membrane surface [26]. Finally, the

carbonization of the superimposed film was carried out in a horizontal tubular furnace (Kosmon S.A., Barcelona) under constant nitrogen gas flow (1.5 $L \cdot min^{1}$), 650 ºC, and atmospheric pressure. Below 350 ºC, the heating ramp rate was set at 4 $ºC \cdot min^{-1}$; over this temperature it was slowed down up to 1 $ºC \cdot min^{-1}$ to prevent the occurrence of fissures throughout the carbon film [26–28]. Afterwards, a complete membrane characterization was carried out through microscopy techniques (ESEM, AFM) and filtration performance tests. This characterization defined its suitability for the proposed application by detecting structural defects, which would prevent their use.

4.2.3 Redox system operation.

Double-cell bioreactors were built using translucent methacrylate; a scheme of the lab-scale double-cell bioreactor is depicted in Figure 1. The unitary cell dimensions were 5 cm width, 10 cm length, and 5 cm height. The total volume of each chamber was approximately 162 ml. Each chamber was designed with five ports (0.35 cm) for the simultaneous and periodic control of parameters such as pH, redox potential (ORP), temperature, and also purge out dissolved gasses (nitrogen or oxygen). Both cells were separated through the previously synthesized CSCM which offered an active area of 15 cm^2. The system was sealed by means of Viton® and Teflon® junctions. The two chambers were vigorously magnetically stirred and heated in a thermostatic bath at 37 ºC throughout the operation.

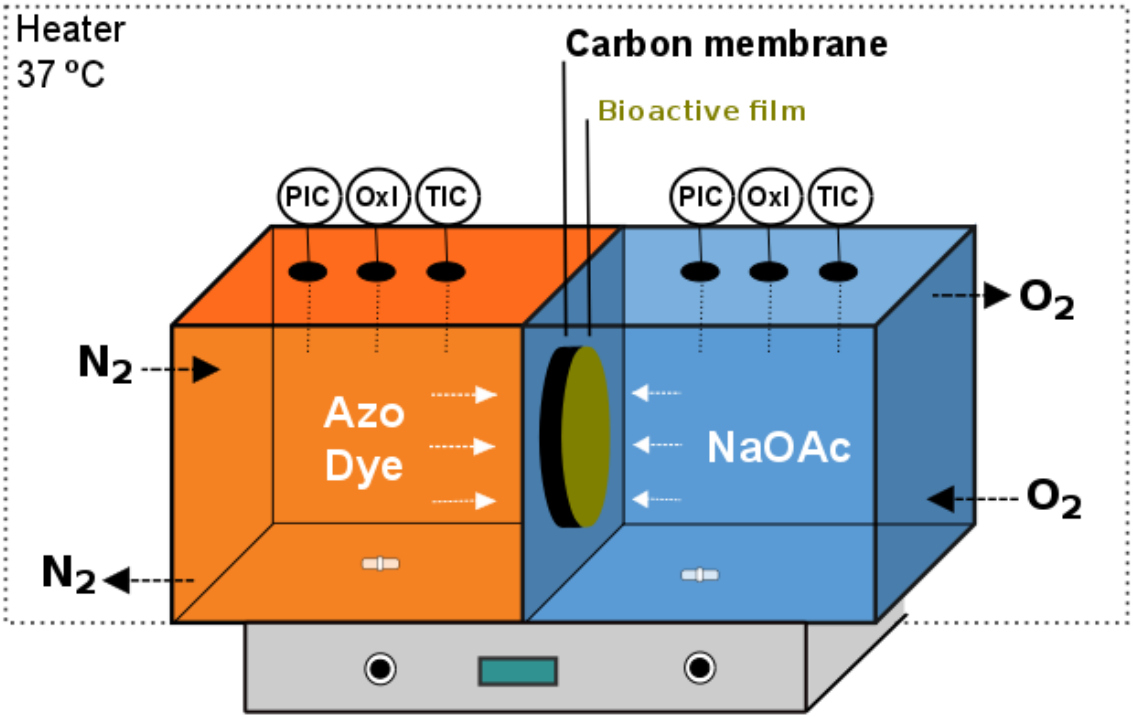

Figure 4.2 Double-cell bioreactor.

In a typical experiment, the oxidation chamber was fed with an external carbon source solution (sodium acetate), an anaerobic microorganism inoculum (3 ml), and the basal media for microorganism growth previously detailed (4.2.1). The sludge containing mixed microbial population was taken from the municipal wastewater plant of Reus (Spain); the inoculum anaerobic conditions were obtained by partial digestion of aerobic sludge for a week. In turn, the reduction cell was only fed with the azo dye solution. As can be seen from Figure 4.2, the membrane was placed separating both chambers; the active part of the membrane, the carbon film, was placed towards the oxidation cell. Thus, the biofilm only grew over the carbon membrane in the oxidation cell.

The batch-wise mode experiments were performed under continuous stirring till the dye was completely removed. The pH was monitored in both cells (Crison pH-meter BASIC 20), its value varied from 6.7 to 7.3. The redox potential (ORP) was maintained and controlled under -300 mV in the reduction cell by purging the dissolved oxygen with nitrogen gas. Note that the solutions were initially saturated with nitrogen gas. Otherwise, the oxidation cell was kept under positive redox potentials (100-300 mV) by continuous flow of oxygen. The temperature was set and monitored in both chambers at 37 ºC throughout the experiments. Samples of both chambers (1 ml) were periodically

taken. The system was run under batch-mode, thus, after taking and analyzing each sample, the compartments were refilled with the corresponding volume and concentration to reestablish the previous conditions.

AO7 was the model compound chosen for the main part of this study. The influence of different parameters on its degradation as the secondary carbon source to dye mass ratios was investigated (10:5:3). The rate of degradation of the simple secondary substrate, sodium acetate, was considerably higher in comparison with the azo dye, thus, it was continuously feed so as to maintain constant ratios over the experiment. A different parameter, the initial dye concentration was also under study (50, 75 and 100 $mg \cdot L^{-1}$). The experiments were reproduced with commercial ceramic membranes (1 kDa) so as to evaluate the influence of the active carbon film over this process. Diffusion and membrane adsorption tests were also carried out following the same experimental conditions as the biological tests in order to investigate its impact. AO7 was the model compound chosen for the main part of this study. Finally, a comparative study including other dyes, i.e. AOG and TAR, was also carried out.

The first-order kinetic constants (k_{DEG}) of degradation can be estimated using the integrated first-order rate law.

$$\ln (c_t) = (-)\, k_{DEG} \cdot t + \ln (c_o) \qquad (1)$$

where c_t and c_o are the dye concentration values at a given time during the degradation process and in the feed solution, respectively.

4.2.4 Analytical techniques.

A high performance liquid chromatography system (HPLC) was used to carry out the identification of the dyes (AO7, AOG and TAR) and sodium acetate. The chromatograph (Agilent 1100 LC) was equipped with a C18 reverse phase column (Hypersil ODS 5.0 µm, 4.6 x 250 mm, Agilent) and a UV detector. The mobile phases were methanol-water ranged from 0-100% to 100-0% in 10 min with a flow rate of 1 $ml \cdot min^{-1}$. The specific chromatographic method for each compound has been included in the supplementary material. The retention times of AO7, AOG, and TAR were 11.2, 8.4, and 7.2 min, respectively. AO7, TAR, AOG and Sodium Acetate were determined

at 487, 427, 252 nm, and 210 nm. All the effluent samples (1.5 ml) were pre-filtered through a 0.22 µm PVDF filter (Whatman®) at room temperature before the analysis.

Transmission electron microscopy (TEM JEOL, JEM-1011, USA) and environmental scanning electron microscopy (ESEM QUANTA 600, FEI, Dawson Creek Drive, Hillsboro, OR, USA) were used to examine the biofilm created over the support. For the ESEM analysis, the samples were dried in air at room temperature for 24 h. In case of TEM analysis, a rapid bacterial acid staining method was applied.

The chemical oxygen demand (COD) after the biotreatment was determined by a DR 6000™ UV-VIS Spectrophotometer from HACH (USA) [13]. Total organic carbon (TOC) was determined with an Analytik Jena multi N/C 2100 TOC analyzer. Each measurement was the average of three replicates tests.

4.3 Results

4.3.1 Membranes characterization.

Commercial ceramic and synthesized membranes tested show different properties in terms of pore size and porosity although the synthesis of the carbon membrane was designed to prepare materials in a close pore size range as the commercial substrates. A rough study of the CSCM pore size distribution based on AFM imaging was performed by SPIP™ software. More than 80% of the total carbon pores were found in the range 1-20 nm, thus the original size of the ceramic support pores was reduced more than 50%. Note that the commercial CS used in this study without any modification present a pore size equivalent to 1 kDa, which is accepted to be in the range of 1 nm pores.

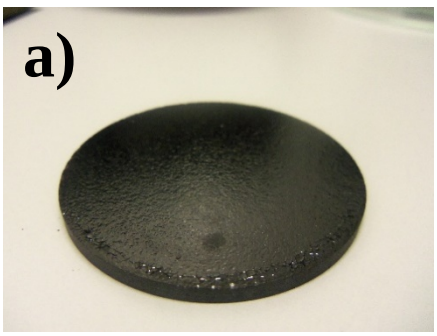

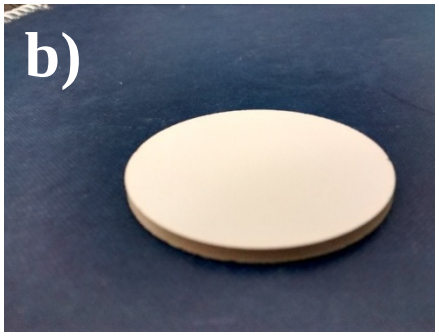

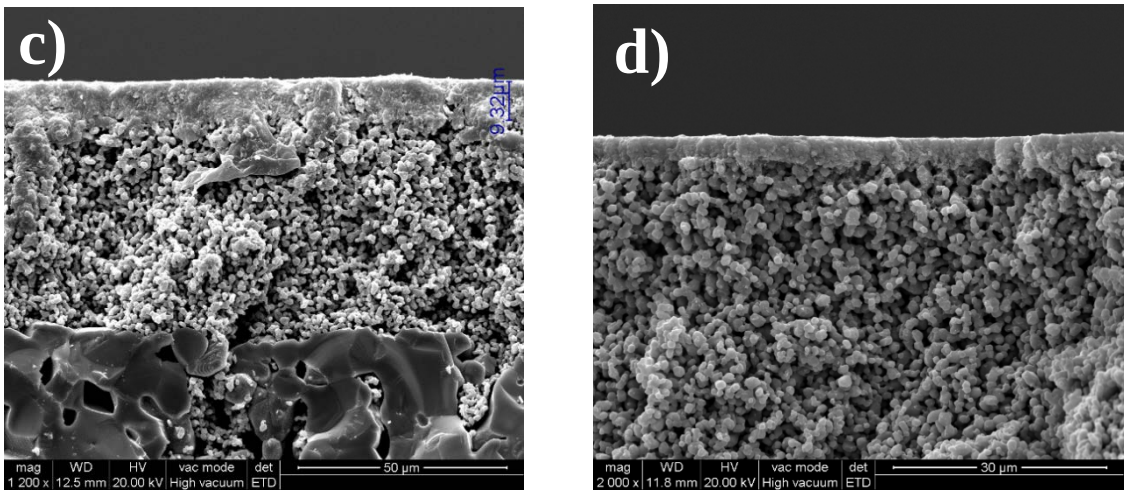

Figure 4.3 Carbon membrane (a, c) and Ceramic support (b, d) surfaces and thickness, respectively.

The synthesized membrane surface was characterized by microscopy techniques (ESEM). A visual inspection discarded important defects over the commercial and synthesized disks, figures 4.3a and b, respectively. The microscopy characterization through ESEM technique evidences also a homogeneous and defect-free carbon membrane cross-section (Figure 4.3c). The CSCM thickness was found almost two times higher than the zirconium layer of the ceramic support, figures 4c and d, respectively.

4.3.2 AO7 biodegradation.

The AO7 biodegradation was evaluated with a synthesized carbon-based membrane (CSCM) and a commercial TiO_2-AlO_2 support (1 kDa) under exactly the same experimental conditions. The commercial membranes were included in this study as a reference to estimate the influence of supported carbon layer over the dye removal. However, note that both types of membranes do not present exactly the same properties such as the porosity or pore size so the membrane adsorption and diffusion through the membranes were also investigated. In all the experiments, the membrane was vertically mounted into the system, separating both chambers.

Four different scenarios were thus examined. In first place, a non-modified ceramic disk of 1 kDa (CS) was mounted to check the dye transport through the membrane (Figure 4.5a), this is, in absence of microorganisms. Later, microorganisms were added to

follow the dye transport and potential consumption (Figure 4.5b). These two tests were later reproduced replacing the CS by the synthetized CSCMs (Figs. 4.5c, d respectively).

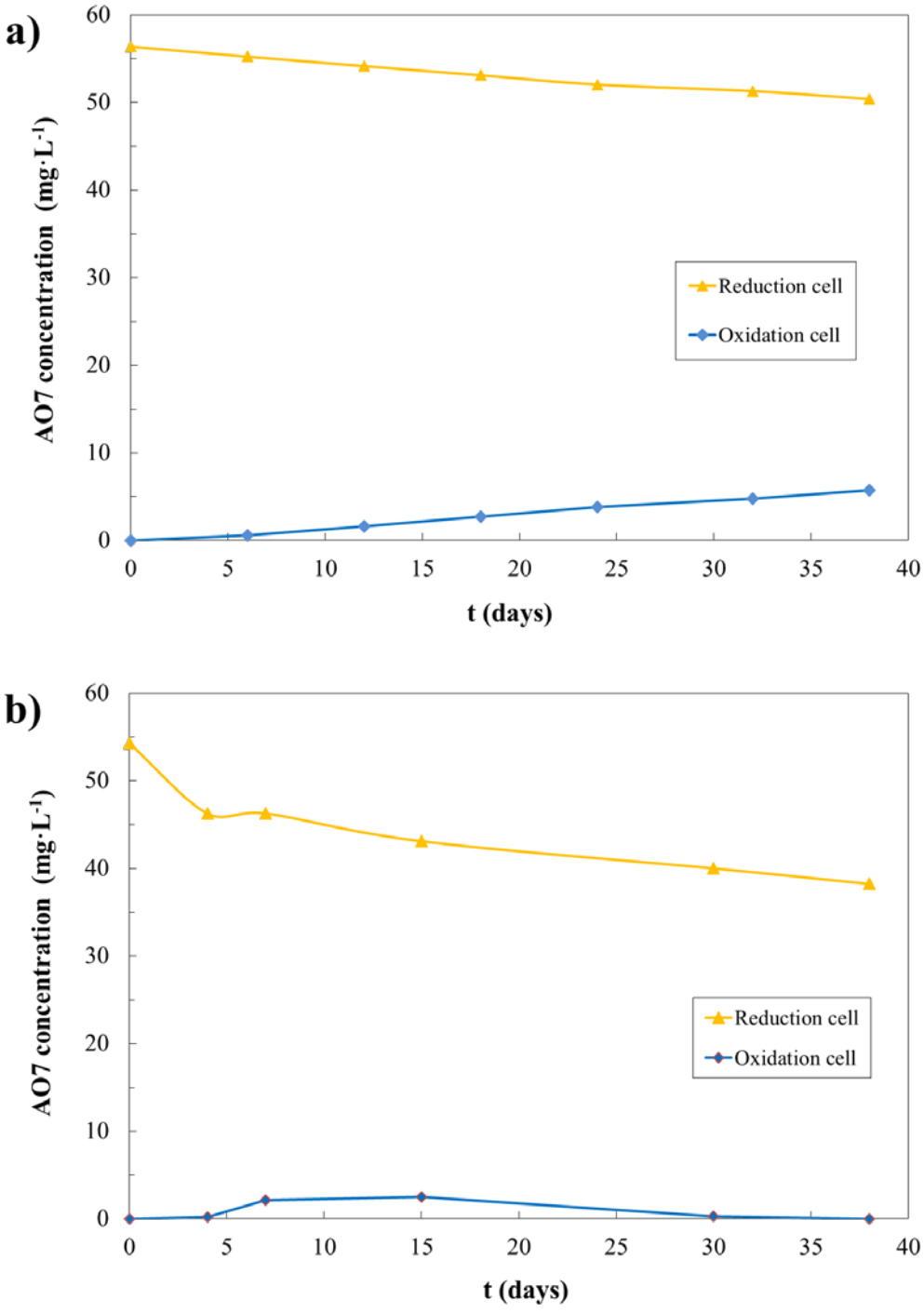

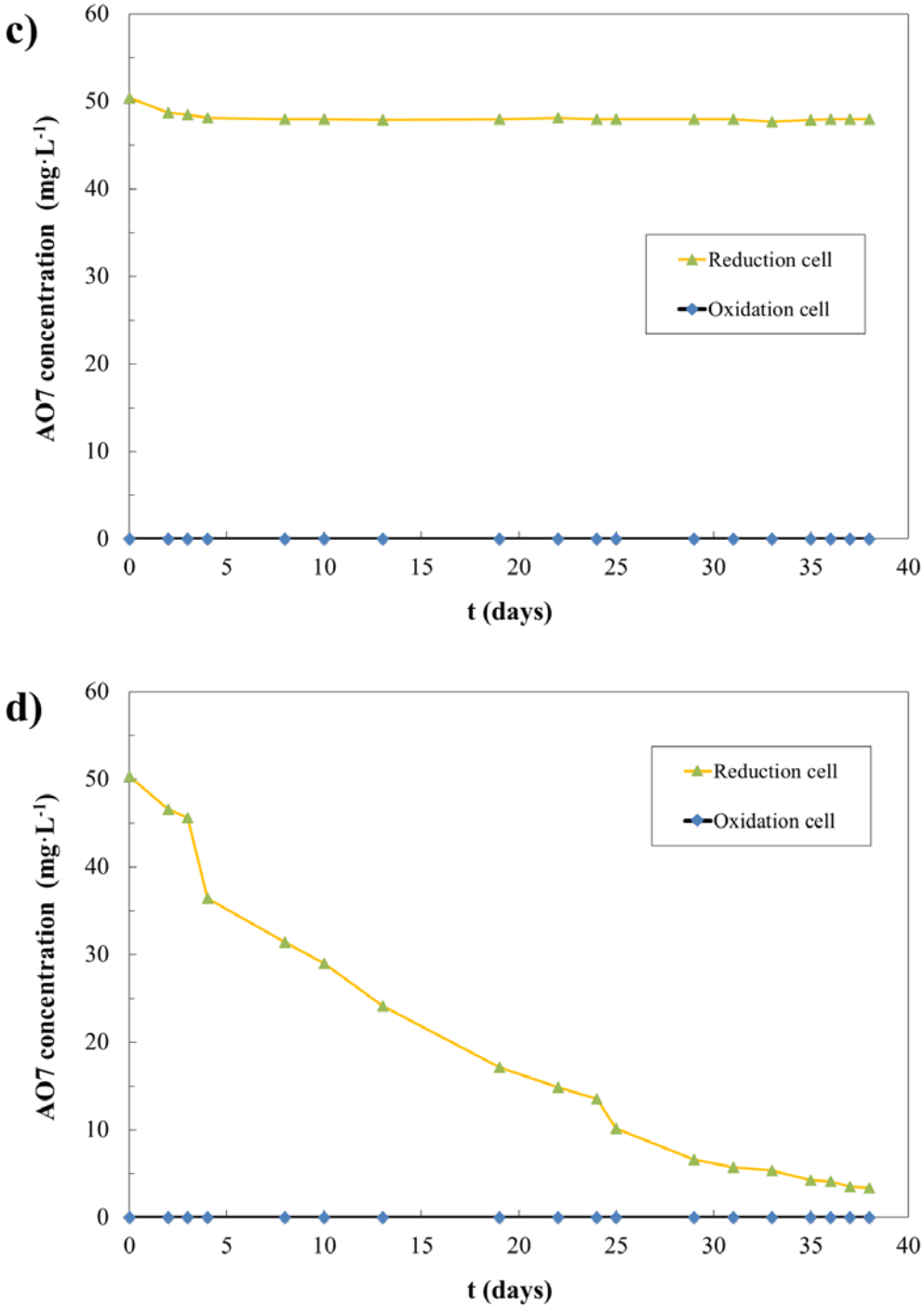

Figure 4.4 Double-cell bioreactor performance under different experimental conditions. CS (a) and CSCM (c) without microorganisms; CS (b) and CSCM (d) with microorganisms. [Feed dye concentration: 50 mg·mL^{-1}, Sodium acetate: AO7 2:1, temperature 37ºC]

An inspection of the Figs. 4.4a-d clearly evidences that only the combination of a carbon layer with a supported biofilm gives significant biodegradation rates (Figure

4.4d). Under these conditions, the concentration of AO7 in the reduction chamber was brought below 5 $mg \cdot L^{-1}$ in less than 40 days, without appearance of color in the oxidation chamber. An appreciable biofilm progressively grew over the carbon membrane after some days of operation as can be seen in Figure 4.5 and, simultaneously, the bioreactor activity increased notably. The equivalent biological experiment was also performed with commercial CS and the results are showed in Figure 4.4b. The AO7 concentration just decreased from 55 to 35 $mg \cdot L^{-1}$ at the end of the experimental time. Therefore, poorer removal rates were achieved in comparison with the CSCM. The experiments were also reproduced in absence of the microorganisms, Figure 4.4c, where the dye concentration remained over 45 $mg \cdot L^{-1}$ after 40 days by using the CSCM. In turn, the same experiment but using the commercial CS showed that the dye concentration progressively decreased up to around 10 mg/L, basically due to the higher transport to the oxidation chamber where the dye concentration correspondingly increased. Therefore, taking into account the four scenarios, it was proven that the carbon material allows higher biodegradation of this azo compound. As it was previously reported in the literature [16], the biologically active carbon is able to act as redox mediator, here facilitating the exchange of electrons between the chambers. At the end of the experimental period, the AO7 removal reached with the CSCMs was three times higher in comparison with the non-modified membranes. However, the experiments with CSs suggest that the diffusion take an important role over this process. Thus, the removal of the AO7 could be even higher increasing the diffusion through the CSCMs. The presence of the carbon layer in the CSCM adds an additional barrier to the dye diffusion that is not as effective as in the CS (Figure 4a and 4c). It could be possible through applying a small positive transmembrane pressure or by physical modification of the membrane surface.

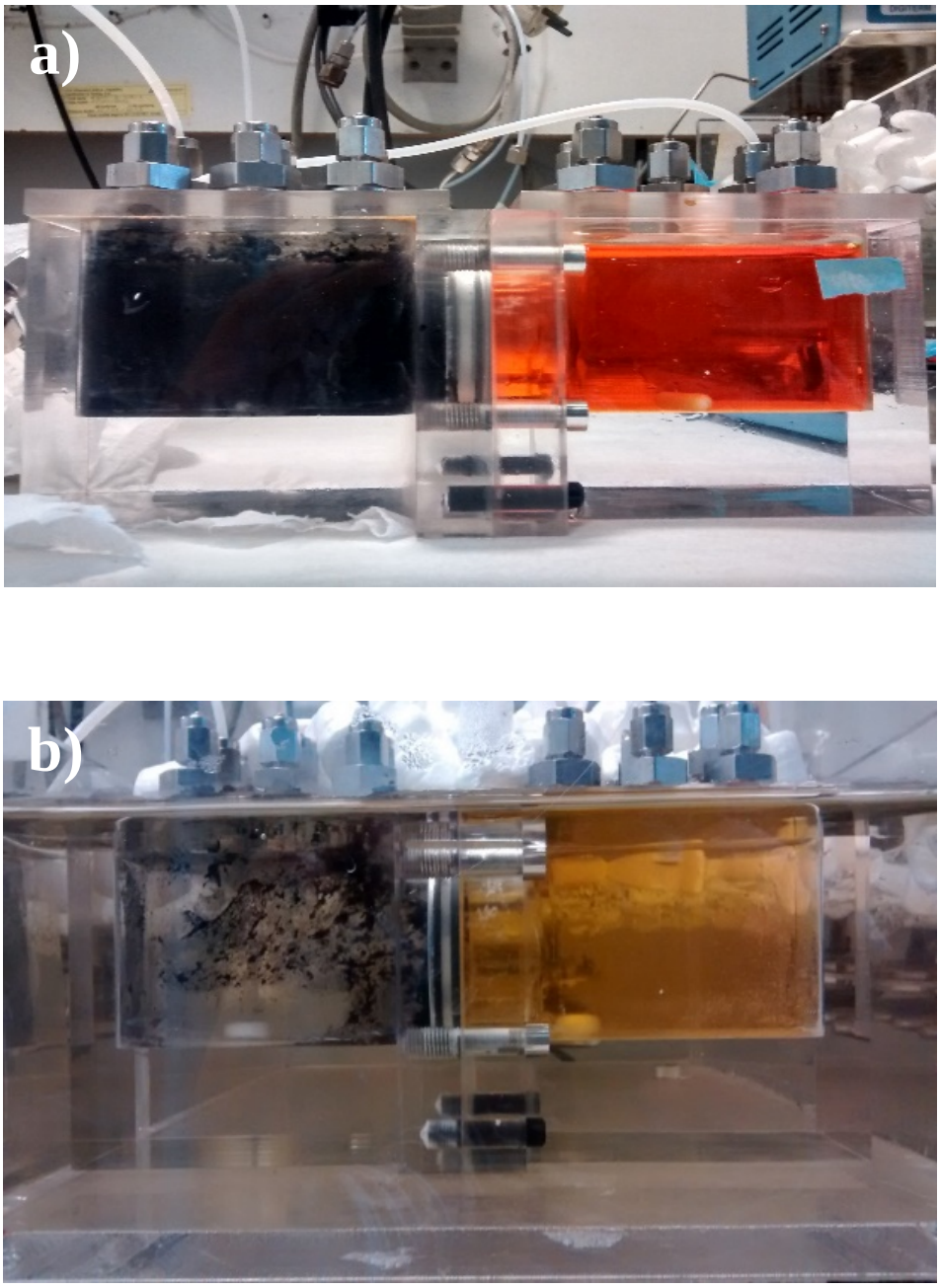

Figure 4.5 CSCM Bioreactors after 0 (a) and 15 (b) days of operation.

4.3.2.1 Influence of the dye concentration.

The concentration of the target compound was modified to study the influence of this parameter and the results are presented in Figure 4.6. As can be expected, highly concentrated solutions of AO7 required longer periods for a complete disappearance; the batches loading dye concentrations of 50 and 100 $mg \cdot L^{-1}$ were completely degraded after 15 and 25 days, respectively. Taking into account the experimental results, the

process was not significantly affected by the toxic nature of these compounds under the concentrations tested in this study.

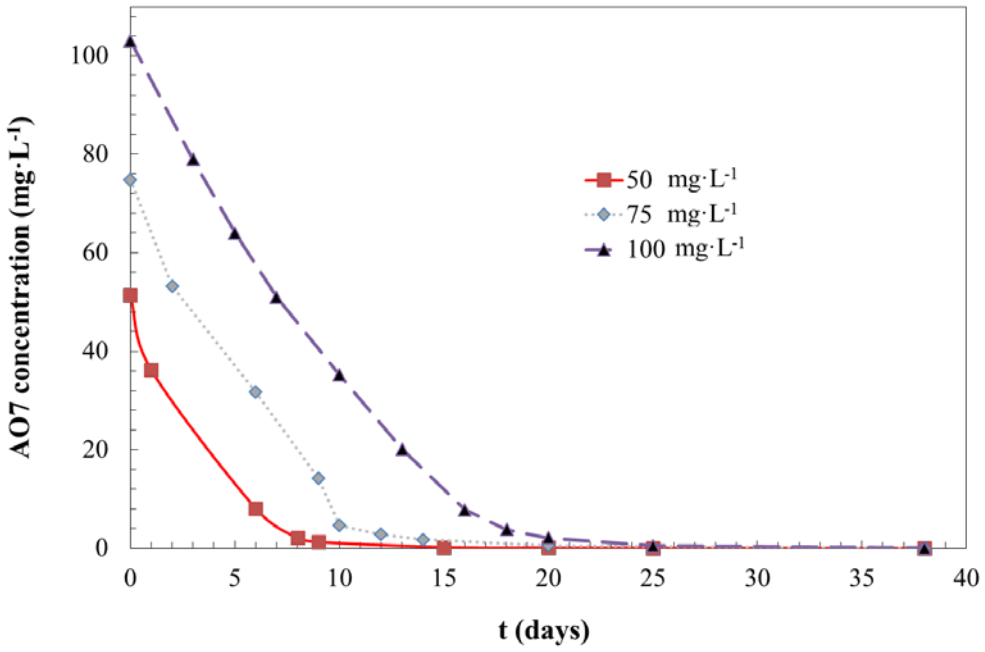

Figure 4.6 Influence of the dye concentration ([NaAc:AO7] 10:1, temperature 37ºC).

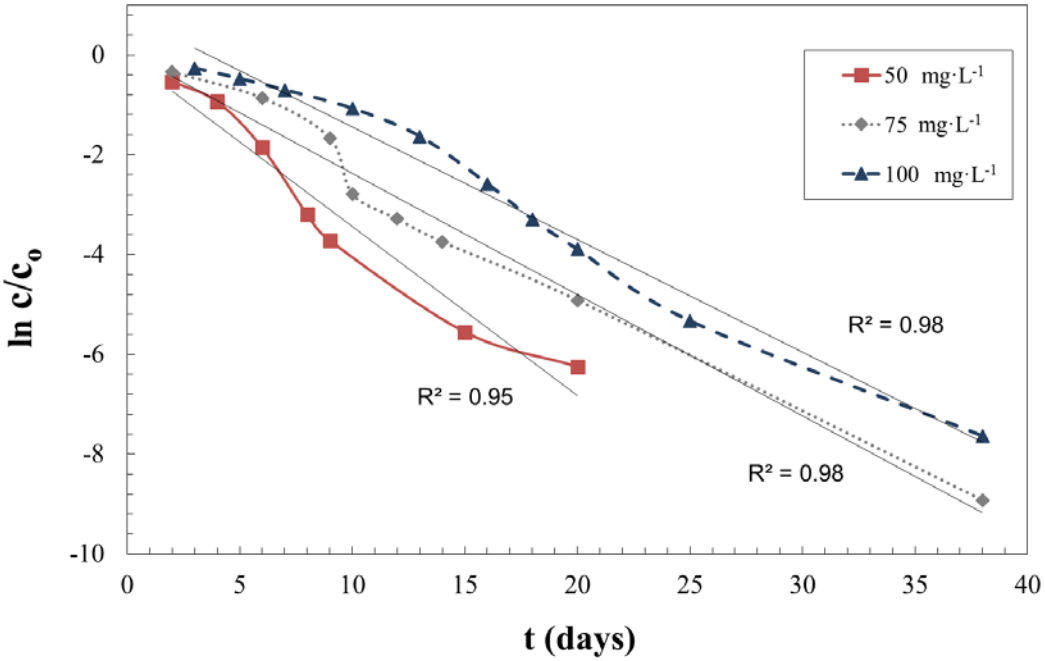

Figure 4.7 First-order kinetic model for the AO7 ([NaAc:AO7] 10:1, temperature 37ºC).

As seen in the Figure 4.7, the reduction of AO7 closely obeyed the first-order kinetics for all the feed dye concentrations tested, which is in agreement with the literature [29]. It suggests that, under the studied operating conditions, the azo dye reduction is related to the dye concentration. In fact, many previous studies pointed out that this process follows first-order kinetic models [30–34]. The kinetic constants were 0.22, 0.24, and 0.34 day^{-1} in case of dye solutions of 50, 75, and 100 $mg \cdot L^{-1}$, respectively. Higher concentrations of the target compound in the membrane may promote a biofilm with different microorganisms and probably more adapted to this toxic compound, increasing this way the biodegradation rates.

4.3.2.2 Influence of the external carbon source and dye ratio

The impact of the mass ratio between the sodium acetate and the AO7 on the biodegradation was also evaluated. As can be seen in Figure 4.8, a complete degradation of the loaded AO7 required about 12 and 38 days in case of [10:1] and [2:1] ratios, respectively. Therefore, there is an evident influence of this relation; an increase of the electron source promotes a faster degradation of the azo dye solution. It suggests that a denser current of electrons enhances the reductive break of the azo dye. On the other hand, as evidenced from Figure 4.8, the operation with low ratios of external carbon source [2:1] shows an initial period of low activity or acclimation. On the contrary, the increase of the external carbon source [5:1, 10:1] promotes a faster development of the biofilm. This fact allows reaching appreciable dye removal rates from the beginning of the operation.

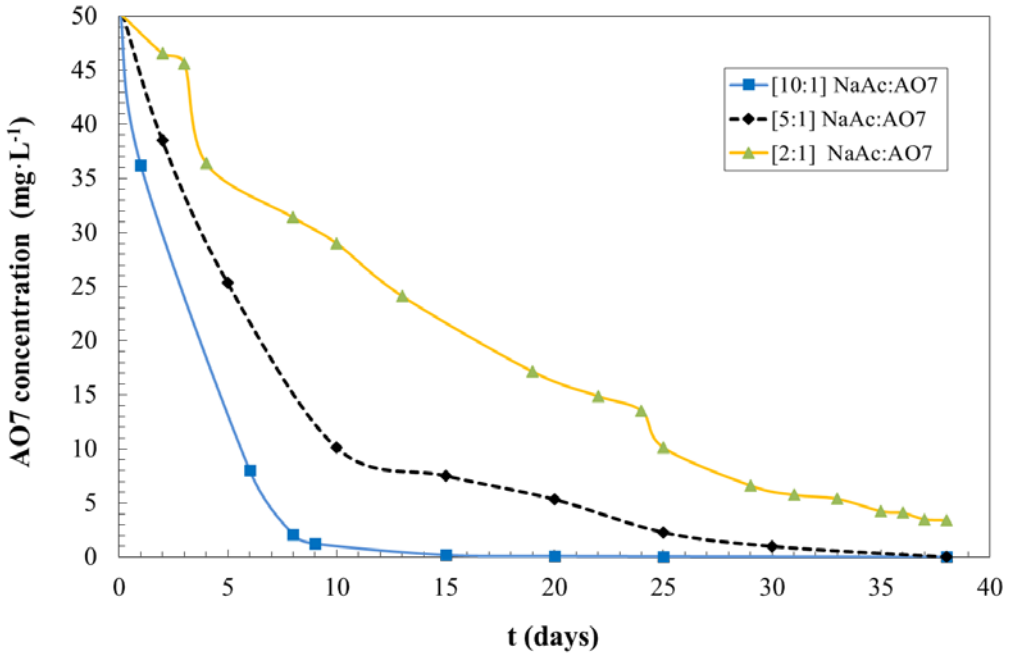

Figure 4.8 Effect of the mass ratio between the external carbon source and the azo dye. [AO7 initial concentration: 50 mg·L^{-1}, [NaAc: AO7] = 2:1, temperature 37ºC].

4.3.2.3 Biodegradation of different azo dyes

The biodegradation of different azo dyes, TAR, AOG and AO7 was evaluated under the same conditions, i.e. feed dye concentration 50 mg·L^{-1}. The CSCM was prepared under the procedure previously detailed. The external carbon source to dye ratio selected was 10:1. The same inoculum of anaerobic mixed sludge was introduced in all the bioreactors. The temperature of operation was again 37 ºC.

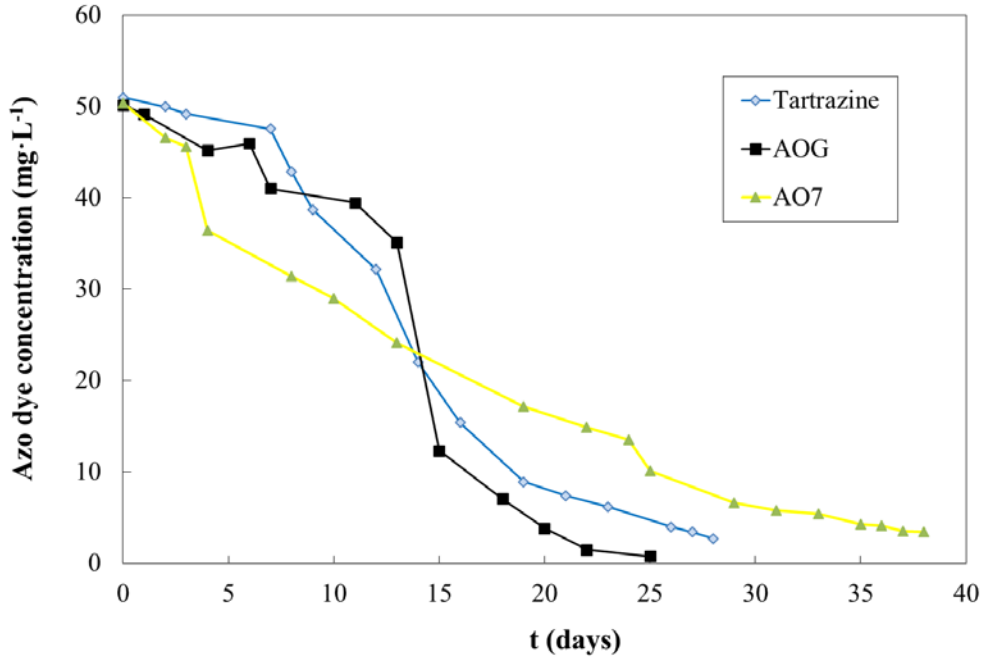

Figure 4.9 Comparison of the biodegradation of different azo dyes.

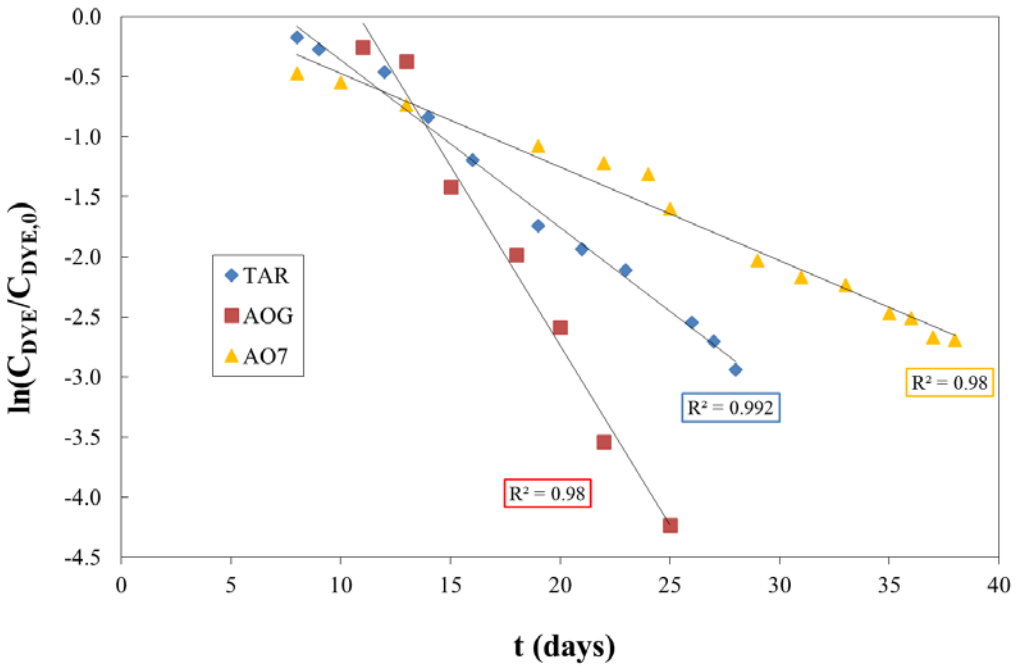

Figure 4.10 Kinetic of the biodegradation of different azo dyes.

As can be seen in Figure 4.9, the acclimation period is longer for TAR, although later the biodegradation is faster than for AOG and AO7. However, the biodegradation rate progressively speeds down, which indicates a potential inhibition due to the by-products, probably due to the occurrence of more complex amines. The rate of

degradation of AOG was higher than that of TAR or AO7, i.e. 90% was reached after 20, 27 and 37 days for AOG, TAR and AO7, respectively. This reactivity coincides with previous reports in the literature [5]. It can be also related to the chemical structure of each compound. As can be noted in Figure 4.1, TAR molecule presents a more complex structure than AOG, i.e. number of functional groups and double bonds, so this complicates its degradation and prolongs the needed time of operation for a complete removal. The slower biodegradation of AO7 in comparison with the other azo dyes can be related to different reasons such as potential inhibition due to the by-products or the presence of different mixed culture carrying out the bioprocess. Note that the AO7 experiment was not performed simultaneously with the AOG and TAR ones; thus, the inoculum, a microbial consortium taken from a conventional wastewater plant, may present different microorganisms. Regarding the kinetic of these processes, it was found that all fit a first-order model (Figure 4.10) in concordance with previous reports of azo dyes degradation kinetic studies [29,35]. The first-order constants were 0.30, 0,14 and 0.08 d^{-1} for AOG, TAR, and AO7, respectively. Therefore, under the operation conditions chosen in this study, the degradation rate is proportional to the dye concentration in all cases [29].

4.3.2.4 Characterization of the biofilm over the carbon membrane.

At the beginning of the operation, the biomass was totally dispersed around the bioreactor chamber (Figure 4.5a). Progressively, the mixed culture was creating a film over the carbon membrane (Figure 4.11a). At the end of the operation, the stable biofilm was characterized by TEM analysis. The samples of the carbon membrane biofilm (0.25 µL) were taken after 10 days of operation. Figures 4.11a-d show the microscopy characterization of the biofilm created over the carbon membrane processing TAR.

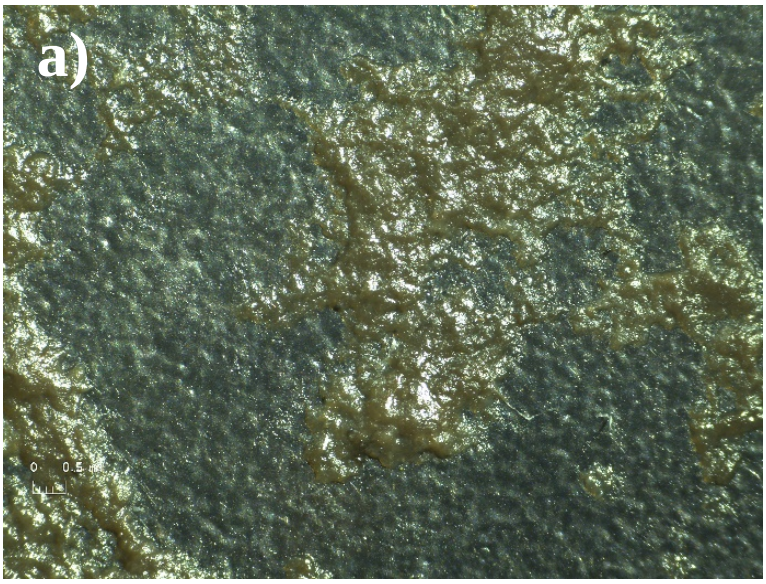
a)

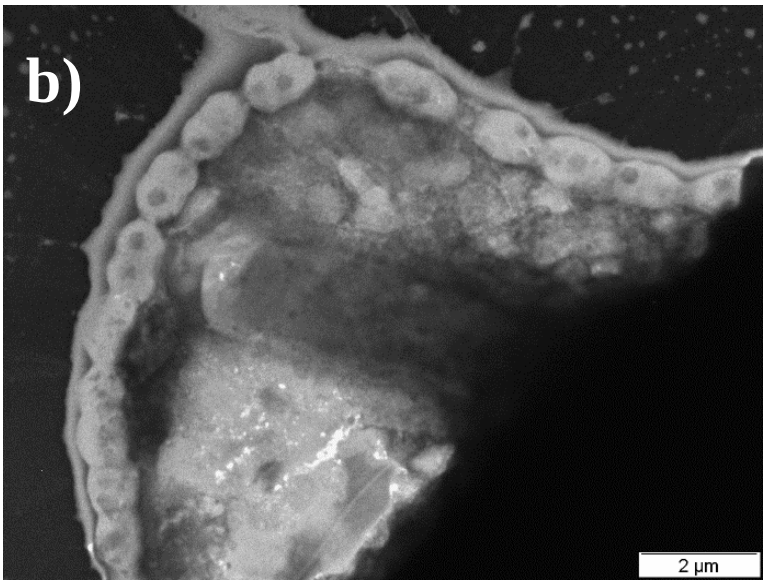
b)
2 µm

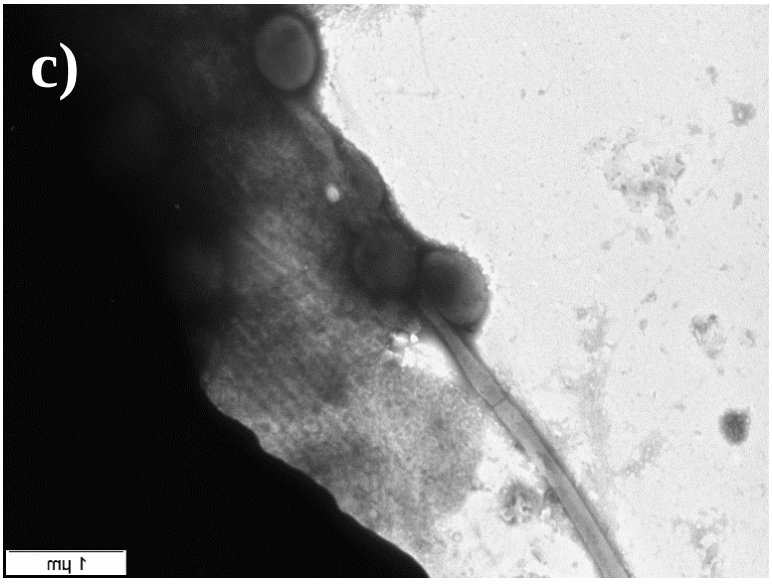
c)

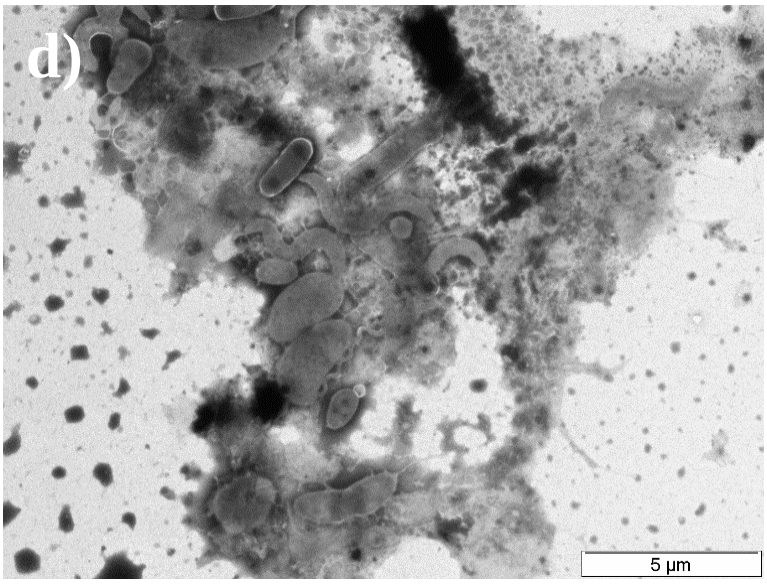

Figure 4.11 Optical microscope (a) and TEM (b-d) images of a biofilm sample.

As commented, the creation of a robust biofilm was found critical in order to reach high azo dye removal rates. The microscopy pictures suggest that most of the identified microorganisms belong to the bacillus bacteria group (Figure 4.11b). However, there were also observed some fungi (Figure 4.11c) and spirochaetes (Figure 4.11d). This microorganism consortium could be expected since the inoculum was prepared from a mixed anaerobic sludge collected from a conventional wastewater treatment plant, where a large number of microorganism groups are typically present. The synergy of all these groups allows reaching a higher level of mineralization of these azo dyes.

4.4 Conclusions.

A novel double chamber bioreactor was successfully tested as an alternative technique for the removal of azo dyes. The redox system was operated under batch-mode degrading completely AO7 solutions with an initial concentration of 50 or 150 $mg \cdot L^{-1}$ after 8 and 28 days, respectively. This system was also able to reduce effectively different azo dyes, although the oxidation of the secondary carbon source, which furnishes the required electrons, was conducted in a separate chamber. The key of the process was a synthesized carbon membrane, used as an efficient connector between

both cells, because it keeps segregated the oxidation and reduction media but allows the transfer of electrons between both. Therefore, the carbon film consistently acted as redox mediator. This study proved a new configuration that allows treating independently different wastewater effluents either by biological oxidation or reduction.

In addition, it was evidenced that a greater ratio between the electron donor, i.e. sodium acetate, and the azo dye enhances the biodegradation process. This fact suggests that denser electron currents make easier the anaerobic reductive cleavage of the azo bonds.

With respect to the biodegradation of several azo dyes, it was observed that longer operation times were needed to achieve complete removal of the more complex compounds such as TAR in comparison with other simpler compounds, i.e. AOG.

Finally, the microscopy characterization of the biofilm evidenced a mixed microbial consortium in the biomass present at the steady operation of this redox system. It could be expected since the inoculum was taken from the biological treatment of a municipal WWTP.

Acknowledgements

The Spanish MINECO and FEDER funded this project through the grant (CTM2011-23069 and CTM2015-67970-P). Moreover, the Spanish Ministry of Education, Culture and Sports is greatly acknowledged by providing a pre-doctoral scholarship (BES-2012-059675). The authors' research group is recognized by the *Comissionat per a Universitats i Recerca del DIUE de la Generalitat de Catalunya (2014 SGR 1065)* and supported by the Universitat Rovira i Virgili (2014PFR-URV-B2-35).

References

[1] R.G. Saratale, G.D. Saratale, J.S. Chang, S.P. Govindwar, Bacterial decolorization and degradation of azo dyes: A review, J. Taiwan Inst. Chem. Eng. 42 (2011) 138–157. doi:10.1016/j.jtice.2010.06.006.

[2] H. Ollgaard, L. Frost, J. Galster, O.C. Hensen, Survey of azo-colorants in Denmark: Consumption, use, health and environmental aspects, Danish Environmental Protection Agency, Copenhagen (DK), 1998. http://www2.mst.dk/udgiv/publications/1999/87-7909-548-8/pdf/87-7909-546-1.pdf.

[3] A. Gottlieb, C. Shaw, A. Smith, A. Wheatley, S. Forsythe, The toxicity of textile reactive azo dyes after hydrolysis and decolourisation, J. Biotechnol. 101 (2003) 49–56. doi:10.1016/S0168-1656(02)00302-4.

[4] J. Feng, C.E. Cerniglia, H. Chen, Toxicological significance of azo dye metabolism by human intestinal microbiota, Front. Biosci. (Elite Ed). 4 (2012) 568–86. doi:10.2741/400.

[5] M. Solís, A. Solís, H.I. Pérez, N. Manjarrez, M. Flores, Microbial decolouration of azo dyes: A review, Process Biochem. 47 (2012) 1723–1748. doi:10.1016/j.procbio.2012.08.014.

[6] B. Zhang, Z. Wang, X. Zhou, C. Shi, H. Guo, C. Feng, Electrochemical decolorization of methyl orange powered by bioelectricity from single-chamber microbial fuel cells., Bioresour. Technol. 181 (2015) 360–2. doi:10.1016/j.biortech.2015.01.076.

[7] A.H. Konsowa, H.B. Abd El-Rahman, M.A. Moustafa, Removal of azo dye acid orange 7 using aerobic membrane bioreactor, Alexandria Eng. J. 50 (2011) 117–125. http://dx.doi.org/10.1016/j.aej.2011.01.014.

[8] F.P. van der Zee, S. Villaverde, Combined anaerobic–aerobic treatment of azo dyes—A short review of bioreactor studies, Water Res. 39 (2005) 1425–1440. doi:10.1016/j.watres.2005.03.007.

[9] G. Mezohegyi, C. Bengoa, F. Stuber, J. Font, A. Fabregat, A. Fortuny, Novel bioreactor design for decolourisation of azo dye effluents, Chem. Eng. J. 143 (2008) 293–298. doi:10.1016/j.cej.2008.05.006.

[10] G. Mezohegyi, F.P. van der Zee, J. Font, A. Fortuny, A. Fabregat, Towards advanced aqueous dye removal processes: A short review on the versatile role of activated carbon, J. Environ. Manage. 102 (2012) 148–164. http://dx.doi.org/10.1016/j.jenvman.2012.02.021.

[11] A. Cardenas-Robles, E. Martinez, I. Rendon-Alcantar, C. Frontana, L. Gonzalez-Gutierrez, Development of an activated carbon-packed microbial bioelectrochemical system for azo dye degradation., Bioresour. Technol. 127 (2013) 37–43. doi:10.1016/j.biortech.2012.09.066.

[12] Y. García-Martínez, C. Bengoa, F. Stüber, A. Fortuny, J. Font, A. Fabregat, Biodegradation of acid orange 7 in an anaerobic–aerobic sequential treatment system, Chem. Eng. Process. Process Intensif. 94 (2015) 99–104. doi:http://dx.doi.org/10.1016/j.cep.2014.12.011.

[13] Y. Matsui, T. Sanogawa, N. Aoki, S. Mima, T. Matsushita, Evaluating submicron-sized activated carbon adsorption for microfiltration pretreatment, Water Sci. Technol. Water Supply. 6 (2006) 149–155. doi:10.2166/ws.2006.017.

[14] G.T. Seo, S. Ohgaki, Y. Suzuki, Sorption characteristics of biological powdered activated carbon in BPAC-MF (biological powdered activated carbon-microfiltration) system for refractory organic removal, Adsorpt. Water Environ. Treat. Process. Sel. Proc. 1st Int. Spec. Conf. Adsorpt. Water Environ. Treat. Process. 35 (1997) 163–170. doi:10.1016/S0273-1223(97)00127-3.

[15] S. Chang, T.D. Waite, P.E.A. Ong, A.I. Schäfer, A.G. Fane, Assessment of trace estrogenic contaminants removal by coagulant addition, powdered activated carbon adsorption and powdered activated carbon/microfiltration processes, J. Environ. Eng. 130 (2004) 736–742. doi:10.1061/(ASCE)0733-9372(2004)130:7(736).

[16] G. Mezohegyi, F. Gonçalves, J.J.M. Órfão, A. Fabregat, A. Fortuny, J. Font, et al., Tailored activated carbons as catalysts in biodecolourisation of textile azo dyes, Appl. Catal. B Environ. 94 (2010) 179–185. doi:10.1016/j.apcatb.2009.11.007.

[17] A.D. Bokare, R.C. Chikate, C. V. Rode, K.M. Paknikar, Iron-nickel bimetallic nanoparticles for reductive degradation of azo dye Orange G in aqueous solution, Appl. Catal. B Environ. 79 (2008) 270–278. doi:10.1016/j.apcatb.2007.10.033.

[18] Z. Li, X. Zhang, J. Lin, S. Han, L. Lei, Azo dye treatment with simultaneous electricity production in an anaerobic-aerobic sequential reactor and microbial fuel cell coupled system., Bioresour. Technol. 101 (2010) 4440–5.

doi:10.1016/j.biortech.2010.01.114.

[19] B.E.L. Baêta, H.J. Luna, A.L. Sanson, S.Q. Silva, S.F. Aquino, Degradation of a model azo dye in submerged anaerobic membrane bioreactor (SAMBR) operated with powdered activated carbon (PAC)., J. Environ. Manage. 128 (2013) 462–70. doi:10.1016/j.jenvman.2013.05.038.

[20] R.A. Pereira, A.F. Salvador, P. Dias, M.F.R. Pereira, M.M. Alves, L. Pereira, Perspectives on carbon materials as powerful catalysts in continuous anaerobic bioreactors, Water Res. 101 (2016) 441–447. doi:10.1016/j.watres.2016.06.004.

[21] S. Gurunathan, J.W. Han, V. Eppakayala, J.H. Kim, Microbial reduction of graphene oxide by Escherichia coli: A green chemistry approach, Colloids Surfaces B Biointerfaces. 102 (2013) 772–777. doi:10.1016/j.colsurfb.2012.09.011.

[22] F. Kong, A. Wang, B. Liang, W. Liu, H. Cheng, Improved azo dye decolorization in a modified sleeve-type bioelectrochemical system., Bioresour. Technol. 143 (2013) 669–73. doi:10.1016/j.biortech.2013.06.050.

[23] H.-Y. Wang, A. Bernarda, C.-Y. Huang, D.-J. Lee, J.-S. Chang, Micro-sized microbial fuel cell: a mini-review., Bioresour. Technol. 102 (2011) 235–43. doi:10.1016/j.biortech.2010.07.007.

[24] H. Ding, Y. Li, A. Lu, S. Jin, C. Quan, C. Wang, et al., Photocatalytically improved azo dye reduction in a microbial fuel cell with rutile-cathode., Bioresour. Technol. 101 (2010) 3500–5. doi:10.1016/j.biortech.2009.11.107.

[25] E. Fernando, T. Keshavarz, G. Kyazze, Complete degradation of the azo dye Acid Orange-7 and bioelectricity generation in an integrated microbial fuel cell, aerobic two-stage bioreactor system in continuous flow mode at ambient temperature, Bioresour. Technol. 156 (2014) 155–162. doi:10.1016/j.biortech.2014.01.036.

[26] K. Briceño, D. Montané, R. Garcia-Valls, A. Iulianelli, A. Basile, Fabrication variables affecting the structure and properties of supported carbon molecular sieve membranes for hydrogen separation, J. Memb. Sci. 415–416 (2012) 288–297. doi:10.1016/j.memsci.2012.05.015.

[27] K. Briceño, A. Iulianelli, D. Montané, R. Garcia-Valls, A. Basile, Carbon

molecular sieve membranes supported on non-modified ceramic tubes for hydrogen separation in membrane reactors, ICCE-2011. 37 (2012) 13536–13544. doi:10.1016/j.ijhydene.2012.06.069.

[28] A.F. Ismail, L.I.B. David, A review on the latest development of carbon membranes for gas separation, J. Memb. Sci. 193 (2001) 1–18. doi:10.1016/S0376-7388(01)00510-5.

[29] S. Kalyuzhnyi, N. Yemashova, V. Fedorovich, Kinetics of anaerobic biodecolourisation of azo dyes., Water Sci. Technol. 54 (2006) 73–9. doi: 10.2166/wst.2006.488.

[30] D. Méndez-Paz, F. Omil, J.M. Lema, Anaerobic treatment of azo dye Acid Orange 7 under fed-batch and continuous conditions, Water Res. 39 (2005) 771–778. http://dx.doi.org/10.1016/j.watres.2004.11.022.

[31] K. Wuhrmann, K. Mechsner, T. Kappeler, Investigation on rate --- Determining factors in the microbial reduction of azo dyes, Eur. J. Appl. Microbiol. Biotechnol. 9 (1980) 325–338. doi:10.1007/BF00508109.

[32] K. Mechsner, K. Wuhrmann, Cell permeability as a rate limiting factor in the microbial reduction of sulfonated azo dyes, Eur. J. Appl. Microbiol. Biotechnol. 15 (1982) 123–126. doi:10.1007/BF00499518.

[33] F.P. van der Zee, G. Lettinga, J.A. Field, Azo dye decolourisation by anaerobic granular sludge, Chemosphere. 44 (2001) 1169–1176. doi:http://dx.doi.org/10.1016/S0045-6535(00)00270-8.

[34] C.M. Carliell, S.J. Barclay, N. Naidoo, C.A. Buckley, D.A. Mulholland, E. Senior, Anaerobic decolorisation of reactive dyes in conventional sewage treatment processes, Water SA. 20 (1994) 341–344.

[35] E. Fernando, T. Keshavarz, G. Kyazze, Simultaneous co-metabolic decolourisation of azo dye mixtures and bio-electricity generation under thermophillic (50 °C) and saline conditions by an adapted anaerobic mixed culture in microbial fuel cells., Bioresour. Technol. 127 (2013) 1–8. doi:10.1016/j.biortech.2012.09.065.

UNIVERSITAT ROVIRA I VIRGILI
COMPACT CARBON-BASED MEMBRANE REACTORS FOR ANAEROBIC BIODEGRADATION OF AZO-DYES FROM WASTEWATER
Alberto Giménez Pérez

CHAPTER 5

Synthesis of N-doped and non-doped partially oxidised graphene membranes supported over ceramic materials

The last chapter deals with the preparation of a novel advanced material with an enormous potential to be applied in similar processes as those discussed in this thesis. The study presents a novel graphene-based membrane supported over a ceramic filtration element, including a complete characterization by different techniques such as ESEM or AFM.

Published research paper

Synthesis of N-doped and non-doped partially oxidised graphene membranes supported over ceramic materials

Alberto Giménez-Pérez, Santosh Bikkarolla, John Benson, Christophe Bengoa, Azael Fabregat, Agustí Fortuny, Frank Stüber, Josep Font, Pagona Papakonstantinou.

*Journal of Materials Science 51: 8346–8360 (2016).*DOI: 10.1007/s10853-016-0075-5

UNIVERSITAT ROVIRA I VIRGILI
COMPACT CARBON-BASED MEMBRANE REACTORS FOR ANAEROBIC BIODEGRADATION OF AZO-DYES FROM WASTEWATER
Alberto Giménez Pérez

5.1 Introduction.

From its first report in 2004, graphene has become one of the main attractions of the scientific world due to its outstanding electrical, optical and mechanical properties [1]. Monolayer graphene shows 1 TPa Young's modulus and 130±10 GPa fracture strength being considered the world's strongest material [2]. Some studies have estimated its electrical resistance as only 20.16 Ω/sq [3] and optical transparency around 97.7% [4]. Initially, single layer graphene nanosheets were prepared by mechanical exfoliation of bulk graphite, also known as the "scotch tape" method [5]. However, the exfoliation of highly ordered pyrolytic graphite allows the preparation of only small areas between nanometres and micrometres in lateral dimension [6]. A different approach to synthesise graphene, epitaxial chemical vapor deposition (CVD), is commonly used for applications that require small areas of high quality graphene [7–10]. On the contrary, CVD shows a lack of controllability when transferring graphene films between different substrates and it is not the best technique to synthesise homogeneous large-area size [11].

An absolutely different method is the chemical reduction of exfoliated graphite oxide [12]; unlike the others techniques, this one allows the synthesis of graphene in large scale and reasonable cost [13]. In 1958, Hummers and Offeman [14] developed a rapid and relatively safe method to synthesise highly oxidised graphene oxide (GO) from graphite. This technique introduced a new via to prepare graphene oxide by using $KMnO_4$ and $NaNO_3$ in concentrated H_2SO_4, which is suitable for large scale production [15] and is commonly used to prepare large GO films [16–19]. GO oxygen groups can be removed by different physical [20] or chemical methods [21]. In this study, GO was reduced by the solvo-thermal method [22].

GO is a promising material to fabricate membranes because of its hydrophilicity, excellent strength, large surface area, low flux resistance and relevant permeation [23]. In addition, the intrinsic 3D heterogeneous structure of GO films may also help to improve the selectivity [24, 25], since open gaps between the stacked platelets are approximately 1 nm wide [26], thus these gaps can act as nanopores for molecular transport [27]. GO membranes can be useful in many applications, such as filters for water treatment, catalysis, electrical devices, or molecular sieving processes [28–30]. The fabrication of these GO films involves different techniques including Langmuir–

Blodgett assembly [31], vacuum filtration [24], molecular templates [19], spin-coating [13, 32], and spray-coating. On the contrary, reduced graphene oxide (RGO), yet showing hydrophobic properties, provides higher electrical conductivity than GO. For these reasons, RGO membranes can be applied in water processes where minimizing the electrical resistance is needed [33]. Great efforts have been devoted on depositing uniform films onto substrates, which has been considered as a major hurdle; this study is focused on the vacuum filtration technique, which has been successfully applied to prepare graphene films with different oxidation degree. A notable advantage is the possibility of controlling perfectly the membrane thickness [24, 29].

Graphene membranes are reported as freestanding films [34–39] or supported ones [40, 41]. However, most water treatment processes are subjected to high pressures so membranes must be robust enough as to operate for long periods, therefore supported membranes are preferred. Ceramic materials have been reported as membrane support because they possess many important advantages such as high thermal and chemical stability, pressure resistance, long lifetime, and catalytic properties coming from their intrinsic nature [42, 43]. Specially, the chemical stability is highly significant for membrane modification or preparation processes. Hence, ceramic porous elements offer the possibility to be used as support for the graphene layer becoming a composite membrane.

This study deals with the preparation of graphene oxide and nitrogenated reduced graphene oxide (GO and NrGO) membranes supported over ceramic porous materials. To the best of our knowledge, there are not previous studies involving the synthesis of GO or NrGO membranes supported over ceramics (ZrO_2-TiO_2) focused on the influence of the graphene oxidising degree, amount of membrane precursor employed for the preparation or the pore size of the ceramic support. These membranes could enhance many environmental processes where other adsorbent and conductive materials are currently being used [44, 45], such as activated carbon filters [46]. Potential applications include photocatalytic or biological processes. Photocatalysis is a clean technology, which uses semiconductor-based nanomaterials such as carbon-based films (TiO_2 /activated carbon) [47] to separate and remediate contaminated organic wastewater [48]. However, decorating titania photocatalyst with graphene oxide (GO) is of particular interest due to GO's ability to increase the photocatalytic activity of TiO_2 [49]. On the other hand, graphene-based membranes can be employed to intensify the

biodegradation of recalcitrant pollutants present in wastewater, which cannot be efficiently removed by conventional methods. Some of these processes are limited by the electron transfer in redox systems [46]; at this point both GO and specially NrGO provide better properties as electron mediator than other ones such as activated carbon that have been widely employed last decades [50]. Moreover, GO offers a 3D sponge structure favouring the microbial growth and presents excellent adsorption capacity [51]. The adsorption capacity and the presence of an electron shuttle are highly beneficial for the degradation of recalcitrant organic compounds from wastewater [52]. Additionally, the proposed catalytic membrane allows the degradation, separation, and microorganism retention in a single stage thus intensifying the process.

5.2 Experimental.

5.2.1 Membrane precursor preparation.

5.2.1.1 Highly oxidised graphene powder (GO).

Highly oxidised graphene (GO) was synthesised following a modified Hummer's process [22]. Pristine graphite powder was purchased by Fluka with average particle size $\leq$ 20 μm. The starting material, i.e. graphite powder, was ground for 30 min by using mortar and pestle, and then 2.5 g of ground graphite were mixed with 2 g of $NaNO_3$ in a 250 ml flask. Sulphuric acid (70 ml) was added to the blend and stirred until homogenised. The mixture was cooled in an ice bath, 10 g of $KMnO_4$ were then added, and left overnight followed by heating at 50 ºC for 24 h. Subsequently, 10 g of $KMnO_4$ and 70 ml of water were slowly added to the mixture and kept stirring for 24 h. The graphite oxide formed was poured into 400 ml of ice water and then 3 ml of H_2O_2 were added and stirred overnight. The graphite oxide mixture was purified by dispersing in 500 ml aqueous solution of 3 wt. % H_2SO_4 and 0.5 wt. % H_2O_2. After 24 h, the graphite oxide pellet was collected by centrifuging at 3000 rpm for 30 min and the supernatant was removed. This process was repeated 5 times. The solid product obtained was rinsed with copious water and dried in oven. Graphite oxide was exfoliated in water by ultrasonication for 2 h to obtain GO sheets. The GO dispersion was centrifuged at 1000 rpm for 5 min to remove any thicker sheets and the supernatant was again centrifuged at 3000 rpm for 30 min. The obtained GO pellet was dried in

oven at 60 ºC for 48 h. Before sonication and separation the material is called as graphite oxide and after sonication and separation the material is referred to as GO. All the chemicals were purchased from Sigma-Aldrich.

5.2.1.2 Nitrogen doped reduced graphene oxide powder (NrGO).

The preparation of N-doped graphene oxide is based on previous studies showing that N-doped graphene exhibits better electrocatalytic activity than graphene [53]. The enhanced performance of N-graphene is mainly attributed to the existence of nitrogen functional groups, oxygen-containing groups and structural defects.

Nitrogen doped reduced graphene oxide (NrGO) was synthesised through solvothermal reaction of GO with ammonia and hydrazine [54]. In a typical experiment synthesised GO was suspended in water to give a concentration of 1 $mg \cdot ml^{-1}$ followed by sonication for 30 min to disperse the material in water. The pH of the solution was adjusted to 10 by using ammonia hydroxide and then 1 ml of hydrazine (35 wt. % in H_2O) was added to the solution and stirred for 15 min. The resultant solution was transferred to a 100 ml Teflon lined vessel to carry out the solvothermal reaction at 160 ºC and 5 bar for 3 h. The resultant product was cleaned with plenty of deionised (DI) water and collected by centrifugation at 3000 rpm for 45 min. The pellet was dried under vacuum at 60 ºC for 48 h.

5.2.2 Membrane supports.

Composite ceramic disks (Ø 47 mm; thickness 28 mm) made of TiO_2 with a slender superficial layer of ZrO_2-TiO_2 were provided by TAMI Industries (France); these are filtration elements in the range of ultrafiltration or fine ultrafiltration with different pore sizes equivalent to 1, 15, 50, and 150 kDa molecular weight cut off (MWCO). Their intrinsic properties ─physical strength, chemical and thermal inertia or solvent insensitivity─ make them suitable for synthesising membranes with relatively long-life and reusability after an adequate chemical cleaning procedure involving diluted nitric, phosphoric acid or sodium hydroxide. This fact is extremely beneficial with a view to a potential application in wastewater treatments or water purification.

5.2.3 Synthesis of graphene (GO or NrGO) membranes.

Homogeneous GO or NrGO solutions were prepared by dispersing a certain amount (10 mg) of previously synthesised graphene powder into deionised water by sonication for 45 min. These solutions (GO or NrGO) were vacuum-filtrated through the final membrane support, forming a superimposed film with controllable thickness on the surface of the ceramic support. The absence of requirement for peeling-off the deposited film reduces the time of preparation. This length of time was around 5-15 minutes depending on the ceramic support pore size. After the preparation, the membrane was dried for 24 h at 40 °C and ready to be used.

5.2.4 Membrane characterisation.

Transmission electron microscopy (TEM JEOL, JEM-1011, USA) and environmental scanning electron microscopy (ESEM QUANTA 600, FEI, Dawson Creek Drive, Hillsboro, OR, USA) were used to study the synthesised material.

Membrane microstructure was examined by AFM (Pico Plus 2500 from Molecular Imaging, Bid-Service, LLC, Freehold, NJ, and USA) operating in the tapping mode.

Membrane precursor properties were further studied by conducting Raman spectroscopy. The analyses were performed at room temperature with a LabRAM 300 Raman spectrometer (Horiba Jobin Yvon) equipped with a HeNe (633nm) laser and a motorized XYZ mapping stage.

X-Ray diffraction (XRD) measurements were also performed using a Bruker-AXS D8-Discover diffractometer equipped with parallel incident beam (Göbel mirror), vertical θ-θ goniometer, XYZ motorized stage and with a GADDS (General Area Diffraction System). Samples were placed directly on the sample holder and the area of interest was selected with the aid of a video-laser focusing system. An X-ray collimator system allowed analyzing areas of 500 μm. The X-ray diffractometer was operated at 40 kV and 20 mA employing a monochromatic CuK_{α} radiation source (λ = 1.54 Å). The GADDS detector was a HI-STAR (multiwire proportional counter of 30x30 cm with a 1024x1024 pixel) placed at 15 cm from the sample and covering a range of 3-37º 2θ.

The synthesised powders were also examined with an X-ray photoelectron spectroscopy (XPS) system (Kratos Axis Ultra DLD spectrometer) equipped with a monochromatic AlK_{α} X-ray (1486.6 eV). The chamber pressure was maintained below $2.39 \cdot 10^{-11}$ bar and surface charging was compensated with a secondary electron gun.

The membrane electrical resistance was measured through a multi height microposition four point probing system combined with a Keithley K2420 SourceMeter.

5.2.5 Membrane filtration tests.

The deionised (DI) water flux of the prepared membranes was measured in a dead-end cell (TAMI Industries) equipped to hold ceramic membranes in form of disks. The effective area of membrane surface was 13.1 cm^2. All the experiments were carried out until steady state at 25 ºC and a constant trans-membrane pressure (TMP) of 0.2 bar. The permeate flux was continuously monitored by a precision balance and automatically recorded in a computer database. A scheme of the experimental setup is shown in Fig. 5.1.

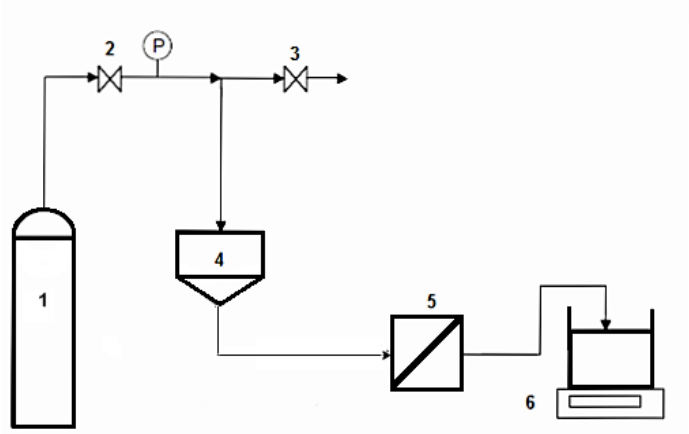

Figure 5.1 Dead-end filtration experimental setup: (1) nitrogen gas cylinder; (2) gas pressure regulator; (3) relief valve; (4) feed tank; (5) membrane holder; (6) weighing scale.

Permeation flux is calculated according to the Equation 1 [55].

$$J_w = \frac{V}{A \cdot t} \quad (1)$$

where, J_w is the pure water flux ($m^3 \cdot m^{-2} \cdot h^{-1}$), V is the collected permeate volume (m^3), A is the membrane active area (m^2), and t is the permeation time (h).

5.3 Results and discussion

5.3.1 Graphene (GO or NrGO) synthesised powder characterisation.

GO powder (1 mg) in N-methyl-2-pyrrolidone (NMP) solutions were characterised by ESEM and TEM (Fig. 2-3) after applying ultrasounds for 15 minutes and next quick solvent evaporation through infrared lamp. The powder sample was deposited onto an aluminium support, the solvent was evaporated and immediately introduced into the ESEM. In the case of TEM analysis, a drop of sample was placed on a *200 μm mesh copper grid* with a *Formvar* film.

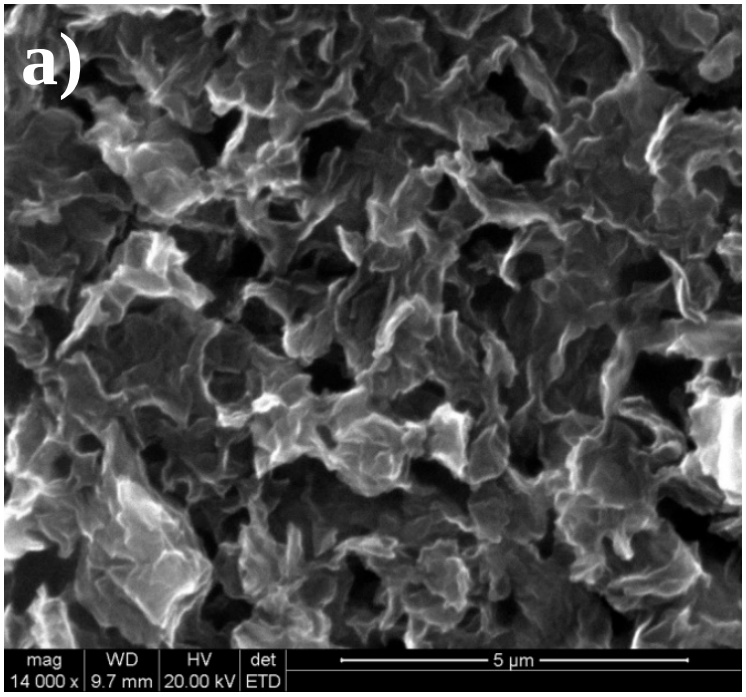

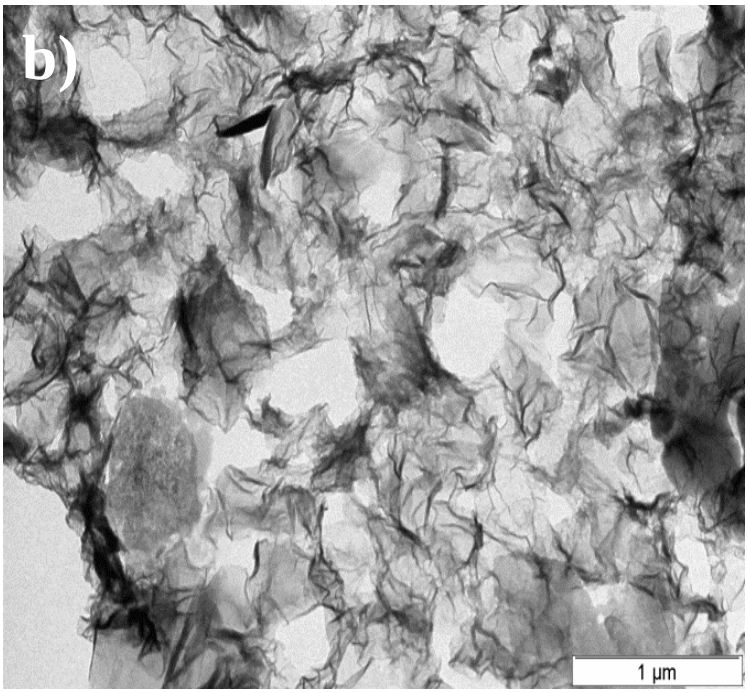

Figure 5.2 ESEM (a) and TEM (b) images of GO powder synthesised by a modification of Hummer's method.

Hydrophilic GO powder (Fig. 2a-b) showed a 3D homogenous material distribution of particle aggregates.

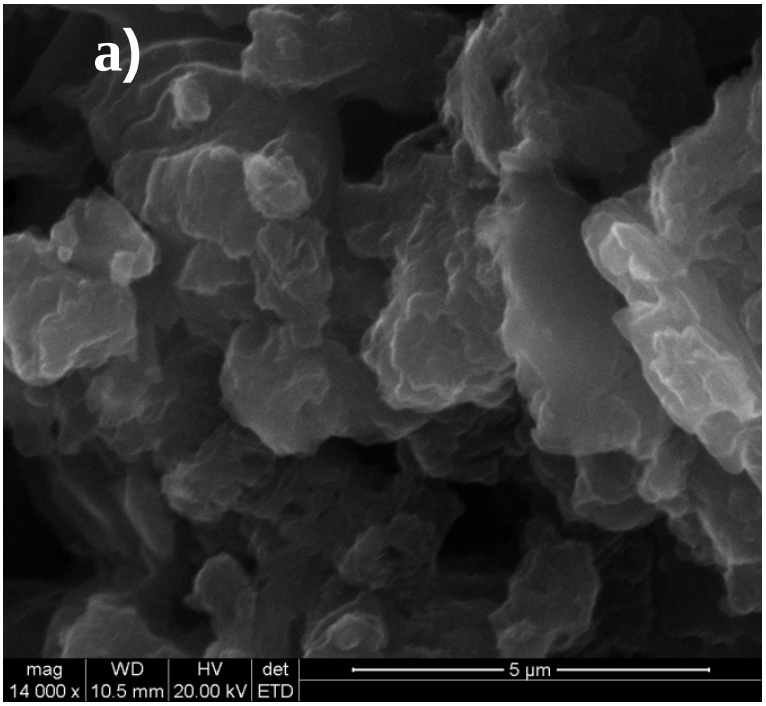

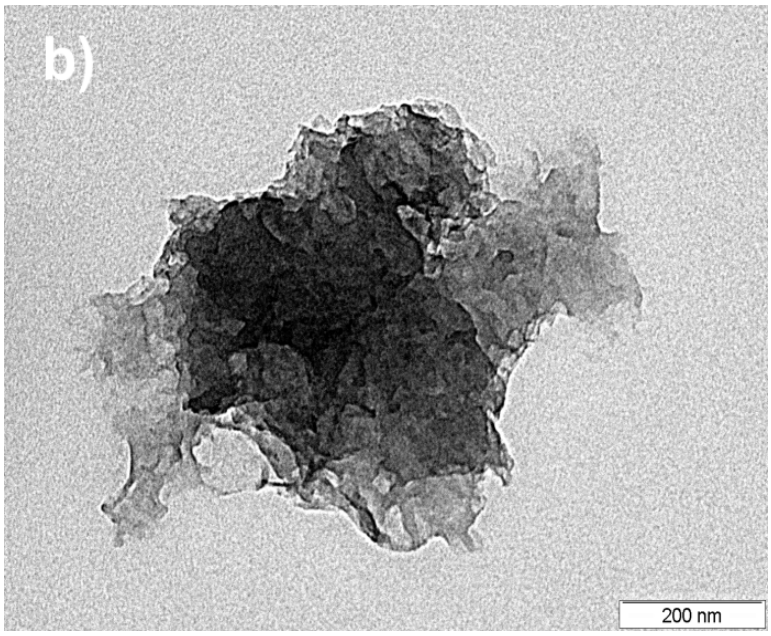

Figure 5.3 ESEM (a) and TEM (b) images of NrGO powder synthesised by Solvo-thermal method.

On the other hand, NrGO sheets demonstrated a 3D wrinkled appearance of particle clusters with an interconnected porous network as elsewhere observed [22, 56]. Low magnification TEM image (Fig. 3b) exhibited the same morphology, which is characteristic of NrGO powder produced by harsh oxidative and reductive treatments, and is indicative of defective structure.

The Raman spectra of GO and NrGO powders are shown in Fig. 4. The G and D bands in the case of graphene oxide are at 1584 cm^{-1} and 1330 cm^{-1}. The G and D bands for NrGO are at 1574 cm^{-1} and 1323 cm^{-1}, respectively. The shift in the G band position of NrGO towards lower wavelengths indicates decrease of the oxygen functional groups and recovery of sp^2 network following the solvothermal reduction. The I_D/I_G intensity ratio increased from 1.05 for GO to 1.4 for NrGO, suggesting the decrease in the size of sp^2 domains [54, 57]. It should be noted that in our study an additional factor could be the incorporation of N dopants, which contributed to the enhancement of the D band intensity upon solvothermal reduction.

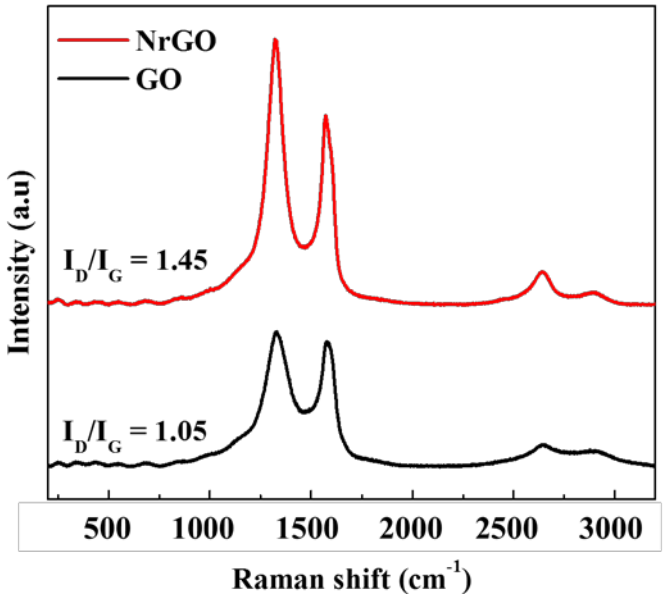

Figure 5.4 Raman spectrum of GO and NrGO powder.

Fig. 5 shows the XRD patterns of GO and NrGO powder. The XRD pattern of pristine graphite consists of a sharp peak at 26°, which corresponds to an interlayer spacing of 0.33 nm [58]. The complete absence of any peak at 2θ of 26º suggests that there are no graphitic contaminants present in the GO. Moreover, the GO pattern shows a characteristic peak at 11.9º, which corresponds to an interlayer distance of 0.7 nm. This indicates that the distance between the (002) planes of the graphite was increased due to the presence of high amount of oxygen functional groups produced through oxidation by the Hummer's method. After the solvothermal reduction with hydrazine, NrGO has two characteristic peaks at 2θ angles of 24º and 44º. The interlayer spacing of (002) plane of NrGO was calculated as 0.362 nm, which is greater than the atomic spacing of graphite (0.33 nm). This indicates that only a moderate level of oxidation is present in the NrGO.

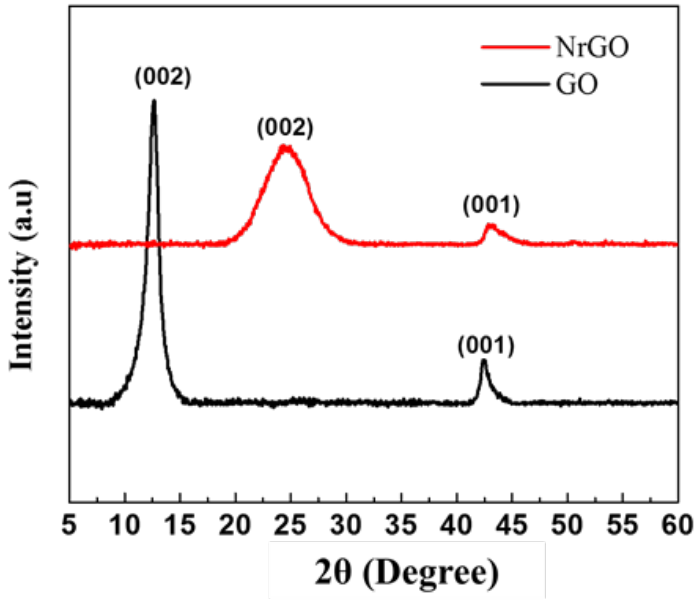

Figure 5.5 XRD characterisation of GO and NrGO powder.

X-ray Photoelectron Spectrometer (XPS) was used to determine the elemental composition and bonding states of GO and NrGO. Fig. 6a-b shows the C 1s of GO and NrGO. The high resolution C 1s of GO shows a well-defined peak at 286.46 eV, in addition to sp^2 carbon peak at 284.5 eV, which is a signature of extreme oxidation of GO. It can be noted that C 1s core level spectra for GO contain four major peaks at 284.4 eV, 285.1 eV, 286.4 eV and 287.9 eV, which are attributed to the sp^2 carbon, hydroxyl (C-OH), epoxide (C-O-C) groups, and the combined contribution from carbonyl (>C=O) and carboxyl (HO-C=O) groups respectively [57]. The C 1s of NrGO can be fitted with three components at 284.4 eV, 285.1 eV and 287.7 eV, which correspond to sp^2 carbon, C-N and also contributions from carbonyl and carboxylic groups [54].

Fig. 6c shows the N 1s of NrGO, which can be considered as divided into four components: pyridinic N (398.8 eV), pyrrolic N (400.0 eV), graphitic N (401.54 eV), pyridine N-oxide (403.4 eV) and these assignments are in agreement with the literature [59]. Fig. 6d shows the elemental composition of GO and NrGO. The C/O ratio in the case of GO and NrGO are 2.5 and 9.6 respectively, which shows that oxygen content has been considerable reduced after solvothermal reduction with ammonia and hydrazine.

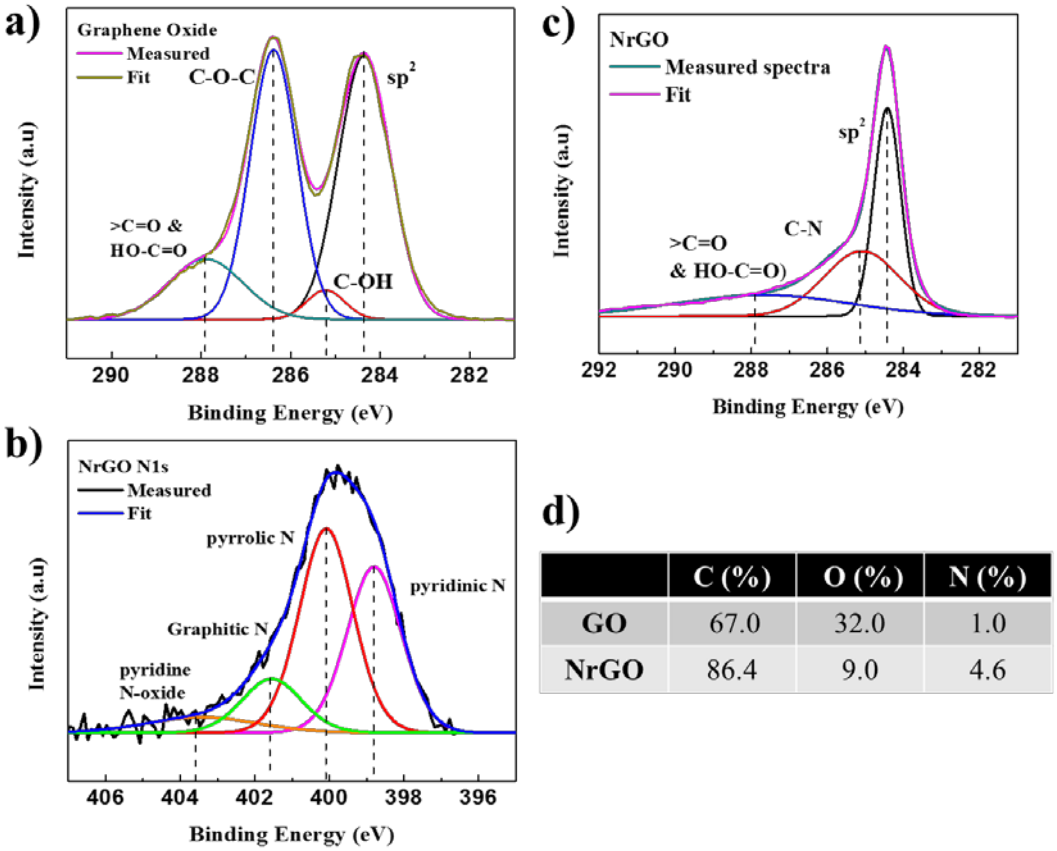

d)

	C (%)	O (%)	N (%)
GO	67.0	32.0	1.0
NrGO	86.4	9.0	4.6

Figure 5.6 High resolution C 1s XPS spectra of GO (a) and NrGO (b); high resolution N 1s XPS spectra of NrGO (c); elemental composition of GO and NrGO (d).

5.3.2 Membrane characterisation.

Fig. 7a-b shows the GO and NrGO membrane surface, respectively, which evidence that homogeneous coating was performed since no significant defects were detected. However, in a potential application the main role of the graphene would be catalysing the process, but also helping the separation. In the specific case of GO membranes, the superficial layer adopted the same homogeneous porous structure as the conglomerate powder precursor (Fig. 2 and 7c). On the contrary, the NrGO surface (Fig. 7d) exhibited a heterogeneous distribution in consonance with the powder precursor structure.

ESEM X-ray (EDX) system for chemical analysis was applied in the graphene (GO or NrGO)-ceramic membrane surface and pointed out the overall composition shown in Table 5.1.

Table 5.1 Elemental composition of GO or NrGO composite membranes (wt. %). [Ceramic support: 50 kDa; deposited graphene amount: 0.1 mg].

	C	O	Zr	Ti
GO	14.17	28.00	57.60	0.23
NrGO	33.48	23.49	41.73	1.30

It must be taken into account that the deposited GO is fragmented into particles or aggregates of different size, a fraction of them being of small size; therefore they are probably able to penetrate into the ceramic support pores thus conforming a sort of composite (graphene-ceramic). Once the pores are constricted, on top of this composite the GO sheets settle down and form a homogeneous GO layer. Therefore, the membrane is probably composed by a thin superficial layer of graphene (either GO or NrGO) followed by a composite of these compounds and ZrO_2 due to the graphene intrusion into the porous surface layer of the support, rich in ZrO_2. The membrane surface composition varied in both cases, the use of reduced graphene oxide as membrane precursor increased the ratio C/O which is in concordance with the synthesised powder composition described in Fig. 6d. Note that the X-ray penetration depth under the operating conditions is estimated around 5 µm (20 kV) assuming the only presence of graphene (GO or NrGO). The detection of zirconia reduces this electron penetration depth to even lower values.

On the other hand, as can be seen in Fig. 7e-f, the GO and NrGO membrane thickness were about 4 and 7 µm, respectively.

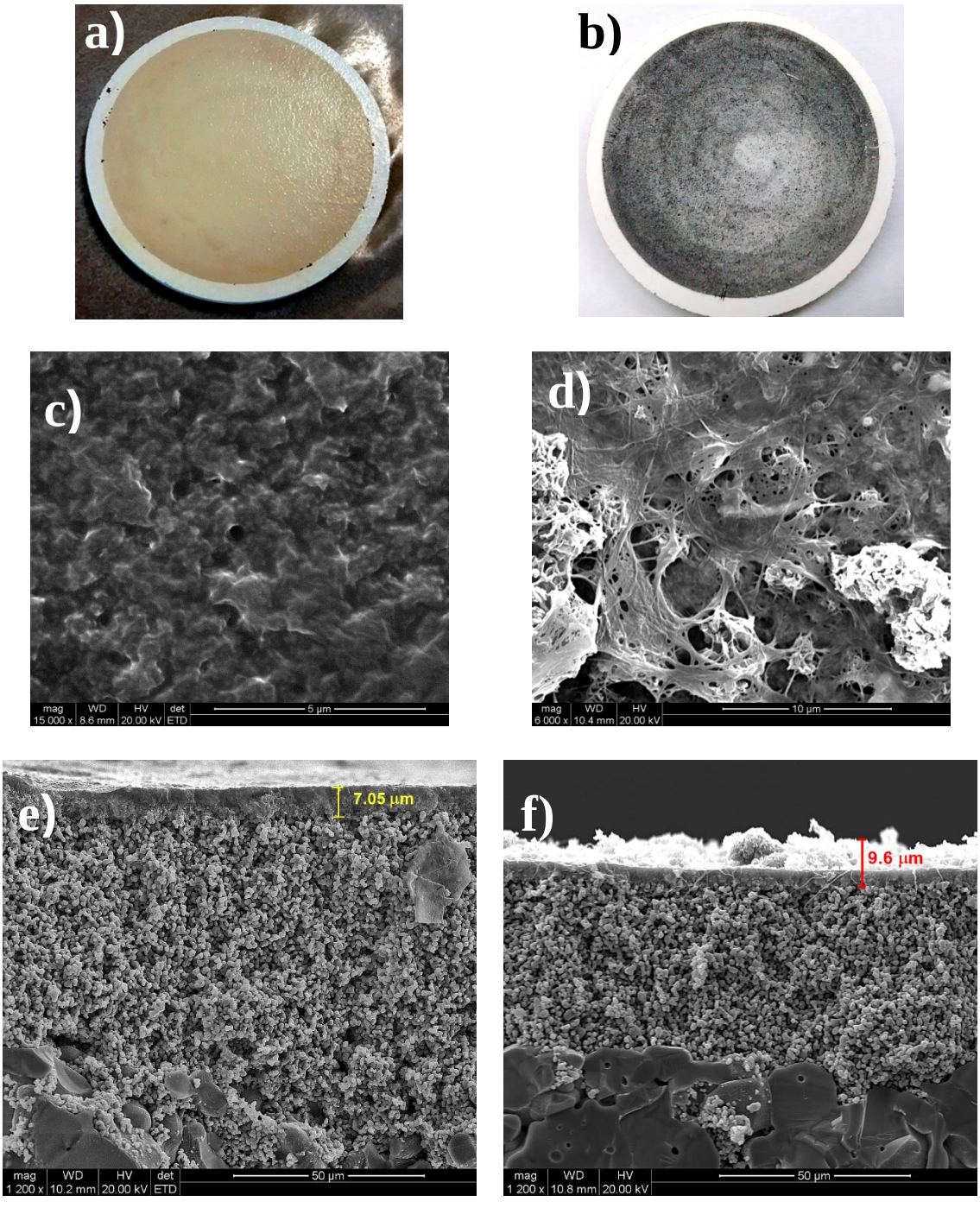

Figure 5.7 ESEM images: GO (a, c, e) and NrGO (b, d, f) disks, membrane surface, and cross-sectional view, respectively. [Ceramic support: 50 kDa; deposited GO or NrGO amount: 0.1 mg].

The membrane surface was further investigated by AFM and the height profiles are depicted in Fig. 8. A root mean square (RMS) roughness analysis was also applied to the membrane surface, as expected, GO membrane showed much more roughness

(136.1) than NrGO ones (0.2). Both materials present a 3D multi-layer structure, however, NrGO shows a less porous structure with punctual irregularities on its topography. GO membrane shows a porous structure with larger surface area, which could be interesting in specific applications where, besides the electrical conductivity, the adsorption plays an important role.

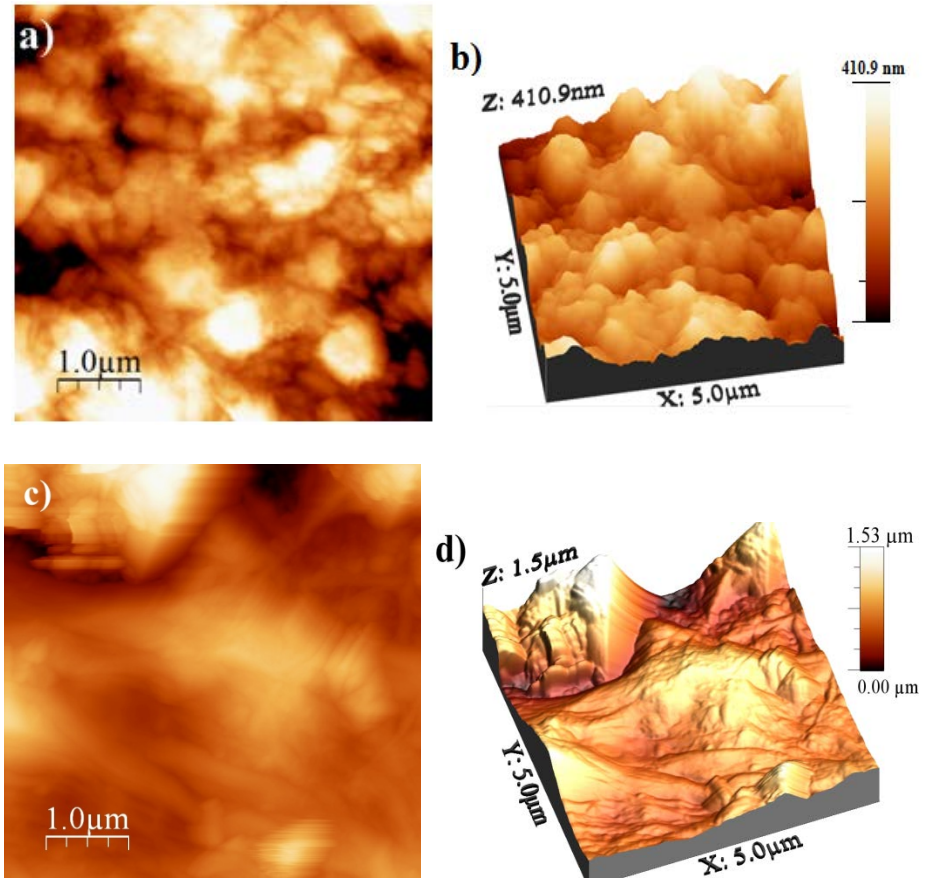

Figure 5.8 AFM images: GO (a, b) and NrGO (c, d) membrane topography 2D, and 3D, respectively. [Ceramic support: 50 kDa; deposited GO or NrGO amount: 0.1 mg].

A rough estimation based on AFM imaging through SPIP^{TM} software indicates that both membranes present most of the pores in the range 20-40 µm. Nevertheless, the significant difference can be found on the area occupied by these pores, 29.8 and 7.6 % for GO and NrGO membranes, respectively.

On the other hand, the electrical properties of the carbon membranes are a measure of its suitability in some wastewater processes such as photocatalytic degradation [60] or anaerobic biodegradation [50]. The electrical resistance was measured through a multi height microposition four point probing system. On the contrary, the membrane thickness was defined by ESEM. Thus, the resistivity (Ω·m) could be calculated using the Equation 2:

$$\rho = R_S \cdot t \tag{2}$$

where, Rs (Ω) defines the electrical resistance and t (m) correspond to the sheet thickness. The calculated value for NrGO sheets was ~$2.8 \cdot 10^{-5}$ (Ω·m) in agreement with

previous studies [61]. This is more than 10-100 times lower resistance than similar sheets of amorphous carbon [62] typically used in such environmental applications.

5.3.3 Interactions on the membrane surface.

Hydroxyl groups always exist on the surface of metal oxides such as ZrO_2 [60]; on the other hand, carboxyl groups are one of the main forms of oxygen-containing functions in oxidised graphene [63]. It has been reported that there is a significant attraction between hydroxyl and carboxyl groups [64]. For this reason, oxidised graphene would be partially ionised creating anions and hydrogen cations, which would react with the hydroxyl groups on ZrO_2 surface. This phenomenon makes easier the synthesis of strong, continuous and homogeneous coatings over this type of ceramic materials. The interactions taking part of a similar process were already described by Hu et al. [40]. Despite their study involved alumina modifications (AlO_2) with highly oxidised graphene, the mechanism could be assimilated in our study as illustrated in Fig. 9.

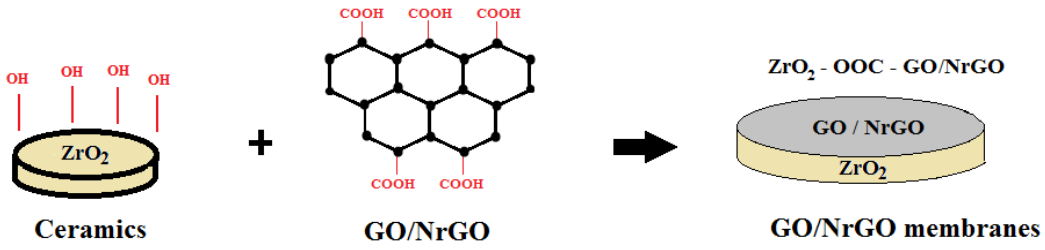

Figure 5.9 GO membrane over ZrO_2 surfaces. Interaction mechanism.

The use of reduced graphene oxide implies a decrease in the presence of carboxyl groups weaken the interactions between both materials. Thus, highly reduced graphene oxide may complicate the preparation of these composites.

5.3.4 Membrane permeation tests.

DI water flux of the filtration element was measured before and after coating with GO or NrGO. Fig. 10 plots the evolution of the water flux over the time.

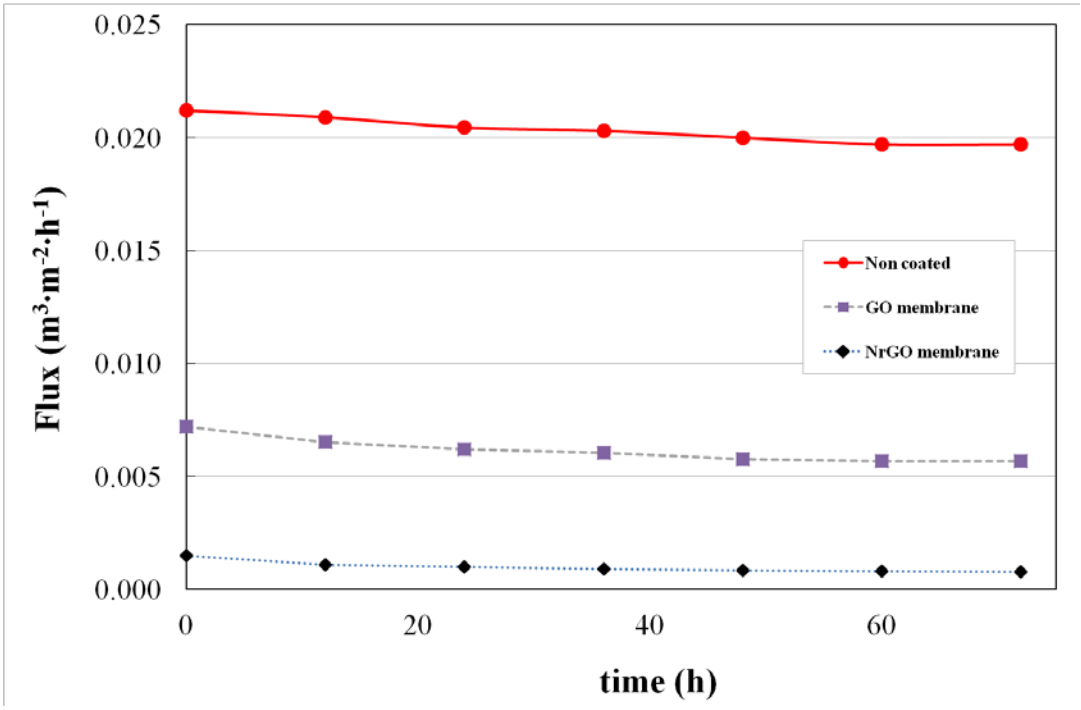

Figure 5.10 Pure water flux. [GO or NrGO deposited: 0.1 mg; ceramic support: 0.04 µm; hydraulic pressure difference: 0.2 bar].

As can be seen, the permeability decreases significantly due to the graphene layer deposition. Several empirical equations correlate permeability and membrane pore size. The Hagen-Poiseuille equation [65] is defined by Equation 3:

$$J_w = \frac{\varepsilon \cdot r^2}{8 \cdot \mu \cdot \tau} \cdot \frac{\Delta P}{d} \quad (3)$$

where, ΔP is the hydraulic pressure difference (Pa), µ is the viscosity (Pa·s) and J_w is the pure water flux ($m^3 \cdot m^{-2} \cdot s$), ε is the porosity, r is the pore radius (m), τ is the tortuosity and d is the membrane thickness (m).

Taking into account the Hagen-Poiseuille dependence and the experimental pure water flux reduction (71%), the pore diameter in the GO membrane would be reduced around 46% with respect to the original size (assuming similar porosity, tortuosity and flux resistance controlled by the GO membrane). The pore constriction is usually associated with an increase of the separation ability and lower permeations. However, in case of high demanding fluxes, the pore size reduction can be limited by depositing smaller amounts of the membrane precursor. In addition, note that filtration experiments were

carried out at very low transmembrane pressures (0.2 bar), thus higher driving forces may be applied in case of specific requirements.

GO presents a 3D structure and relatively thick layers regarding graphene (2D) sheets. This fact has a clear detrimental impact on the permeation but also increases the surface area which is of great value in specific applications such as organic removal, e.g. photocatalytic degradation or anaerobic biodegradation, in wastewaters conducted over surface. The permeation was even lower for NrGO films probably due to its hydrophobic properties [66]. However, NrGO membranes offer less liquid permeation but higher electrical conductivity than GO layers do. Therefore, the election of the proper membrane must be taken depending on the requirements of a specific application.

In addition, potential applications such as water purification demand a stable performance for long periods. Tests conducted for three weeks showed that the flux was almost constant, which suggests no changes on membrane structure and guarantees their use for relatively long periods.

Some studies of GO membranes on alumina hollow fibre substrates reported drying-related shrinkage and instability at the dry state [41]. To check this effect, the disk membranes were subjected to drying for 24 h at 40 ºC between two consecutives filtration tests. The experimental cycle was repeated twice in order to subject the membrane to further mechanical stress. After that, no differences of permeability were found, thus refuting any drying-related problems. However, it must be noted that this phenomenon was indeed observed in case of depositing 1 mg or higher GO amounts (results not shown). In that case, membranes must be maintained in wet state in order to avoid any drying-related shrinkage and subsequent cracks.

5.3.5 Influence of membrane thickness.

The impact of depositing different amounts of membrane precursor was studied. GO was chosen to carried out this investigation. The amount of GO deposited on the ceramic support can be easily controlled by using the vacuum filtration technique. The volume filtrated and corresponding GO concentration define the ultimate film thickness. As can be seen in Fig. 11, an increase of any of these variables provides thicker membranes.

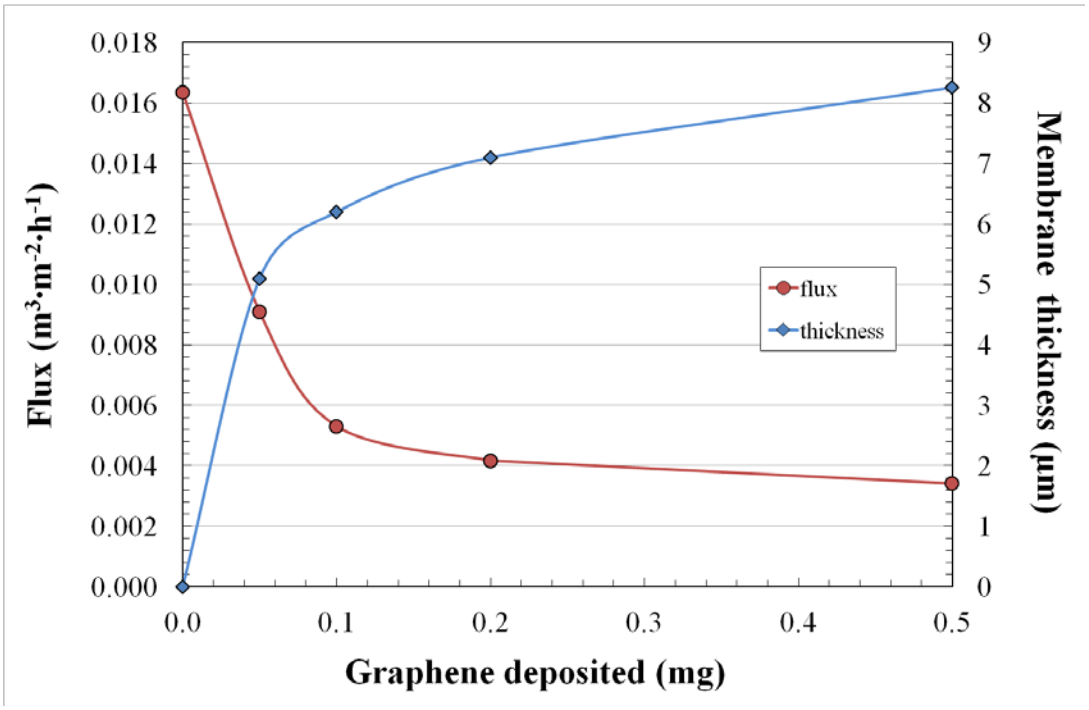

Figure 5.11 Dependence of the pure water flux on the GO deposited [ceramic support: 0.4 µm].

In comparison to the ceramic support, the most important flux reduction (81%) took place depositing small amounts (below 0.1 g) of GO. At this point, likely, the material filled completely the ceramic disk pores and the pure water flux decreased notably from 0.027 to 0.005 $m^3 \cdot m^{-2} \cdot h^{-1}$ (Fig. 11). For this reason, the deposition of larger amounts (0.5 g) of GO showed little additional impact on reducing the flux (4%). Therefore, the graphene-ceramic composite zone exercises control over permeation, while superimposed GO layers only slightly impact the flux. This behaviour could be positive for specific applications where denser films of GO are needed.

In fact, the GO membrane physical structure as 3D aggregates and not 2D crystalline planes could be detrimental for filtration applications because of the additional membrane resistance and derived reduction on the permeation. However, GO membrane structure may benefit its performance in other processes where thicker and rougher films are preferable.

5.3.6 Support pore size influence on membrane preparation.

The effect of the support pore size (SPS) in the preparation of highly oxidised graphene membranes was further studied. GO membranes were synthesised under identical conditions with the exception of the SPS. The permeability and membrane resistances, assuming a resistance in series model, are displayed in Fig. 12 and Table 5.2, respectively.

The overall membrane resistance R_m (m^{-1}) was calculated using the Equation 4:

$$R_m = \sum R_i = R_S + R_{GO} = \frac{\Delta P}{\eta \cdot J_w} \quad (4)$$

where, R_s is the ceramic support resistance (m^{-1}), R_{GO} is the graphene oxide membrane resistance (m^{-1}), ΔP is the hydraulic pressure difference (Pa), J_w is the pure water flux ($m^3 \cdot m^{-2} \cdot s^{-1}$), and η is the viscosity ($kg \cdot m^{-1} \cdot s^{-1}$).

As the resistance of the support, R_S, can be obtained from its original pure water flux, the additional resistance provided by the GO layer, R_{GO}, can be calculated.

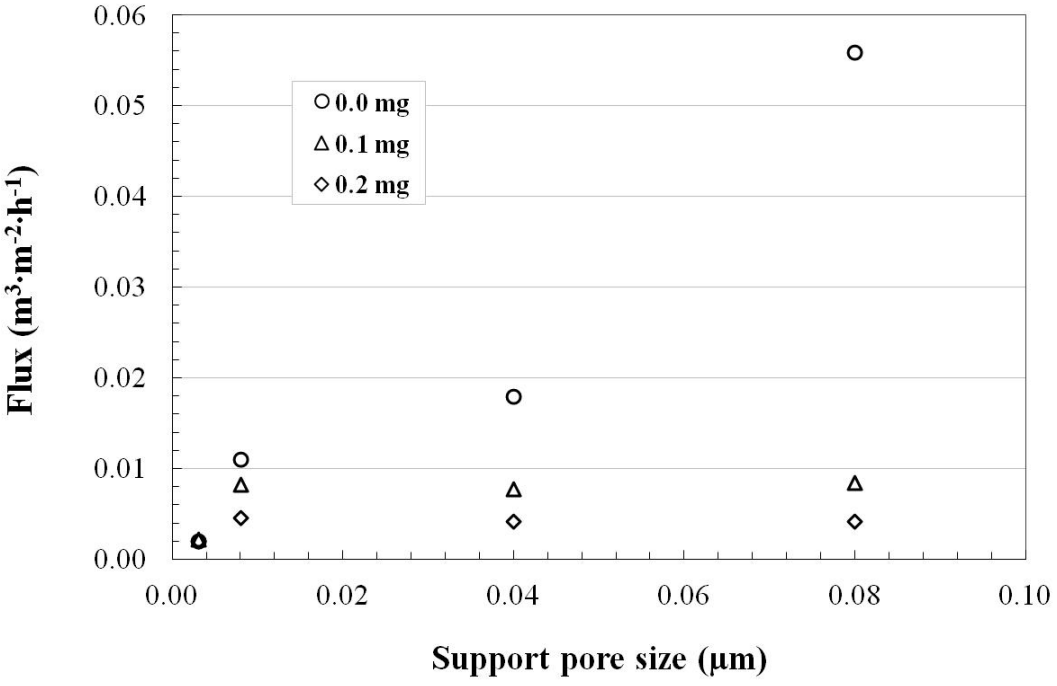

Figure 5.12 Influence of the support pore size on the permeate flux.
[GO coated: 0.1 and 0.2 mg; hydraulic pressure difference: 0.2 bar; T = 20 ºC].

Table 5.2 Intrinsic GO layer and support resistances.

[Hydraulic pressure difference = 0.2 bar; T = 20 ºC; GO coated: 0.1 mg].

SPS (μm)[a]	**GO coated** (mg)	**$J \cdot 10^6$** ($m^3 m^{-2} s^{-1}$)	**$R_m \cdot 10^{-12}$** (m^{-1})	**$R_s \cdot 10^{-12}$** (m^{-1})	**$R_{GO} \cdot 10^{-12}$** (m^{-1})
0.003	0.0	0.6	34.7	34.7	0.0
0.003	0.1	0.4	47.3	34.7	12.6
0.003	0.2	0.3	59.5	34.7	24.8
0.008	0.0	3.1	6.5	6.5	0.0
0.008	0.1	2.3	8.7	6.5	2.2
0.008	0.2	1.3	15.8	6.5	9.3
0.040	0.0	5.0	4.0	4.0	0.0
0.040	0.1	2.2	9.3	4.0	5.3
0.040	0.2	1.2	17.2	4.0	13.2
0.080	0.0	15.5	1.3	1.3	0.0
0.080	0.1	2.4	8.5	1.3	7.2
0.080	0.2	1.2	17.2	1.3	15.9

[a] Estimated from the molecular weight cut-off (MWCO) by Crystal water manufacturer.

Non-significant membrane resistance differences (≤ 10%) were detected by modifying the support pore size from 0.008 to 0.08 μm. As can be observed in Table 5.2, the pure water permeability was mostly governed by the GO layer intrinsic resistance independently of the support pore size used. This can be explained by the ceramic disk pores constriction, which takes place in a greater or lesser extent depending on the initial pore size when the graphene sets down, yet reaching the same final state defined by the particles or aggregates deposited.

Note that the initial GO particles aggregates size, which was estimated to be around 1 μm (Fig. 2-3), changes after sonication and vacuum filtration due to the physical forces involved in these processes, and thus reaches smaller single particle or aggregate sizes allowing the penetration into the greater pores.

On the contrary, the permeability of the ceramic support with the smallest pore size (0.003 μm) was only slightly diminished after depositing the carbon film. In this specific case, as can be observed in Table 5.2, the flux resistance is controlled by the ceramic support instead of the ultrathin GO layer. The most likely reason may be that the GO particles or aggregates settled onto the ceramic surface as they presented a

bigger size than most ceramic pores (0.003 µm), so there were not able to penetrate the support pores. Therefore, the pore size was only slightly reduced and its derived impact on the overall membrane resistance was less pronounced.

5.4 Conclusions.

GO-ZrO_2 and NrGO-ZrO_2 membranes have been synthesised by using the vacuum filtration technique. GO hydrophilicity favours the preparation of homogeneous precursor solutions and coatings. Moreover, the interactions between GO carboxyl and ceramic hydroxyl groups increase the robustness of these composites. In the specific case of NrGO-ZrO_2, although stable ultra-thin coatings were achieved, the coating was not as homogeneous as those derived from using GO powder because functional groups resulting from the chemical reduction of GO impart a hydrophobic character. These should be removed to improve the quality of these coatings.

GO-ZrO_2 membranes showed higher roughness than NrGO/ZrO_2. Their associated large surface area is required in specific applications where, besides the electrical conductivity, the adsorption plays an important role. On the other hand, NrGO membranes electroconductivity was found to be many orders of magnitude higher than that offered by other carbon forms such as GO or activated carbon. For this reason, these materials may enhance any water process such as photocatalytic decolourisation or anaerobic biodegradation of wastewaters where separation, surface area and electrical conductivity are simultaneously necessary.

In relation to the membrane synthesis, as expected, the precursor amount used determines the thickness. Thicker membranes provided lower permeability. However, note that the study is focused on composite membranes, thus the first GO layers deposited promoted the constriction of the support pores reducing its original flux to a greater extend. On the other hand, the support pore size was changed in order to study the derived impact on the synthesised membrane. Non-differences were detected on the permeation that could be defined by the membrane precursor size.

References

1. Novoselov KS, Geim AK, Morozov S V, et al (2004) Electric Field Effect in Atomically Thin Carbon Films. Sci 306 :666–669. doi: 10.1126/science.1102896
2. Lee C, Wei X, Kysar JW, Hone J (2008) Measurement of the Elastic Properties and Intrinsic Strength of Monolayer Graphene. Sci 321 :385–388. doi: 10.1126/science.1157996
3. Ning J, Wang D, Zhang C, et al (2015) Electrical and optical properties of layer-stacked graphene transparent electrodes using self-supporting transfer method. Synth Met 203:215–220. doi: 10.1016/j.synthmet.2015.02.007
4. Kang S-H, Fang T-H, Hong Z-H, Chuang C-H (2013) Mechanical properties of free-standing graphene oxide. Diam Relat Mater 38:73–78. doi: 10.1016/j.diamond.2013.06.016
5. Jagiello J, Judek J, Zdrojek M, et al (2014) Production of graphene composite by direct graphite exfoliation with chitosan. Mater Chem Phys 148:507–511. doi: 10.1016/j.matchemphys.2014.09.043
6. Liu F, Seo TS (2010) Large scale synthetic method for free standing graphene film and graphene sponges. In: 10th IEEE Int. Conf. Nanotechnol. IEEE, pp 696–699
7. Campos-Delgado J, Botello-Méndez AR, Algara-Siller G, et al (2013) CVD synthesis of mono- and few-layer graphene using alcohols at low hydrogen concentration and atmospheric pressure. Chem Phys Lett 584:142–146. doi: 10.1016/j.cplett.2013.08.031
8. Radchenko TM, Shylau AA, Zozoulenko IV (2014) Conductivity of epitaxial and CVD graphene with correlated line defects. Solid State Commun 195:88–94. doi: 10.1016/j.ssc.2014.07.012
9. Wu B, Tuncer HM, Katsounaros A, et al (2014) Microwave absorption and radiation from large-area multilayer CVD graphene. Carbon 77:814–822. doi: 10.1016/j.carbon.2014.05.086
10. Grennberg H, Jansson U (2012) Advanced Functional Materials. Sci Technol At Mol Condens Matter Biol Syst. doi: 10.1016/B978-0-44-453681-5.00005-4
11. Whitener KE, Sheehan PE (2014) Graphene synthesis. Diam Relat Mater 46:25–34. doi: 10.1016/j.diamond.2014.04.006
12. Potts JR, Dreyer DR, Bielawski CW, Ruoff RS (2011) Graphene-based polymer

nanocomposites. Polymer (Guildf) 52:5–25. doi: 10.1016/j.polymer.2010.11.042

13. Zhao C, Xing L, Xiang J, et al (2014) Formation of uniform reduced graphene oxide films on modified PET substrates using drop-casting method. Particuology 17:66–73. doi: 10.1016/j.partic.2014.02.005
14. William S. Hummers J, Offeman RE (1958) Preparation of Graphitic Oxide. J Am Chem Soc 80:1339. doi: 10.1021/ja01539a017
15. Nekahi A, Marashi PH, Haghshenas D (2014) Transparent conductive thin film of ultra large reduced graphene oxide monolayers. Appl Surf Sci 295:59–65. doi: 10.1016/j.apsusc.2014.01.004
16. Xu Y, Bai H, Lu G, et al (2008) Flexible graphene films via the filtration of water-soluble noncovalent functionalized graphene sheets. J Am Chem Soc 130:5856–5857. doi: 10.1021/ja800745y
17. Chen C-M, Huang J-Q, Zhang Q, et al (2012) Annealing a graphene oxide film to produce a free standing high conductive graphene film. Carbon 50:659–667. doi: 10.1016/j.carbon.2011.09.022
18. Noerochim L, Wang JZ, Wexler D, et al (2013) Rapid synthesis of free-standing MoO3 / Graphene films by the microwave hydrothermal method as cathode for bendable lithium batteries. J Power Sources 228:198–205. doi: 10.1016/j.jpowsour.2012.11.113
19. Wei Z, Barlow DE, Sheehan PE (2008) The assembly of single-layer graphene oxide and graphene using molecular templates. Nano Lett 8:3141–3145. doi: 10.1021/nl801301a
20. Dolbin A V., Khlistyuck M V., Esel'son VB, et al (2015) The effect of the thermal reduction temperature on the structure and sorption capacity of reduced graphene oxide materials. Appl Surf Sci. doi: 10.1016/j.apsusc.2015.11.167
21. Du X, Zhou C, Liu H-Y, et al (2013) Facile chemical synthesis of nitrogen-doped graphene sheets and their electrochemical capacitance. J Power Sources 241:460–466. doi: 10.1016/j.jpowsour.2013.04.138
22. Bikkarolla SK, Papakonstantinou P (2015) CuCo2O4 nanoparticles on nitrogenated graphene as highly efficient oxygen evolution catalyst. J Power Sources 281:243–251. doi: 10.1016/j.jpowsour.2015.01.192
23. Li H, Song Z, Zhang X, et al (2013) Ultrathin, Molecular-Sieving Graphene Oxide Membranes for Selective Hydrogen Separation. Science (80-) 342:95–98. doi: 10.1126/science.1236686

24. Liu R, Arabale G, Kim J, et al (2014) Graphene oxide membrane for liquid phase organic molecular separation. Carbon 77:933–938. doi: 10.1016/j.carbon.2014.06.007
25. Li H, Song Z, Zhang X, et al (2013) Ultrathin, Molecular-Sieving Graphene Oxide Membranes for Selective Hydrogen Separation. Sci 342 :95–98. doi: 10.1126/science.1236686
26. Eda G, Chhowalla M (2010) Chemically Derived Graphene Oxide: Towards Large-Area Thin-Film Electronics and Optoelectronics. Adv Mater 22:2392–2415. doi: 10.1002/adma.200903689
27. Paul DR (2012) Creating New Types of Carbon-Based Membranes. Sci 335:413–414. doi: 10.1126/science.1216923
28. Geim AK, Novoselov KSS (2007) The rise of graphene. Nat Mater 6:183–191. doi: 10.1038/nmat1849
29. Chen J, Guo Y, Huang L, et al (2014) Controllable fabrication of ultrathin free-standing graphene films. Philos Trans R Soc A Math Phys Eng Sci 372:20130017. doi: 10.1098/rsta.2013.0017
30. Zheng Q, Li Z, Yang J, Kim J (2014) Graphene oxide-based transparent conductive films. Prog Mater Sci 64:200–247. doi: 10.1016/j.pmatsci.2014.03.004
31. Zheng Q, Shi L, Yang J (2012) Langmuir-Blodgett assembly of ultra-large graphene oxide films for transparent electrodes. Trans Nonferrous Met Soc China 22:2504–2511. doi: 10.1016/S1003-6326(11)61492-1
32. Xu Y, Long G, Huang L, et al (2010) Polymer photovoltaic devices with transparent graphene electrodes produced by spin-casting. Carbon 48:3308–3311. doi: 10.1016/j.carbon.2010.05.017
33. Chowdhury S, Balasubramanian R (2014) Graphene/semiconductor nanocomposites (GSNs) for heterogeneous photocatalytic decolorization of wastewaters contaminated with synthetic dyes: A review. Appl Catal B Environ 160-161:307–324. doi: 10.1016/j.apcatb.2014.05.035
34. Berdova M, Perros AP, Kim W, et al (2014) Exceptionally strong and robust millimeter-scale graphene-alumina composite membranes. Nanotechnology 25:355701. doi: 10.1088/0957-4484/25/35/355701
35. Li N, Yang G, Sun Y, et al (2015) Free-Standing and Transparent Graphene Membrane of Polyhedron Box-Shaped Basic Building Units Directly Grown

Using a NaCl Template for Flexible Transparent and Stretchable Solid-State Supercapacitors. Nano Lett 15:3195–3203. doi: 10.1021/acs.nanolett.5b00364

36. Feng X, Chen W, Yan L (2015) Free-standing dried foam films of graphene oxide for humidity sensing. Sensors Actuators B Chem 215:316–322. doi: 10.1016/j.snb.2015.03.068
37. Dikin DA, Stankovich S, Zimney EJ, et al (2007) Preparation and characterization of graphene oxide paper. Nature 448:457–460. doi: 10.1038/nature06016
38. Rana K, Singh J, Lee JT, et al (2014) Highly conductive freestanding graphene films as anode current collectors for flexible lithium-ion batteries. ACS Appl Mater Interfaces 6:11158–11166. doi: 10.1021/am500996c
39. Liu Y, Zhang D, Shang Y, Liu Y (2014) A simple route to prepare free-standing graphene thin film for high-performance flexible electrode materials. RSC Adv 4:30422. doi: 10.1039/C4RA04031G
40. Hu X, Yu Y, Zhou J, et al (2015) The improved oil/water separation performance of graphene oxide modified Al2O3 microfiltration membrane. J Memb Sci 476:200–204. doi: 10.1016/j.memsci.2014.11.043
41. Aba NFD, Chong JY, Wang B, et al (2015) Graphene oxide membranes on ceramic hollow fibers – Microstructural stability and nanofiltration performance. J Memb Sci 484:87–94. doi: 10.1016/j.memsci.2015.03.001
42. Almandoz MC, Pagliero CL, Ochoa NA, Marchese J (2015) Composite ceramic membranes from natural aluminosilicates for microfiltration applications. Ceram Int 41:5621–5633. doi: 10.1016/j.ceramint.2014.12.144
43. Hatori H, Takagi H, Yamada Y (2004) Gas separation properties of molecular sieving carbon membranes with nanopore channels. Carbon N Y 42:1169–1173.
44. Chen X, Dai Y, Wang X, et al (2015) Synthesis and characterization of Ag_3PO_4 immobilized with graphene oxide (GO) for enhanced photocatalytic activity and stability over 2,4-dichlorophenol under visible light irradiation. J Hazard Mater 292:9–18. doi: 10.1016/j.jhazmat.2015.01.032
45. Kim H-S, Takizawa S, Ohgaki S (2007) Application of microfiltration systems coupled with powdered activated carbon to river water treatment. Wastewater Reclam Reuse Sustain 202:271–277. doi: 10.1016/j.desal.2005.12.064
46. Mezohegyi G, Bengoa C, Stuber F, et al (2008) Novel bioreactor design for decolourisation of azo dye effluents. Chem Eng J 143:293–298.

47. Fu X, Yang H, Lu G, et al (2015) Improved performance of surface functionalized TiO2/activated carbon for adsorption–photocatalytic reduction of Cr(VI) in aqueous solution. Mater Sci Semicond Process 39:362–370. doi: 10.1016/j.mssp.2015.05.034
48. Chen J, Zhang F, Zhao Y-L, et al (2016) Facile synthesis of CdS/C core–shell nanospheres with ultrathin carbon layer for enhanced photocatalytic properties and stability. Appl Surf Sci 362:126–131. doi: 10.1016/j.apsusc.2015.11.197
49. Fagan R, McCormack DE, Dionysiou DD, Pillai SC (2015) A review of solar and visible light active TiO2 photocatalysis for treating bacteria, cyanotoxins and contaminants of emerging concern. Mater Sci Semicond Process 42:2–14. doi: 10.1016/j.mssp.2015.07.052
50. Mezohegyi G, Gonçalves F, Órfão JJM, et al (2010) Tailored activated carbons as catalysts in biodecolourisation of textile azo dyes. Appl Catal B Environ 94:179–185. doi: 10.1016/j.apcatb.2009.11.007
51. Sun L, Yu H, Fugetsu B (2012) Graphene oxide adsorption enhanced by in situ reduction with sodium hydrosulfite to remove acridine orange from aqueous solution. J Hazard Mater 203-204:101–10. doi: 10.1016/j.jhazmat.2011.11.097
52. Mezohegyi G, van der Zee FP, Font J, et al (2012) Towards advanced aqueous dye removal processes: A short review on the versatile role of activated carbon. J Environ Manage 102:148–164.
53. Shao Y, Zhang S, Engelhard MH, et al (2010) Nitrogen-doped graphene and its electrochemical applications. J Mater Chem 20:7491. doi: 10.1039/c0jm00782j
54. Bikkarolla SK, Yu F, Zhou W, et al (2014) A three-dimensional Mn3O4 network supported on a nitrogenated graphene electrocatalyst for efficient oxygen reduction reaction in alkaline media. J Mater Chem A 2:14493–14501. doi: 10.1039/C4TA02279C
55. Mobarakabad P, Moghadassi AR, Hosseini SM (2015) Fabrication and characterization of poly(phenylene ether-ether sulfone) based nanofiltration membranes modified by titanium dioxide nanoparticles for water desalination. Desalination 365:227–233. doi: 10.1016/j.desal.2015.03.002
56. Centeno A, Rocha VG, Alonso B, et al (2013) Graphene for tough and electroconductive alumina ceramics. J Eur Ceram Soc 33:3201–3210. doi: 10.1016/j.jeurceramsoc.2013.07.007
57. Ganguly A, Sharma S, Papakonstantinou P, Hamilton J (2011) Probing the

Thermal Deoxygenation of Graphene Oxide using High Resolution In Situ X-Ray based Spectroscopies. J Phys Chem C 115:17009–17019. doi: 10.1021/jp203741y

58. Bikkarolla SK, Cumpson P, Joseph P, Papakonstantinou P (2014) Oxygen reduction reaction by electrochemically reduced graphene oxide. Faraday Discuss 173:415–28. doi: 10.1039/c4fd00088a
59. Long D, Li W, Ling L, et al (2010) Preparation of Nitrogen-Doped Graphene Sheets by a Combined Chemical and Hydrothermal Reduction of Graphene Oxide. Langmuir 26:16096–16102. doi: 10.1021/la102425a
60. Seven O, Dindar B, Aydemir S, et al (2004) Solar photocatalytic disinfection of a group of bacteria and fungi aqueous suspensions with TiO2, ZnO and Sahara desert dust. J Photochem Photobiol A Chem 165:103–107. doi: 10.1016/j.jphotochem.2004.03.005
61. Pei S, Cheng HM (2012) The reduction of graphene oxide. Carbon N Y 50:3210–3228. doi: 10.1016/j.carbon.2011.11.010
62. Ishak A, Rusop M (2014) Electrical Properties Of Intrinsic Amorphous Carbon Films From Ethanol Precursor. 3:305–308.
63. Oh YJ, Yoo JJ, Kim YI, et al (2014) Oxygen functional groups and electrochemical capacitive behavior of incompletely reduced graphene oxides as a thin-film electrode of supercapacitor. Electrochim Acta 116:118–128. doi: 10.1016/j.electacta.2013.11.040
64. Wang L, Zhao J, Bai S, et al (2014) Significant catalytic effects induced by the electronic interactions between carboxyl and hydroxyl group modified carbon nanotube supports and vanadium species for NO reduction with NH3 at low temperature. Chem Eng J 254:399–409. doi: 10.1016/j.cej.2014.05.096
65. Chen L, Feng H, Xie Z, Sun F (2014) “Disc-point” mass transfer Constructal optimizations with Darcy and Hagen–Poiseuille flows in porous media. Appl Math Model 38:1288–1299. doi: 10.1016/j.apm.2013.08.015
66. Fan L, Harris JL, Roddick FA, Booker NA (2001) Influence of the characteristics of natural organic matter on the fouling of microfiltration membranes. Water Res 35:4455–4463. doi: 10.1016/S0043-1354(01)00183-X

. Supplementary material

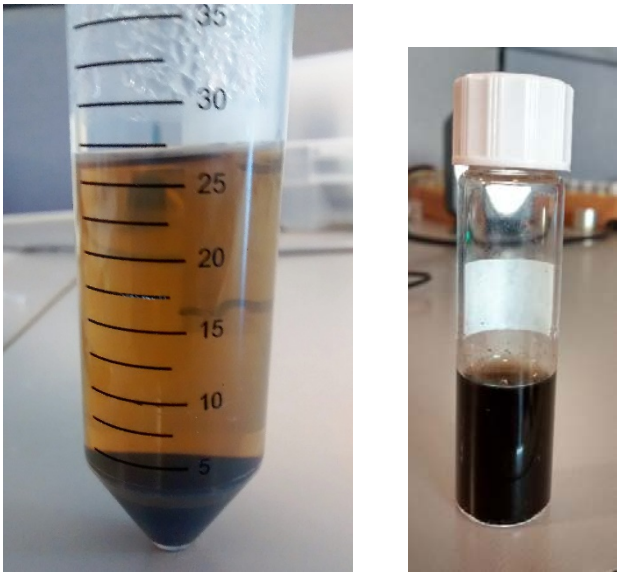

Figure A5.1 Synthesised GO after (a) and before (b) the centrifuge process.

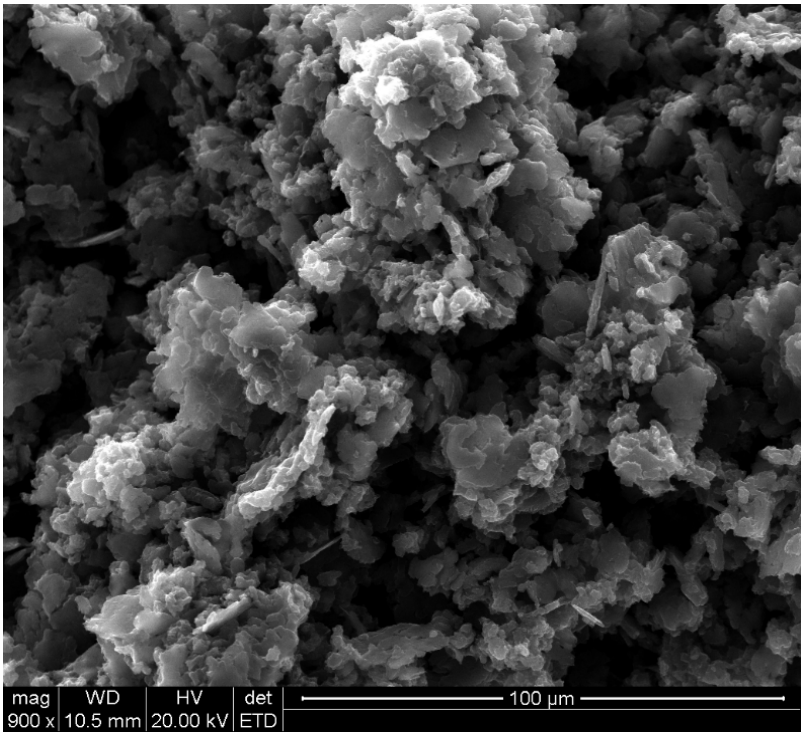

Fig A5.2 Synthesised NrGO powder (reflux method).

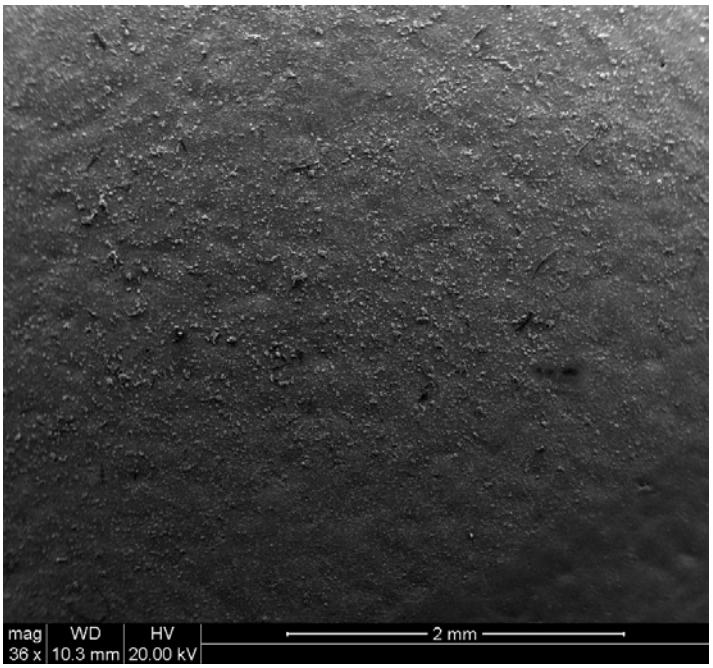

Figure A5.3 Synthesised NrGO membrane (Solvothermal method).

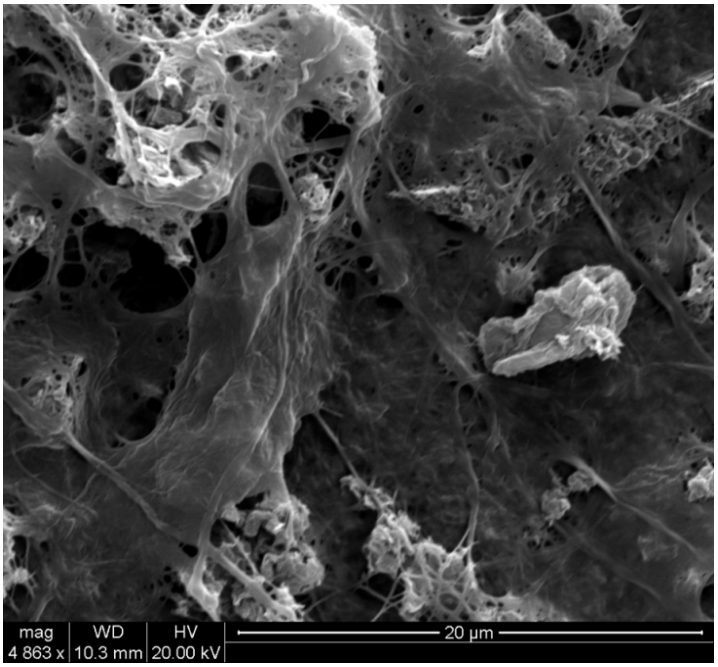

Figure A5.4 Synthesised NrGO powder (Solvothermal method).

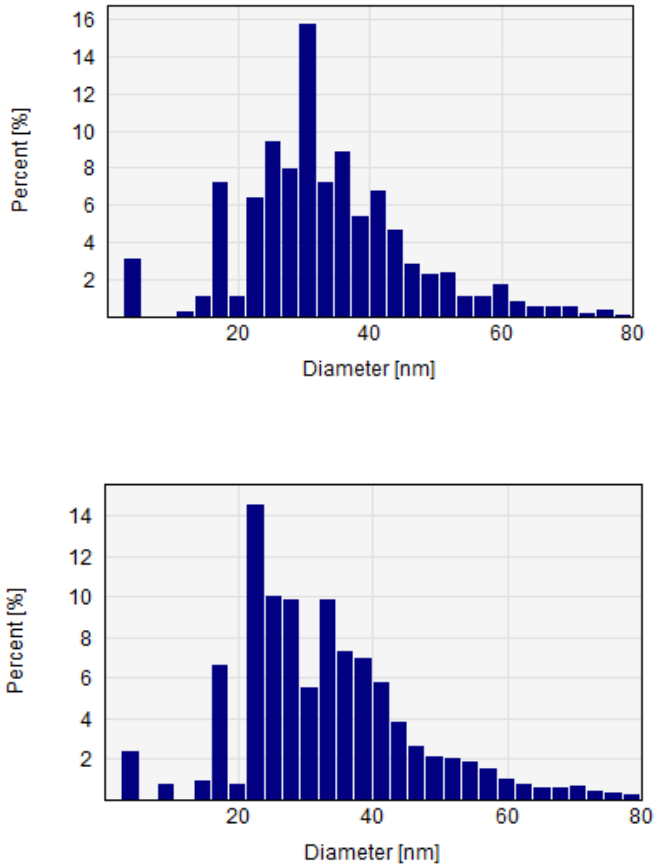

Figure A5.5 GO (a) and NrGO (b) membranes, respectively

CHAPTER 6

General conclusions and future work

The final chapter of this thesis presents a general overview of the main results, along with the most relevant conclusions. Finally, some suggestions about future work are presented.

6.1 General conclusions

Ceramic supported carbon membranes (CSCM) were synthesized and subsequently tested for the azo dye removal by anaerobic biodegradation. The synthesis of the membranes was reproducible under specific conditions. The most critical stage was found to be the deposition of the carbon precursor solution over the ceramic support. The method to carry out this stage was the spin-coating technique. Rotating speeds higher than 3000 rpm favored the deposition of ultrathin (5-15 µm) and homogeneous films of the carbon precursor, which is decisive to synthesize defect-free membranes. The deposited layer was finally carbonized, the atmosphere over this stage was also found crucial for the successful preparation of the carbon membrane; for this reason, an initial purge of the oxygen and subsequent continuous flow of nitrogen was required.

CSCMs were applied to anaerobically process wastewater containing low concentration of Acid Orange 7, as model compound. The degradation was conducted in a biofilm supported over the carbon layer, where the wastewater was continuously filtrated through. After a period of acclimation and incubation, the azo dye conversion exceeded 80% from the feed dye concentration (50 $mg \cdot L^{-1}$) and a flux of 0.05 $L \cdot m^{-2} \cdot h^{-1}$. Thus, The CSCMs were proved to be efficient for the anaerobic biodegradation of AO7. Sulfanilic acid, a derived dye reduction metabolite, was also significantly degraded (> 95%) while the chemical oxygen demand was halved. The presence of a carbon layer enhanced the removal rate over four times in comparison to the performance of commercial ceramic membranes without carbon. Therefore, the carbon layer played an essential role as electron mediator favoring the dye reductive treatment and as retention system for biomass and its derivatives, resulting in an intensified one-step treatment for azo dyes removal from wastewater.

The amount of carbon precursor was found critical for the studied application. Different carbon precursor amounts (2-10% wt.) and ceramic support pore sizes (15, 50, and 150 kDa cutoff) were tested. These factors determined the membrane thickness (5-11 µm) and surface characteristics such as root mean square roughness (31-67 nm). All the membranes were tested for the anaerobic biodegradation of the dye over immobilized biofilms under an equivalent dye loading rate of 38 $g \cdot m^{-3} \cdot day^{-1}$. The presence of the carbon membrane increased two to five times the biodegradation rates. The amount of

active carbon material and the membrane roughness were found to be the responsible of the azo dye removal differences.

Further studies were focused on a novel double-cell bioreactor for the removal of azo dyes from wastewater. This novel double-cell bioreactor was proved to be efficient for the anaerobic biodegradation of AO7. The carbon membrane surface acts as an excellent electron carrier accelerating the removal of these harmful pollutants from wastewater. Dye concentrations from 50 $mg \cdot L^{-1}$ to 150 $mg \cdot L^{-1}$ were processed reaching complete removal of AO7 and soluble COD under batch conditions. It was found that the dye chemical structure influences the biodegradation. More complex compounds such as Tartrazine demands a longer biodegradation period.

Finally, the efforts were focused on the development of novel membranes with higher conductive properties thus enhancing the redox mediator role of these materials. For the first time, a stable graphene layer was deposited over a ceramic disk using a simple casting method. Graphene has a great potential to substitute other amorphous carbon materials which have been widely used in many water and wastewater treatments such as purification or photocatalytic processes. Graphene powder with different degree of oxidation was synthesized and subsequently used to prepare supported membranes. Ceramic porous materials were chosen as membrane support due to the robustness and long-life required in a likely application. Ultrathin membranes (7-9 μm) were successfully prepared through vacuum-filtration of highly oxidized graphene or reduced graphene oxide solutions (1 $mg \cdot mL^{-1}$). The influence of depositing different amounts of membrane precursor was extensively studied (0.003-0.037 $mg \cdot cm^{-2}$); above 0.037 mg/cm^2 drying-related shrinkage problems are detected. Moreover, the ceramic support pore size (0.008-0.08 μm) showed little impact in terms of overall membrane flux resistance and the deposited graphene layer usually governs the membrane permeation. Finally, long-term filtration experiments were also performed for weeks without substantial variation of the membrane structure or permeation ($\leq$ 2%), which is demanded in most conventional water treatments. Overall, the addition of partially oxidized graphene to conventional ceramic membranes greatly decreases their electrical resistivity ($\sim 2.8 \cdot 10^{-5}$ $\Omega \cdot m$) opening the possibility of being employed for many environmental purposes, among, the anaerobic biodegradation of azo dyes.

6.2 Future work

The results and conclusions derived from this thesis must serve as a guideline for future studies in this field. Below, some suggestions about possible future continuations are given.

- GO membranes could be chemically or physically treated for further removal of the oxygen groups increasing this way the surface conductivity.
- Membrane chemical doping with some specific functional groups, such as COOH functionalization, can be investigated in order to increase the surface conductivity.
- It is mandatory in a close future research to assess the applicability of the graphene membranes for the removal of azo dyes.
- It would be of interest the design and operation of double chamber bioreactors on continuous mode and modify the design to be operated as a microbial fuel cell.
- A different application of these conductive materials could be photocatalytic removal of recalcitrant compounds from wastewater through the synthesized graphene membranes.
- The specific identification of the microorganism strains developed preferentially over the carbon membrane must allow their selection as process intensification strategy.